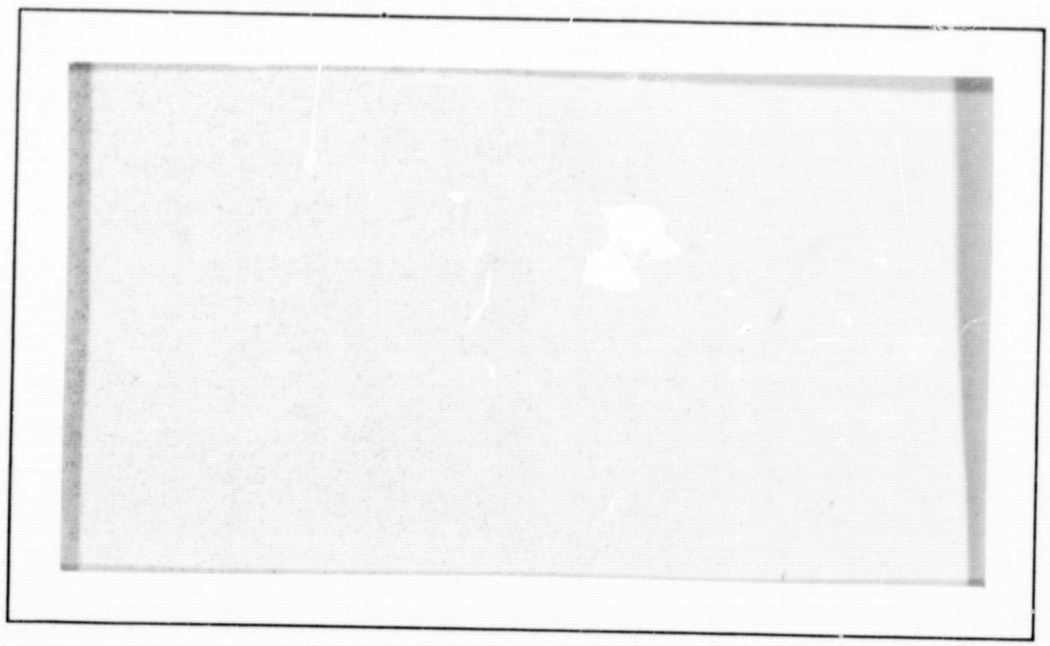

A Publication of the

DEPARTMENT OF MECHANICAL SCIENCES and ENVIRONMENTAL ENGINEERING

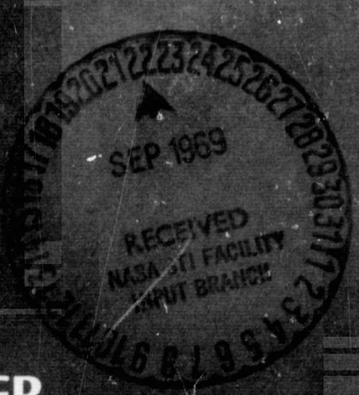

UNIVERSITY OF DENVER

Denver, Colorado

First Annual Report

PROGRAM FOR THE EXPLOITATION OF UNUSED NASA PATENTS

NASA Grant
NGL 06-004-078

June 1, 1968 - May 31, 1969

TABLE OF CONTENTS

TABLE OF CONTENTS (Cont.)

I. PROGRAM GOALS

The purpose of this program is a multidisciplinary research effort for the exploitation of unused NASA patents, using a team of faculty, students and research staff to establish the technical, economic and marketing feasibility of selected NASA patents.

II. THE ORGANIZATION OF THE PROGRAM

During the initial stages of this program during the summer of 1968, there was a skeleton organization consisting of Professor Ezra, and Professor Parks from the Department of Mechanical Sciences and Environmental Engineering, along with Dr. Milliken of the Industrial Economics Division, and two students in Mechanical Engineering. The skeleton organization (shown in Figure 2.1) operated during the summer, concentrating on the patent selection process, policy formulation, interaction with the faculty members of the other departments such as School of Business Administration, Law School, Department of Mass Communications to determine their role in the program and what the multidisciplinary needs of the program would be.

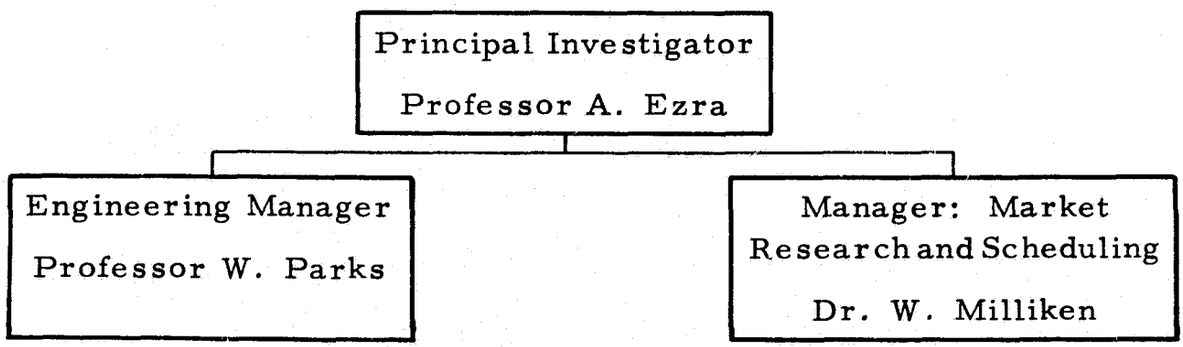

Figure 2.1. Skeleton Organization for Summer of 1968

During the summer, commitments for participation in this program were obtained from the deans and faculty members of the Law School, School of Business Administration, and the Department of Mass Communications. The goals of the program had to be thoroughly explained along with the expected beneficial fall-out. Contrary to

pessimistic predictions from a number of sources. the reaction of the non-engineering faculty to such a program was one of interest and willingness to participate, though on their own terms.

It was finally established that participation in this program by graduate students from non-engineering schools would earn credit for either independent study or thesis. The student's faculty adviser would participate in the program and determine the grades given to his student.

Having laid the foundations of this multidisciplinary program during the summer of 1968, the organization of the program was drawn up with the participation of the students after the beginning of the academic year in September 1968.

The organization structure and assignment of functional responsibilities for the Patent Exploitation Project were patterned after those of an aerospace firm engaged in advanced research and development. That is, the matrix organization concept was used as a basis for establishing a multidisciplinary project structure.

This organization concept is considerably different from the traditional university patterns of work. A departure from the carefully segmented discipline orientation of the academic environment was considered highly desirable in promoting cooperation among the project participants and in creating the right atmosphere for a multidisciplinary effort. Yet, as is typical of a university rather than industry, the decision on organizational pattern evolved from a group consensus, not a unilateral decision from top management.

When the project began, the first area of deliberation by staff and students was that of project organization. Following introductory lectures on the theory of organizational behavior and on comparative patterns of organizational structure by Dr. Milliken, the project participants engaged in discussions of alternative organizations to meet project goals. Each student then prepared a paper recommending an organization structure of his choice. Several of the papers were extremely creative, and showed an unusual ability by students without a business administration background to adapt concepts from other fields to the organization problem. The clear consensus of the participants, faculty and students alike, favored the aerospace-generated matrix organization concept.

Adapting the matrix concept to a university presents certain unusual challenges. The existing university organization is functional, and cooperation between schools and colleges of the university, as well as between departments of the same college, relies on individuals' consent (e.g., participation in committees). The basic University of Denver organization structure (simplified form) is shown in Figure 2.2. There is a considerable diversity among the participating functions. Several of these had no previous history or contact. Few, if any, had developed patterns of interdepartmental cooperation.*

Nevertheless, cooperation began and has continued. Several factors are believed to account for the degree of success thus far in the project. Of these, the most important is believed to be a common perception of the significant value of the R&D goal - the exploitation of unused NASA patents. A significant objective of this nature appears to promote a greater spirit of cooperation and to reduce friction among project participants, than might be the case with a routine project effort. A second factor may be the aerospace R&D experience possessed by key faculty members, which stimulates an attitude of concern for project goals.

The original organization structure, developed in October, 1968, is shown in Figure 2.3. With minor changes in personnel and some evolution of project tasks, the structure still is in effect in May, 1969. The matrix structure depicted promotes simultaneous and continuous attention, both to project objectives and to functional integrity. The project engineers are responsible for product performance, schedule and budget control. The functional unit supervisors are responsible for maintaining quality and design standards and to supply personnel for project activities. The resulting interplay of checks and balances is intended to assure that proper attention is given to all aspects of project activity, and that no responsibility gaps occur to threaten attainment of project objectives.

Reasonably detailed statements of functional responsibility were prepared for each of the project and functional units, by a graduate

---

* Some of the experiences of University of Denver participants parallel recent findings of Syracuse University investigators engaged in a NASA-sponsored study of management of university R&D programs. See Richard J. Hopeman and David L. Wilemon, "Reflections on Interdisciplinary Research," Occasional Paper No. 2, Syracuse, April, 1969.

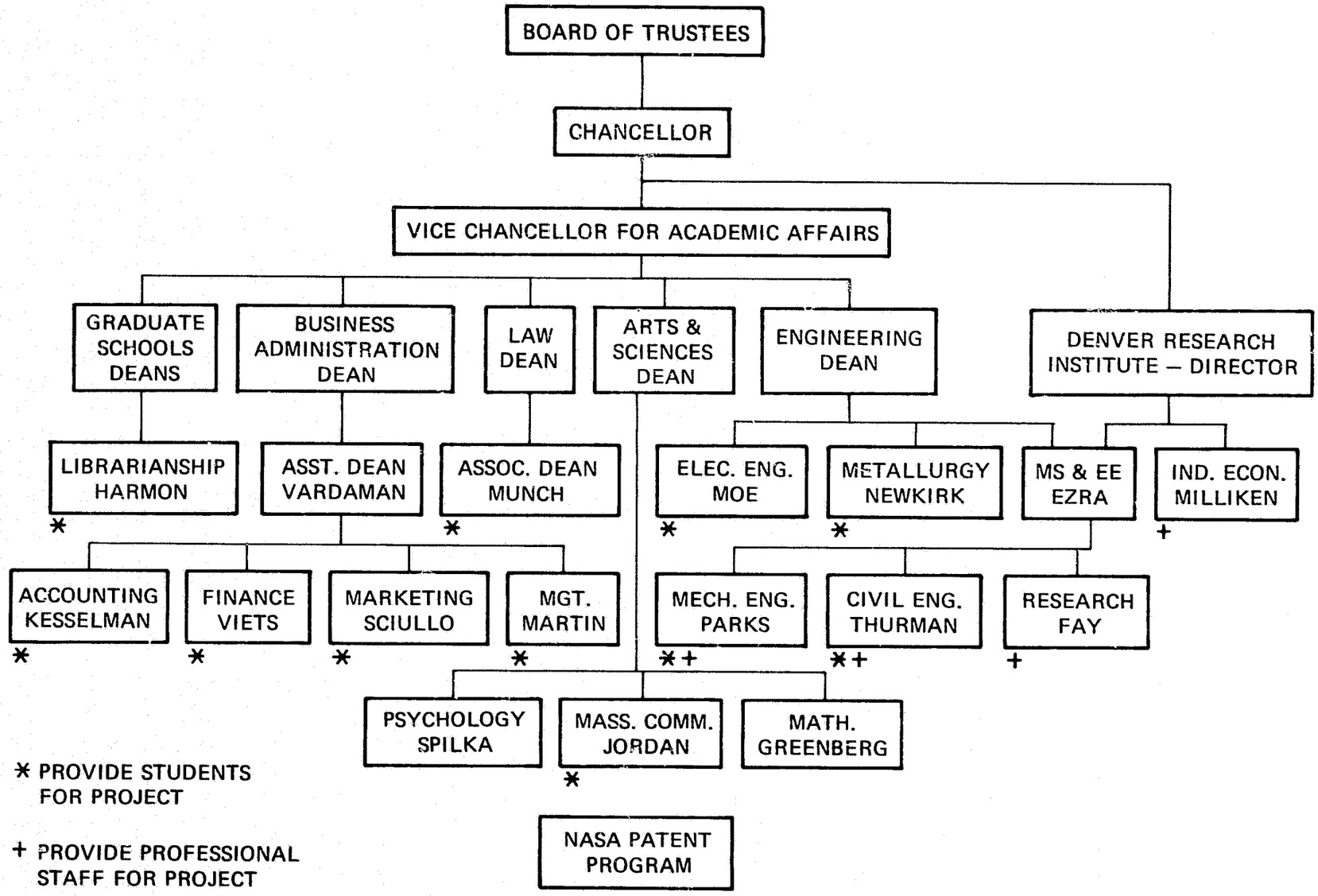

Figure 2.2. Program for Exploitation of Unused NASA Patents University Organization

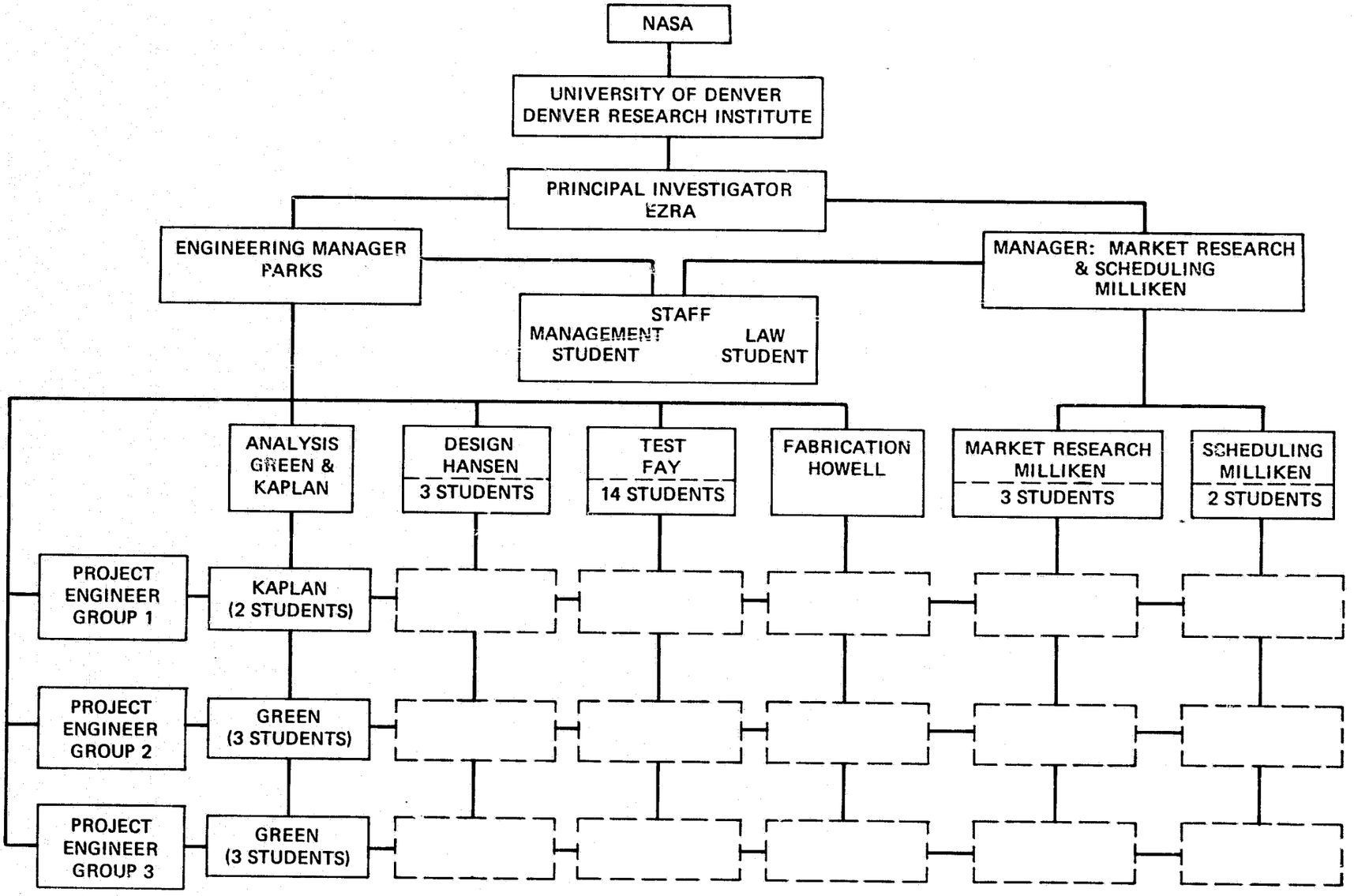

Figure 2.3. Program for Exploitation of Unused NASA Patents Program Organization

student in business administration participating in the project. The integration of the nonengineering activities has been the responsibility of Dr. G. Milliken of the Industrial Economics Division. The participation of the Law School was heaviest in the first semester when policies had to be made about the rights of students in new patents that may emerge from this program, and the legal status of overlapping patents such as the NASA owned patent No. 3,143,321 and Lockheed owned patent 3,236,333, and the question of how the University could benefit legally from the exploitation of unused patents in energy absorbing devices. The results of studies by a law student on the question of student rights and overlapping patents is presented in Appendix 1A & 1B. The last question does not have a completely satisfactory answer as yet; but studies of this question are continuing.

III. THE PROJECT MANAGEMENT CONTROL SYSTEM

A. Purpose and General Description of the System

There was a recognized need for all participants in the program to know and understand how their specific tasks integrate with the total program. A system of communications and control clearly was needed whereby all participants could organize and plan to meet the total objectives of the program. Such a system had to take into account that students and faculty are working on different tasks, at different times, and different places.

Specific purposes of the management control system were:

1. To show the individual tasks of each group/individual that were to be accomplished within the quarter.

2. To show to all members of the team and other interested parties the total interrelated functions and tasks of the total project.

3. To provide a basis of control, through budget and task force performance data so that program management can effectively evaluate the project results in light of the forecasted expectations.

4. To provide a means of communication among the team members as to expectations, problem areas, and results.

5. To provide a meaningful learning experience for the students. It was intended to give the students the responsibility to plan and evaluate their own work in respect to the tasks and due dates that they themselves have planned and established.

6. To provide a summary reference for evaluating past performance and for planning for future tasks.

The faculty-student group responsible for management control suggested and soon established a management information and control board to keep every member of the project informed as to the progress of each task and thus the progress of the total program. This board ultimately will display the work status of each of the task groups under

one of the major subject areas of the board. These subject areas are: production, staff functions, budget control, and an integrated schedule chart. It was the general purpose of the integrated chart to help each individual to plan, staff, control, organize, and provide adequate leadership for his specific task.

B. Development of Management Control System

The first objective of the management control group was to prepare task definitions for each group in the project. It was decided to have each group develop its own task definitions. The results were then consolidated into a general work schedule, using an interrelated network diagram (i.e., PERT). Several gaps and overlaps were immediately apparent, and it was evident that confusion existed in some quarters as to the functions of the technical support groups. Some groups (primarily the patent groups) thought that the design group would handle the designing of their models for fabrication, that the fabrication group would construct the models, and that the test group would handle all testing of the models. In contrast to these attitudes, the design group saw its objective as developing the design constraints made by the applications of the energy absorbing devices. Specifically, the design group planned to study those capabilities that an energy absorption device must possess in order to prevent deaths in automobile collisions. The fabrication group defined its objective as providing technical guidance to the patent groups in the machining of parts for the energy absorbing devices, and as the construction of a test rig for dynamic testing of the models. The test group was concerned with designing and constructing the test rig, as well as developing testing procedures. In short, there was inadequate recognition of the interrelationships of the research groups. Better work planning and communication were needed.

A second ramification of the network diagram was that very few people could easily understand it. Therefore, it was apparent that it would be an inefficient method of disseminating information to the rest of the project members.

During the break between fall and winter quarters, the management control group agreed to develop a new technique of representing the work flow, and to conduct a literature search for such a technique before making a final decision. A second item discussed during this meeting was that of providing more feedback to the rest of the members of the project. It was decided that a weekly newsletter which would be

distributed to all participants in the program would best serve this end. The subject of computerizing the PERT system was briefly discussed but tabled until more urgent tasks were completed.

During the Christmas holidays, there was some reorganizing of the different groups in the project. This reorganization was necessitated by the graduation of some of the participants, the expression from other students of a desire to move from one group to another, and the recruitment of new students into the project.

As a result of the reorganization, two students from the College of Business Administration were added to the management group. In addition to their duties of establishing marketing and budgeting systems, they also assisted in developing a reporting technique for monitoring the project.

The most important item of business at the beginning of the winter quarter (January, 1969) was to obtain new task definitions from each group. It was decided to confine these definitions to work anticipated to be performed during winter quarter only. The experience in the fall quarter had shown that accurate long-range planning was not possible in a R&D program of this type. Library research also was conducted in an attempt to find a better system for displaying work flow. The Vis-A-Plan technique was chosen as a result of the research. This system was designed under another NASA program and reported in NASA Tech Brief No. 67-10240.

The management information and control board includes an integrated schedule chart called Vis-A-Plan - a rectilinear method of charting which presents a PERT-type logic diagram of interrelated project activities in the form of a series of horizontal time bars. The length of the bars is proportional to lengths of time allocated for activities, and the bars are interconnected vertically to indicate necessary group interactions. Each bar is labeled to show responsibility for task completion. Dotted green bars show forecasts of activity, and solid purple bars show tasks completed. The Vis-A-Plan system was invented by a NASA contractor for use at Cape Kennedy. Its use on our project represents a transfer of technology from the space program, analogous to our anticipated transfer of NASA patent technology to use in some aspect of vehicle impact absorption.

The principal advantage of Vis-A-Plan is that it clearly shows both the time sequencing of activities and the interrelationships that exist between activities. A second advantage of this system is that

progress is easily monitored by the use of colored tape which can be attached directly to the Vis-A-Plan. Furthermore, changes in activity performance forecasts is easily shown, again through the use of colored tape. Yet another advantage of Vis-A-Plan is that it is compatible with computerized CPM or PERT systems.

Perhaps the most important aspect of Vis-A-Plan is that it was possible to schedule each group's activities independently of the other group activities without diminishing control of the entire project. The ability to separate group activities is the result of careful task definition. Figure 3.1 illustrates a portion of the Vis-A-Plan, reporting on the scheduling function of the Management Group.

Concurrently with the development of Vis-A-Plan, the Management Group designed a reporting form to be used by each group. This form (Figure 3.2) was to supplement the information of the Vis-A-Plan by providing a verbal description of the activities, and by noting any other information not readily shown on the Vis-A-Plan. At first, some project participants, when filling out the report form, would not bother to relate their report to the schedule that had already been developed by them. Consequently, their reports were inadequate in content, and frequently irrelevant. Therefore, the Management Group made copies of the Vis-A-Plan and requested that all information given on the report form also be shown on the copies of the Vis-A-Plan. This technique of combining Vis-A-Plan with the report form proved very effective in that it forced personnel to become familiar with Vis-A-Plan, helped them learn to plan their activities more carefully, and enhanced their awareness of the other project activities. The scheduling function of the management group was a difficult one for several reasons. Of main concern was the fact that the patent project has no history. In other words, all estimates of time, cost, manpower allocation, etc., must be made as guesses based on personal intuition. Therefore, when a schedule was first set up using these estimates, it was only reasonable to expect that schedules will not always be met. However, setting up a schedule was found to serve several valuable purposes. Most important of these is the examination which follows when schedules are not met, which promotes better understanding of project operations and focuses attention on needed improvements.

In an attempt to set up an organized system in which answers to these questions can be recorded and made available to all persons concerned with this project, a management information and control board was placed on a wall in the project headquarters. The control board

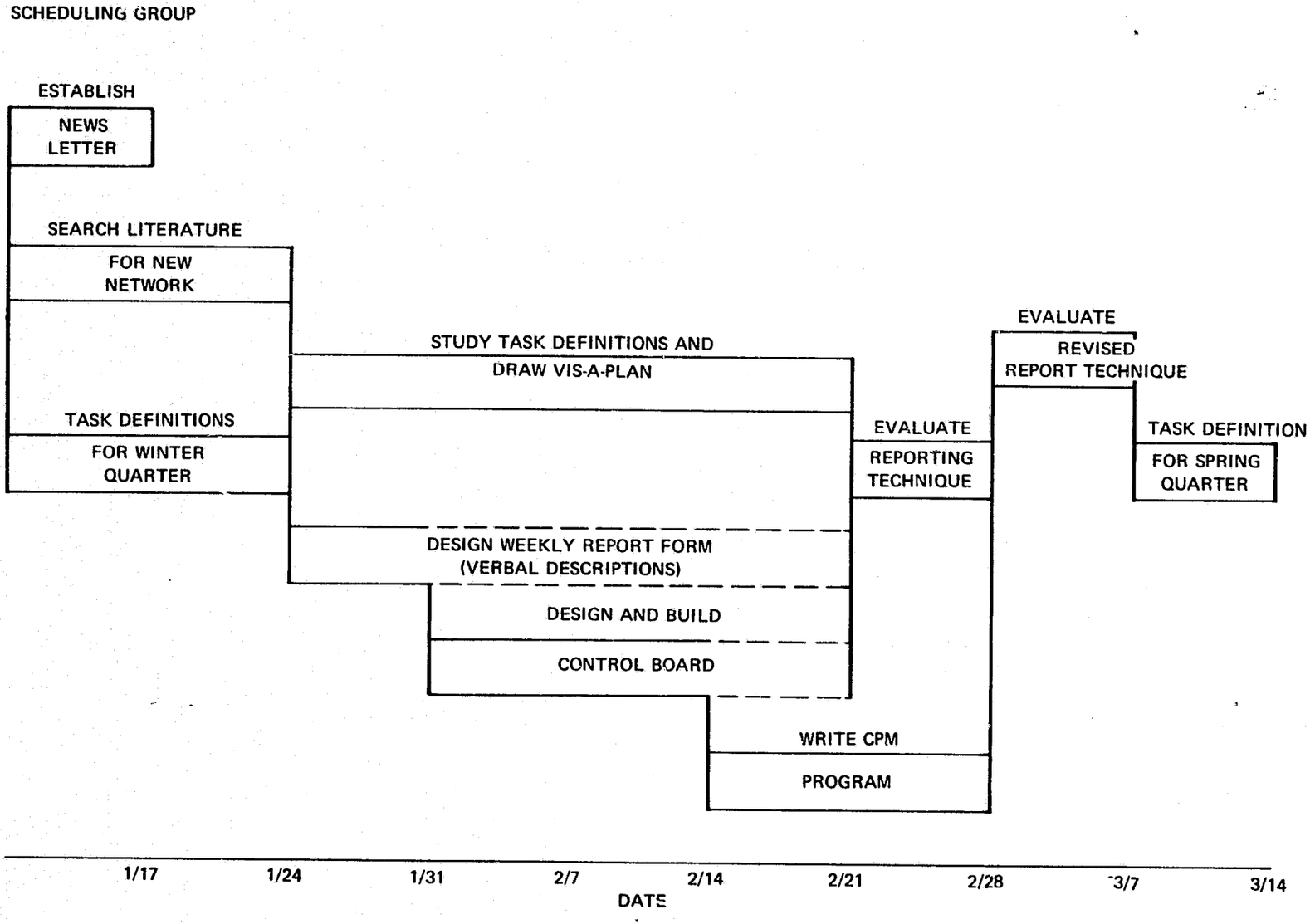

Figure 3.1. NASA Patent Development Project Work Flow-Winter Quarter 1969

contains status report sheets for each project group's major activities. Each report form was set up to identify the group supervisor, project function, and students with the group. Then, in tabular form, the following headings were given: Tasks - This column is to list each of the basic group activities for at least a three-month period; Due Date - This column is for the currently expected date of completion of the respective task. (In some cases this due date will not be the same as that date originally estimated); Completion Date - This column is for the actual date that the task was completed Comments - This column is for remarks concerning progress.

The operating procedures used to implement the management control system are shown in Exhibit 3.1.

Computer scheduling methods have not been used by the Management Group, and probably will not be. Due to the simplicity of each group's work flow, and to the success of the Vis-A-Plan, there is little need for utilizing a computer at this time. Furthermore, the scheduling group is sensitive to the risk of over-regimenting the project by imposing a demanding and rigid control system.

It must be emphasized that we were well aware that the use of such an elaborate control system to manage a research program could have a stifling effect on creativity, and every effort was made to avoid this pitfall. Nevertheless, the complexity of such an interdisciplinary research effort, composed entirely of part-time personnel made a management control system seem advisable.

C. Budget Report and Statement of Accounting Objectives

The budget is the key to financial order and organization and it supplements the overall management function of organization. The general purpose of a budget is to project the amount of funds to be spent on different tasks and on different total account areas such as equipment and salaries.

Considerable effort has been made to clarify and to report publicly the accounts and expenses comprising the budget for Project 4114. This required analyzing the DRI computer accounting system which has a cost reporting lag of almost one month (and for some accounts, two months). A need to revise the original project budget projections became evident, once interrelated task definitions were established.

STATUS AS OF: April 11, 1969

Group: Patent Group I

Students: T. W. Miller
L. V. Hychalk
E. Gruenberg
E. Fernholt

Supervisor: Prof. M. A. Kaplan

Project: Tube Collapse

TASKS	DUE DATE	COMPLETION DATE	COMMENTS
1. Design of tube for first test series.		2/4/69	Manufacture of tubing appeared to be very expensive. Thus, we were led to task # 2.
2. Investigation of commercial cylinders, e.g., beer cans, commercially available piping, and scraps in the shop, to see if any of these would be adequate.	2/18/69		
3. Static testing.			There has been some static testing of beer, soda, and coffee cans. The tests indicate the importance of initial conditions and end effects. Further testing will be done on commercial tubing.
4. Dynamic testing		4/4/69	
5. Receive tubing		3/28/69	
6. Static & dynamic testing of standard tubing.	5/16/69		
7. Receive rollers for pre-weakened sample	4/11/69	4/11/69	
8. Prepare pre-weakened samples	4/25/69		
9. Test (static & dynamic) pre-weakened samples	5/23/69		
10. Analyze all data	5/30/69		
11. Finish report on analysis of tube collapse.	6/6/69		

Figure 3.2. Example of Report Form

EXHIBIT 3.1

The following operating procedures have been established to implement the management control system.

1. During the first week of each quarter, each individual will list all the tasks that he plans to perform during the quarter, and the expected date when the particular task will be completed. This list will then be submitted to the individual's group supervisor. (Individual tasks can be combined into a group task just as long as initials are placed after the task to designate who is responsible for the task completion.) The supervisor will examine each task and due dates and make rearrangements as needed with the student. These task sheets will then be forwarded to the Management Group.

2. As each task is completed, the date completed and the appropriate comments will be reported to the supervisor. He in turn will forward this to the Management Group for posting on the management information and control chart.

3. It is the responsibility of each individual to report his current status to his supervisor, on a weekly basis.

4. As the quarter progresses, new necessary tasks may be identified. These will be reported in the following way:

   a. Delays: If the plan task will not be done on time then "postponed" or "delayed" should be posted in the "Comments" Column and the appropriate reason entered.

   b. Additional Tasks Discovered: A new task can be entered in its chronological sequence if there is room, or inserted at the bottom of the list and integrated with the previous tasks mentioned by revising task numbers.

5. Additional comments can be added on the reverse side of the form. If this is done, some sort of comment should be made on the front side to draw attention to the information on the reverse side.

6. Past task sheets will be kept by the Management Group for permanent reference. At the end of the quarter these task sheets can serve as a vital record for reference, review, critic, summation, and as a stepping stone for future planning.

7. It is the responsibility of all project participants to review the management information and control board weekly, and to identify possible inaccuracies and potential operating problems.

This was accomplished, and monthly budget reports are charted on the control board. The management group is now in the process of creating a reporting and budget system based on the project group organization. A monthly report, by group, of the expenses incurred will be instrumental in developing a cost accounting system. From such a system we hope ultimately to project what it would actually cost to manufacture the different patent devices.

IV. THE SELECTION OF THE TYPE OF PATENTS

Consultation and guidance were obtained from members of the National Inventors Council. Dr. Myron Coler, President of the Markite Corporation, New York, who is a member of the National Inventors Council, was extremely helpful in the selection process. He spent a day in Denver, at the beginning of the program, and discussed the selection process exhaustively. He advised that the consideration of a single patent in a given area would be quite inadequate for its successful exploitation. Based on his past experience he predicted that a block of related patents in a given area rather than a single patent would prove to have a market value. He also advised that the timeliness of a particular set of patents was an important factor in its successful exploitation. The current national awareness of highway safety needs would make patents on energy absorbing devices very timely. The possession by NASA of a number of patents on energy absorbing devices made it seem that we should concentrate on patents in this general technical area.

Another member of the National Inventors Council, Mr. Jack Rabinow, Vice President of Control Data Corporation, was consulted independently. His opinions confirmed those of Dr. Myron Coler.

It was therefore decided to concentrate on patents in the area of energy absorbing devices. With the assistance of Mr. Gayle Parker from the Office of the General Counsel of NASA, a search of the NASA owned patents was conducted. Eleven patents on energy absorbing devices were uncovered. They are the following:

Patent No.	Title	Ownership
3,127,157	Multiple Belleville Spring Assembly	NASA
3,143,321	Frangible Tube Energy Absorber	NASA
3,160,950	Method and Apparatus for Shock Protection	NASA
3,164,222	Nonreuseable Kinetic Energy Absorber	NASA
3,175,789	Landing Pad Assembly for Aerospace Vehicles	NASA
3,181,821	Spacecraft Safe Landing System	NASA
3,228,492	Double Acting Shock Absorber	NASA
3,236,066	Energy Absorption Device	NASA

Patent No.	Title	Ownership
3,330,549	Shock Absorber	NASA
3,337,004	Impact Energy Absorber	NASA
3,381,778	Energy Absorbing Device	NASA

A search in the patent office revealed the existence of 36 additional patents on energy absorbing devices.

At this point it became obvious that the first major barrier to the exploitation of NASA owned patents on energy absorbing devices was the large number of competing patents in this area. The scope of the program would have to change from our initial proposal which undertook to select "two or three of the most promising patents." It was not obvious which two or three of these patents were the most promising and a major part of our effort would have to be devoted to the screening process, within the constraints of the funds and time available.

V. THE SCREENING OF THE PATENTS

This has turned out to be the most difficult and time consuming part of this project, requiring not only detailed technical analyses but fabrication, test and detailed cost analyses. The wide variety of energy absorbing concepts and the wide range of possible applications complicated the screening process still further.

As a first step, each student participating in the research project was required to study two or three patents (there were 16 students and 46 patents) and to present a review of them in joint sessions of faculty, students and research staff. The total of 46 patents were found to fall into eighteen different categories. They are listed below:

PATENT CATEGORIES

Group 1 — Tube and Mandrel

3,143,321 - Frangible Tube Patent (basic) (NASA)

3,181,821 - Spacecraft Safe Landing System (NASA)

3,236,333 - Energy Absorber
Lockheed - Split and roll the tube

3,339,674 - Energy Absorbing Device
General Motors Tube & Mandrel - ductile material - Tube merely becomes a bigger tube.

3,381,778 - Energy Absorbing Device
NASA property - very much like Lockheed 3,236,333. Tube-mandrel split and roll the tube.

Group 2 — Bending Bars

2,835,348 - Retarder Device
Longitudinal displacement taken up in bending of two bars beyond elastic limit.

3,283,857 - Beam Energy Absorbing Device
Cyclic bending with rectilinear motion.
ARA Rube Goldberg mechanism

3,361,475 - Safety Belt with Shock Absorbing Device
Corrugated strip of ductile metal straightens out under impact load.

Group 3 Shear Pins

2,837,176 - Safety Device for Automobiles
Bumper mount. Contains pins which shear one after the other.

2,845,144 - Shear Pin Brake for Auto Bumper
Complex frame arrangement with shear pins to promote glancing blow. Also linkage to close valve in front brake lines.

Group 4 Folding Tube

2,870,871 - Shock Absorber
Folding Tube

3,240,676 - Nuclear Reactor Including Energy Dissipation Device for Falling Bodies
Straight tube preformed at one end, folding like an accordion.

Group 5 Rolling Mill

2,953,189 - Shock Absorber
Rolling mill - bar between rollers

Group 6 Machining Metal

2,961,204 - Deceleration Device
Metal machining with cutters as in key seater

Group 7 Hydraulic Cylinder

2,959,251 - Auxiliary Bumper Type Impact Absorber
Hydraulic cylinder

3,330,549 - Shock Absorber (NASA Patent)
Hydraulic shock absorber to function over wide range of impact loadings in space vehicle docking

Group 8 Belleville Spring Assembly

3,127,157 - Multiple Belleville Spring Assembly (NASA)

3,313,567 - Belleville Spring Biased Bumper
16 claims - dissipates some energy in tube friction.
Locks to avoid rebound.

Group 9 Friction Between Sheets

3,164,222 - Nonreusable Kinetic Energy Absorber
Wound sheets - friction mode of absorption (NASA)

Group 10 Extrusion

3,209,864 - Single Sheet Energy Dissipater
Extrudable material confined behind a piston. The piston has the extrusion hole in it.

3,380,557 - Variable Kinetic Energy Absorber
Various plastic materials forced by a piston to extrude through an orifice.

2,997,325 - Piston and Cylinder
Absorbs energy by extruding plastic material through apertures at end of cylinder.

Group 11 Pulling Strip Between Pins - Wires through Holes

3,211,260 - Energy Absorption Device
Pulls metal strip between pins (Same inventor as 3,366,353).

3,280,942 - Energy Absorber
To anchor airplane seats.
Wires absorb energy as they weave in and out through a series of holes in a metal strip.

3,308,908 - Energy Absorber
Two tubes with helical convolutions. Soft tube screwed into hard tube. Absorbs energy under tensile load by deformation of softer tube.

3,337,004 - Impact Energy Absorber (NASA)
Very low energy absorption. Soft aluminum tape. Plastically deformed when it is wound onto a spool. Is plastically deformed again and absorbs energy as it is unwound from spool.

3,366,353 - Energy Absorbing Device (Variation of 3,211,260)
Pulls metal strip between staggered pins.

3,372,773 - Load Limiter Device
"A plurality of wire strands are looped in and out of longitudinal apertures in platten." Pulling wires alternately bends them.

3,377,044 - Cargo Tie-Down Apparatus
Another application of pulling a metal strip between staggered pins as 3,211,260 and 3,366,353.

Group 12 Annealed, Stranded Cable

3,217,838 - Energy Absorbing Device
Annealing steel cable after stranding & means of anchoring cable.

3,353,768 - Energy Absorbing System
Extensible Cable System with ability to handle light impacts gently and heavier ones more firmly.

Group 13 Crushable Material Instead of Hydraulic Fluid in a Similar Configuration

3,228,492 - Double Acting Shock Absorber (NASA)
Crushable material instead of fluid in a double-acting cylinder. (Same inventor as 3,175,789)

3,175,789 - Landing Pad Assembly for Aerospace Vehicles (A Structure)
A system to take up misalignments and absorbers which are tube-mandrel combinations acting in tension. (NASA)

3,252,548 - Shock Absorber Cartridge
Cylindrical honeycomb to protect an airplane that gets tipped up on its tail during landing or take off.

3,339,673 - Volumetrically Expandable Energy Absorbing Material
Hexcel Corp.

2,966,200 - Shock Absorbent Fitting
Squash a lead or brass washer (Aircraft seats)

3,160,950 - Method of Apparatus for Shock Protection (NASA)
Shock protection of instruments by embedding in a material which can be sublimated.

Group 14 Torus Action

3,231,049 - Energy Absorbing Device
Aerospace Research Associates (See 3,360,080 and 3,360,081) Torus being twisted inside out - Deformation in torsion.

3,360,080 - Energy Absorbing Device
ARA One of the devices shown in 3,231,049.

3,360,081 - Energy Absorbing Device
ARA One of the devices shown in 3,231,049.

3,369,634 - Energy Absorbing Device
ARA Wire coiled into a helix between two tubes.

Group 15 Shearing Sheet Metal

3,232,383 - Energy Absorbing Means (Developed in Sweden)
Shearing of sheet metal.

3,289,792 - Apparatus for Absorption of Energy from a Moving Load
Virtually identical to 3,232,383 (from Sweden) Looks like a maneuver for legal reasons.

Group 16 Overload Relief in Drive Shaft

3,236,066 - Energy Absorption Device (NASA)
Really just an overload relief in a drive shaft.

Group 17 Rolling Tubes

3,301,351 - Energy Absorbing Device
Rolling tubes between plates with friction

Group 18 Knock-over Hydrant

3,331,397 - Resilient Bumper for Vehicles (Incorrect title)
This is a fire hydrant with a localized weakness in a flange resulting in a localized failure when struck by an auto.

Screening criteria had to be developed to narrow down the wide range of choices. The wide range of possible applications for energy absorbing devices also had to be narrowed down. Three relating to traffic safety alone provide a huge potential market, i.e., automobiles, protection for fixed highway obstacles, and seat belts.

The screening criteria were the following:

1. Mechanical efficiency, i.e., energy absorbed per unit weight of the device.
2. Ratio of total length of device to maximum stroke.
3. Reliability and repeatability.
4. Ability to withstand long term exposure to the weather.
5. Cost.

The requirements of reliability and repeatability, and the ability to withstand long term exposure to the weather, eliminated the entire category of devices which rely on friction alone. This is because the friction coefficient between two surfaces can vary over a wide range under different operating and environmental conditions, making it almost impossible to establish a consistent figure for energy absorption capability and mechanical efficiency.

With regard to mechanical efficiency or energy absorption capability, not only must the energy absorption be maximized, but the fullest use must be made of the material in the device. For any given situation there is a maximum allowable value for the deceleration, governed by what the human body will take, and hence a limiting value to the restraining force F. The total distance (or stroke) in which the moving vehicle may be brought to rest is also limited by the configuration of a particular situation. The energy absorption $= \int_0^{L_{max}} F\,dx$ is maximized when the integral is equal to $F_{max}\,L_{max}$, i.e., when the energy absorbing device exerts a constant force throughout its stroke. A

number of the inventors of energy absorbing devices (e.g., Patent Nos. 3,181,821; 3,381,778; 3,143,321) show a clear understanding of this principle in their patents. What most inventors appear unwilling to accept is that just about any device can, in principle, be engineered to give a constant force through the stroke, and that only those devices which give a constant force with the least manufacturing and material cost are the most cost effective, subject of course to the constraints of a given situation such as service life, reliability, resistance to exposure, etc.

The ratio of total length of device to maximum stroke is a very important factor, because every inch of decelerating length in a collision is valuable. Devices which have a stroke of half the total length or less are uneconomical. For example, the simplest extrusion device consists of a piston and cylinder combination as shown below in Figure 5.1.

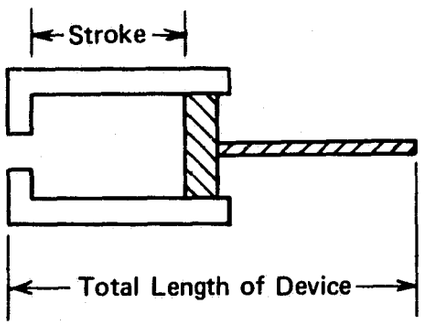

Figure 5.1. Extrusion Device

In this device the total length of the device is at least twice the stroke, and only a fraction of the material in the device absorbs energy - a large proportion of the material in such a device merely acts as a messenger - to deliver the energy to the absorbing portion.

A rolling toroid device, such as that shown in Figure 5.2, can have a total length of as much as three times the stroke, but no less than twice. In this type of device, toroids trapped between two concentric cylinders are turned inside out and absorb energy as the cylinders collapse.

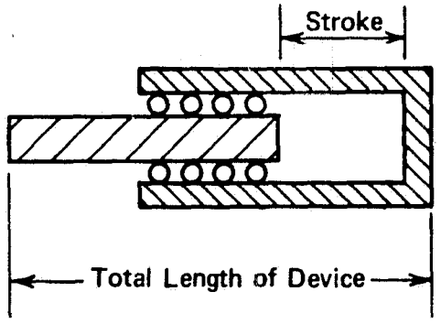

Figure 5.2. Rolling Toroids

For this type of device, an even larger proportion of the material in the device plays a secondary role and does not absorb energy.

In contrast, collapsing tube and tube and mandrel devices have a total length approximately equal to the stroke (see Figure 5.3). Hence for the same resisting force (which is limited by the deceleration a human body can take) and the same total length of device (governed by space limitations) a tube and mandrel or collapsing tube device shown in Figure 5.3, will absorb almost twice as much energy as the extrusion type of device shown in Figure 5.1, and from two to three times as much energy as a rolling torus device as shown in Figure 5.2. It is interesting to note that in spite of these fundamental considerations, the Department of Transportation funded a full scale crash evaluation of the rolling torus device and the New Mexico Highway Department bought and installed three of them.

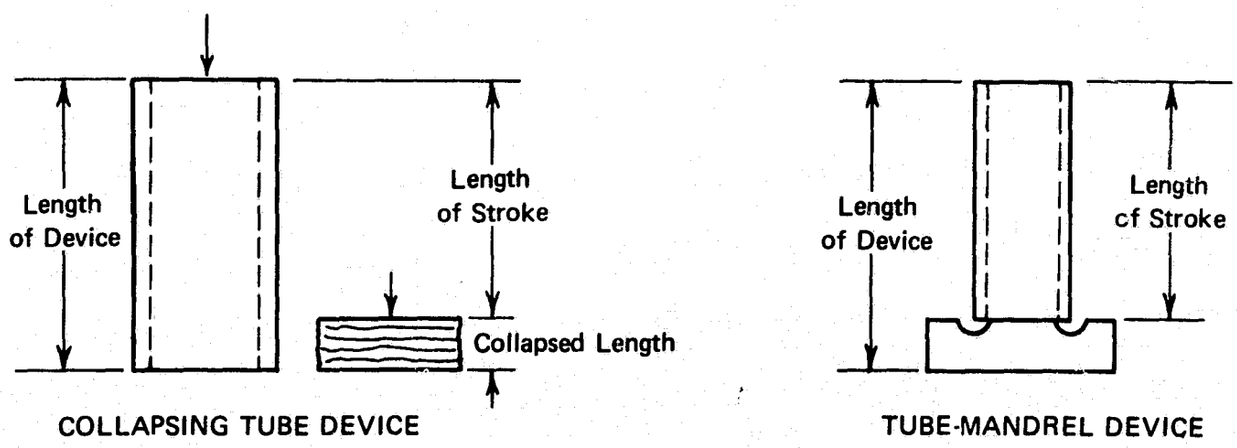

Figure 5.3. Collapsing Tube and Tube-Mandrel Devices

At the end of this screening process, the following patents remained under consideration:

Category	Patent No.
Tube and Mandrel	3,143,321 (NASA) 3,381,778 (NASA) 3,236,333
Cyclic Bending	3,211,260; 3,360,080 2,953,189; 3,369,634 3,301,351
Metal Tearing or Shearing	2,961,204 3,232,383 3,289,792
Collapsing Tube	2,870,871
Extrusion Devices	2,997,325 3,209,864 3,380,557

Detailed analyses were now conducted to provide estimates of energy absorption capability, i.e., mechanical efficiency, neglecting high strain rate effects as a first approximation. Along with these, static tests are being conducted in a standard testing machine while a high velocity tester has been built and calibrated. This has permitted the number of patents to be narrowed down still further and also provided data for the impact tests which would ensure that the impact tester would not deliver more energy than the device could absorb.

The patents still under consideration are the following:

Category	Patent No.
Tube and Mandrel	3,236,333; 3,143,321 (NASA) 3,338,778 (NASA)
Cyclic Bending	3,211,260
Metal Tearing or Shearing	3,232,383
Folding (Collapsing) Tube	2,870,871
Extrusion Device	3,380,557

All the analyses have not yet been completed. However, those that are sufficiently far along will not be presented.

VI. MATHEMATICAL MODELS

The first objective of a mathematical analysis was to provide a basis for comparing the mechanical efficiencies of the different energy absorbing devices which were not screened out on the basis of the other criteria described above.

The first stage was to conduct a static analysis of the different devices. Under static loading, a device will absorb less energy than under dynamic loading since practically no energy is required to accelerate the device. The use of results from static or slowly deforming conditions to predict energy absorption under dynamic or fast moving conditions will therefore be on the safe side, i.e., the device will absorb more energy under dynamic conditions than predicted. Furthermore, if all devices are analyzed on the same basis, a comparative evaluation can be expected to give valid results. Excluding the use of brittle material or material which is so strain rate sensitive that a decrease in ductility will occur at velocities below 60 miles per hour, one can expect static or slowly deforming conditions to give reliable comparative evaluations of energy absorbing capability.

The second stage consists of building and testing the devices under static conditions to verify the mathematical analysis and to ensure the validity of the comparative evaluation.

The third stage consists of testing 1/5 scale models of the devices under dynamic conditions simulating impacts at 60 miles per hour. This will provide performance criteria under crash situations. Where substantial deviations of performance from static predictions are found, more sophisticated mathematical models will be formulated.

These three stages have been running concurrently at the end of the first year, with different devices in different stages of analysis. The following mathematical models have been derived.

1. Cyclic Deformation of Toroids (Patent Nos. 3,231,049; 3,360,080; 3,360,081)

The general operating principle in this device is illustrated in Figure 5.2. Toroids trapped between a piston and a cylinder are turned inside out as the piston moves relative to the cylinder. This type of device has a length from two to three times the stroke, and depends on both tight tolerances and friction for it to work reliably.

Because of the widespread interest that has been shown in this type of device, an analysis was made of its energy absorbing capability and mechanical efficiency, as a means of comparing it with other devices, e. g., the tube and mandrel which has attracted just as much attention.

a. Analysis of Circumferential Stresses Developed in Cyclic Deformations of Toroids

The following derivation is based on the following assumptions.

i. Infinitely rigid cylinder and shaft

ii. Elastic perfectly plastic material

iii. No slipping between walls and torus

iv. Only nonzero deformations are circumferential.

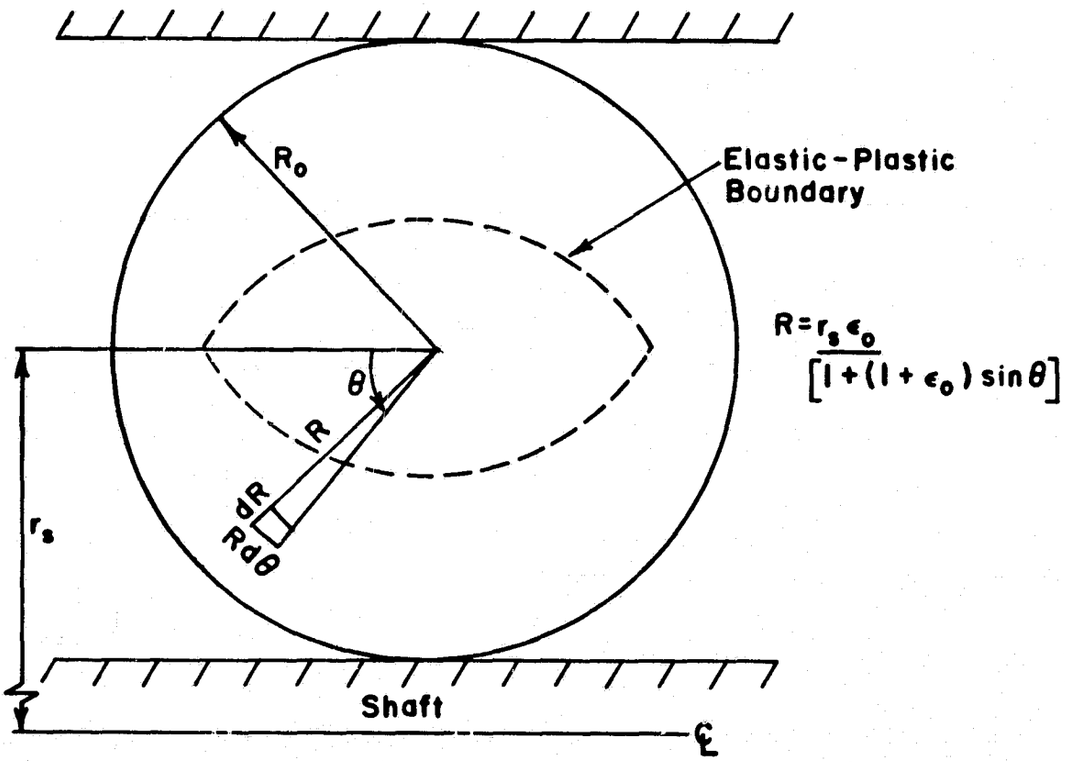

Figure 6. 1. 1. Deformation Analysis of Rolling Toroid

As Figure 6.1.1 indicates, the total strain undergone by a differential chord during one turn of the toroid is given by a ratio of the circumferences of the stretched and relaxed chords.

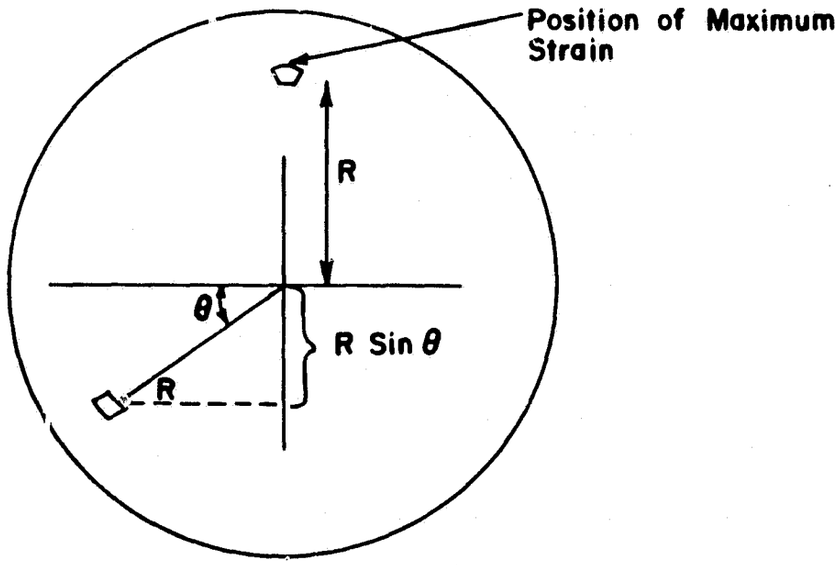

Figure 6.1.2. Strain Analysis

$$\text{Max strain} = \frac{2\pi(r_s + R) - 2\pi(r_s - R\sin\theta)}{2\pi(r_s - R\sin\theta)} = \frac{R + R\sin\theta}{r_s - R\sin\theta} \tag{6.1.1}$$

If the maximum strain (which is a function of R and θ) is less than ϵ_o, where ϵ_o = strain at yield point of the toroid material, then deformation remains within the elastic range and no energy is absorbed. Therefore:

$$R = \frac{r_s \epsilon_o}{[1 + (1 + \epsilon_o)\sin\theta]} \tag{6.1.2}$$

is a boundary condition for minimum plastic strain. Equation (6.1.2) is the polar equation for a hyperbola, and all material within the hyperbola is useless for circumferential energy absorption.

To make maximum use of the plastic portion of the stress strain law, the plastic region should include all points of the circumference. Thus,

$$R_o > r_s \epsilon_o \tag{6.1.3}$$

Furthermore, the torus must be such that the strain never exceeds the strain at rupture of the material designated by ϵ_{ult}. Thus,

$$\epsilon_{ult} > \frac{2R_o}{r_s - R_o}$$

and

$$R_o < \frac{r_s \epsilon_{ult}}{(2 + \epsilon_{ult})} \tag{6.1.4}$$

The ratio of R_o over r_s consequently should fall between these two extremes.

$$\epsilon_o < \frac{R_o}{r_s} < \frac{\epsilon_{ult}}{(2 + \epsilon_{ult})} \tag{6.1.5}$$

This then is a design criteria for the torus. For maximum efficiency this leads to a relation between R_o and r_s.

$$R_o = \frac{r_s \epsilon_{ult}}{(2 + \epsilon_{ult})} \tag{6.1.6}$$

We wish to calculate the amount of energy absorbed by a differential volume element of unit length. Consider the loading path of a typical element of material shown in Figure 6.1.3. During one cycle of the torus the energy absorbed is given by the area enclosed within the parallelogram.

$$\beta = \frac{R[1 - \sin\theta]}{r_s - R\sin\theta}$$

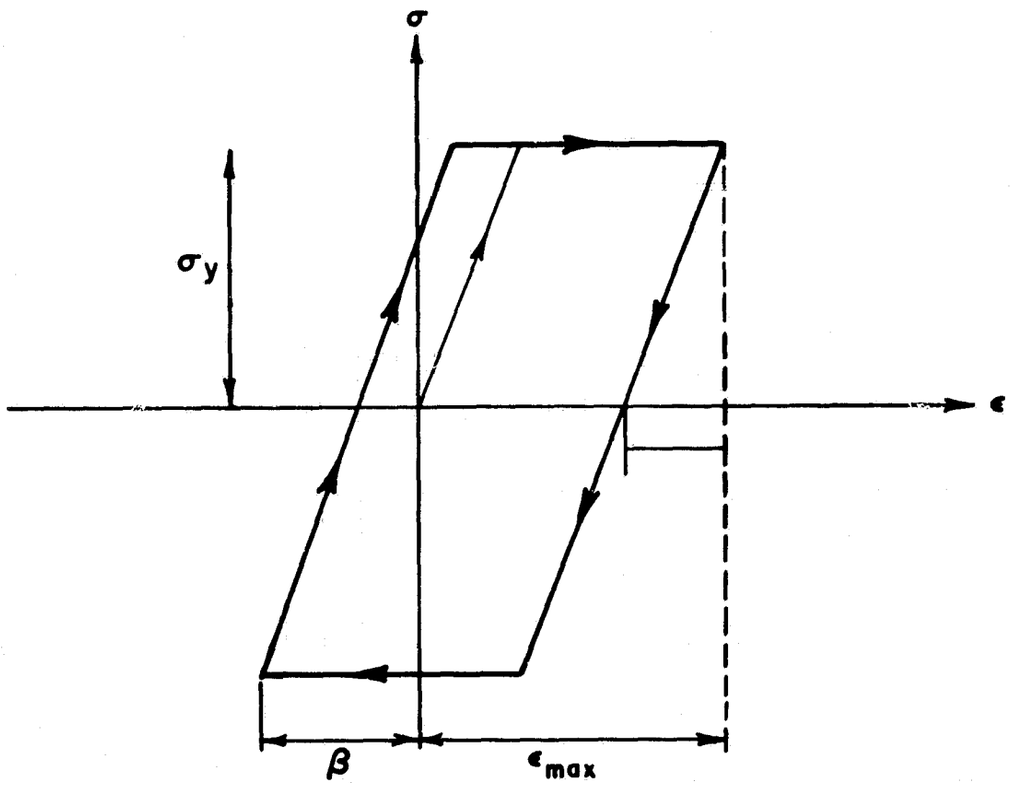

Figure 6.1.3. Loading Path of Material

Therefore

$$W = 2(\sigma_y) \quad [\epsilon_{max} + \beta - 2\epsilon_o]$$

$$W = 2(\sigma_y) \quad \left[\frac{2R}{r_s - R\sin\theta} - 2\epsilon_o\right] \qquad (6.1.7)$$

This has to be integrated over the volume of the torus. The integral for total energy absorbed in one revolution is given by

$$W_T = 4(\sigma_y) \int_0^{\pi} \int_{\epsilon_o r_s}^{R_o} \frac{W\,(r - R\sin\theta)\; 2\pi R\,dR\,d\theta}{[1+(1+\epsilon_o)\sin\theta]} \qquad (6.1.8)$$

The integration can be simplified by approximating the lower limit of R by the average value of R to the elastic-plastic value. This then is given by

$$a_o = \frac{3}{4} \epsilon_o r_s \tag{6.1.9}$$

Integration of equation (7) results in

$$W_T = (\sigma_y) \left\{ 8\pi \left(\frac{2\pi}{3} + \epsilon_o \right) \left[R_o^3 - \frac{27}{64} \epsilon_o^3 r_s^3 \right] - \frac{64}{3} \epsilon_o r_s \pi^2 \left(R_o^2 - \frac{9}{16} \epsilon_o^2 r_s^2 \right) \right\} \tag{6.1.10}$$

As the material approaches a rigid plastic material this equation becomes greatly simplified. As

$$\epsilon_o \rightarrow 0$$

$$W_T = \frac{16}{3} \pi^2 R_o^3 (\sigma_y) \tag{6.1.11}$$

Note that for this type of behavior the dependence on r_s drops out.

Consider now how the toroids function in the device. If the overall length of the device is ℓ, only a fraction of the length will be filled with toroids. A reasonable figure would be $\ell/3$. Each torus would go through $(\ell/6\pi R_o)$ cycles. If the toroids are spaced evenly at one diameter intervals, then the number of toroids is given by $\ell/2R_o$. The total energy available would then be

$$T = W_T \frac{\ell^2}{12\pi R_o^2} \tag{6.1.12}$$

For a rigid-plastic material this gives

$$T = \frac{4}{9} \pi R_o \ell^2 (\sigma_y) \tag{6.1.13}$$

It is desired now to compare a specific device to an aluminum tube and mandrel device of nearly the same overall dimensions. The

tube and mandrel device to be compared has a length of 7.5 inches and a diameter of .75 inch. The wall thickness is .065 inch. Consequently we take

$$r_s = 0.7$$

Using equation 6.1.6 with $\epsilon_{ult} = .2$

$$R_o = .07$$

A rigid-plastic material is assumed with

$$\sigma_y = 20,000 \text{ psi}$$

then

$$T = 12,200 \text{ in-lb}$$

The force exerted is given by

$$F = T\left(\frac{3}{\ell}\right) = 4980 \text{ lb.}$$

	Tube and Mandrel	Rolling Torus
Energy absorbed	15,000 in-lb	12,200 in-lb
Force applied	2,000 lb	4,980 lb
Energy per pound	31,000 ft-lb/lb	10,000 ft-lb/lb

As seen from the table, the toroid device gives much less energy absorption per pound. Furthermore, the figure is based on the weight of the toroids alone. If the encasing tubes were included also the figure would be even lower. Note also that over twice the load is required to move the device which would result in high and unfavorable "g" loads in a real application.

b. Conclusions

i. Length to Stroke Ratio

An important criteria for an energy absorbing device is that as much as possible of the overall length should be available for energy absorption. An efficient device would be one where the length to stroke

ratio is near one. Such a device is the tube and mandrel device. Other devices such as the cyclic bending of a wire may have a ratio very much less than one. The device analyzed here, however, comes out very poorly. The minimum ratio possible would be two. For a working device, however, the ratio would be around 3. Such a high ratio would in itself be enough to rule out the device for most purposes.

ii. Energy Absorption Capacity

As seen by the analysis the torus itself gives low energy absorption per pound as compared to the tube and mandrel. In addition, the device as a whole makes no real use of the two sliding tubes. Thus material is carried along for the ride and a loss in efficiency results. Also the center portion of the toroid is useless for energy absorption.

c. Cost of Manufacture

Compared to some other devices (tube and mandrel, collapsing cylinder) this is a complicated device. Obviously, manufacture of a torus would be a costly operation although use of a wound wire would help considerably in this respect. In order to insure rolling of the toroids, close tolerances are necessary which again would add to the cost. A detailed cost analysis is unnecessary unless it is decided to pursue the patent further.

d. Reliability

To work well there must be little slippage between the tubes and the toroids. Thus close tolerances are required so that rolling action is optimized. Rain, temperature changes and other factors could reduce the reliability.

e. Omnidirectional Capability

Since this device has to be struck directly on end to operate effectively, complex support systems might be necessary for actual installation.

Recommendation

Discard this type of patent.

2. Tube and Mandrel Devices (Patent Nos. 3,143,321 (NASA); 3,338,778 (NASA); 3,236,333 (Lockheed))

The basic principle underlying the tube and mandrel devices is shown in Figure 5.3. A hollow cylinder is forced down over a mandrel which causes the metal to expand, split and curve. This basic concept was patented by McGehee (No. 3,143,321) and the patent is NASA owned. Its efficiency has been investigated by NASA[1] and the results show that 31,000 ft-lbs of energy per lb of tube material can be obtained, using 2024-T3 aluminum. This is comparable to the energy absorption capabilities of balsa wood crushed parallel to the grain. The above reference (TN D-1477) shows that by tapering or pre-splitting the ends, a constant force-displacement curve can be obtained. To be comparable to other devices, the weight of the mandrel should have been included. This device has already been investigated by NASA, although all the information necessary to incorporate this device into a system is not yet available. For example, all the criteria necessary to proportion the hollow tube so as to avoid generalized buckling under impact, or local buckling is not available. These investigations have been deferred until it can be established that this type of device has the maximum efficiency, using established values from previous NASA reports for comparison.

This device not only absorbs energy by splitting the tube material, but also by friction between the tube and mandrel, as well as by bending of the split material. Patent No. 3,338,778 (NASA owned) adds one more mode of energy absorption i.e., metal cutting by placing cutters in the mandrel. Patent No. 3,236,333 (Lockheed owned) maximizes the energy absorbed in the bending mode by shaping the mandrel so that the split strips are bent over into several turns. The energy absorption capability of the basic tube and mandrel is compared with some other typical energy absorbing devices in Figure 6.2.1. The comparative figures on energy absorbing capability in Figure 6.2.1 are taken from Ref. 2.

Up to the present time the tube and mandrel devices appear to have the highest mechanical efficiency. We still have to prove they are also the most cost effective.

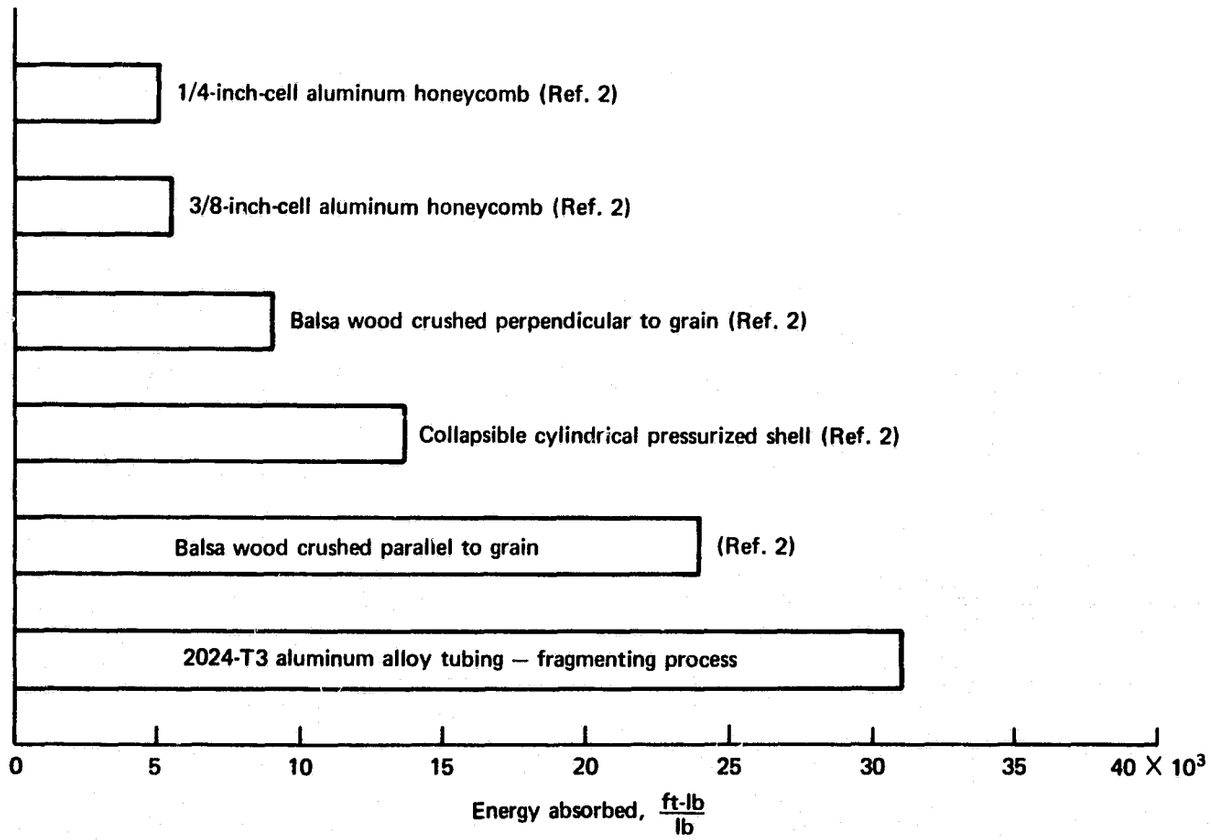

Figure 6.2.1. Comparison of Basic Tube and Mandrel Energy Absorption Capability With Some Other Methods

3. Tube Collapse (Patent No. 2,870,871)

a. Introduction

This device was selected for study because it offers a simple means of producing large plastic deformations and therefore has potential for high energy absorption at relatively low cost.

The mechanism of deformation is the formation and growth of local folds. The number and size of the folds depends on the dimensions of the tube and the strength of the tube material. In the patent, the inventor weakened the tube in several places to encourage folding action. Since this increases the cost of the device and disguises, to some extent, the natural folding process, it was decided to examine unweakened tubing initially. This report, therefore, contains our work on the collapse of standard commercial tubing. Pre-weakened tubing will be examined later in the program.

b. Analysis

The application of large axial loads to metal tubes produces local instability. A short section of tube, generally near either end, begins to buckle plastically by forming a fold (Figure 6.3.1).

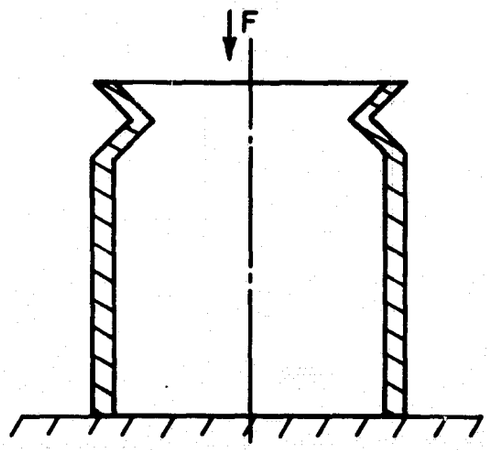

Figure 6.3.1. Collapsing Tube

The cross section of the fold is circular for thick wall tubes.* Thin wall tubes form folds which are n sided regular polygons in cross section, n increasing with decreasing wall thickness. The collapse of the tube section continues until the folds are nearly flat. Then folding is initiated in an adjacent section of the tube. The process of local collapse continues until the entire tube has been folded. This description of the essential geometrical features of tube collapse stems from our experimental observations of both static and dynamic instability. Other experimenters[3, 4, 5, 6, 7] have noted similar behavior.

The analytical situation is, as with most energy absorbing devices, rather complex. The nature of the geometry during folding and the large deformations induced present the major difficulties. The theoretical work which has been done has therefore been limited to specific aspects of the problem. Although no force-displacement relations have been developed, Pugsley[3] develops an expression for the average collapse load of a thin walled cylinder while Alexander[4] examines the average force necessary to collapse a thick walled cylinder.

Pugsley uses the collapse moment** for a thin beam in the determination of the work done in bending the folds, while Alexander modifies this expression somewhat in an attempt to account for the cylinder being an extremely wide beam. Many of the assumptions of thin beam theory, e.g., uniaxial state of stress and free lateral deflection, are inadmissable for the present problem. It is not surprising, therefore, that the error in Pugsley's results is of the order of 100 percent. Alexander's theory appears to give more satisfactory results for both thick and thin walled cylinders. The equation Alexander derives for the average collapse load F is

$$F = 6\,\sigma_y t\sqrt{tD} \qquad (6.3.1)$$

---

* "Thick Walled Cylinder" will be used to denote any tube which collapses by the formation of circular folds. Similarly, any tube which forms polygonal folds will be called a "Thin Walled Cylinder." For the purposes of stress analysis, the tubes we deal with can be treated as cylindrical shells.

** The collapse moment is the bending moment at which the entire cross section of the beam becomes plastic.

where σ_y is the yield strength of the material, t the wall thickness, and D the mean diameter of the tube. The initial height h of each fold is estimated by Alexander to be

$$h = 1.9\sqrt{tD} \qquad (6.3.2)$$

The final height after folding is approximately h - 2t (Figure 6.3.2)

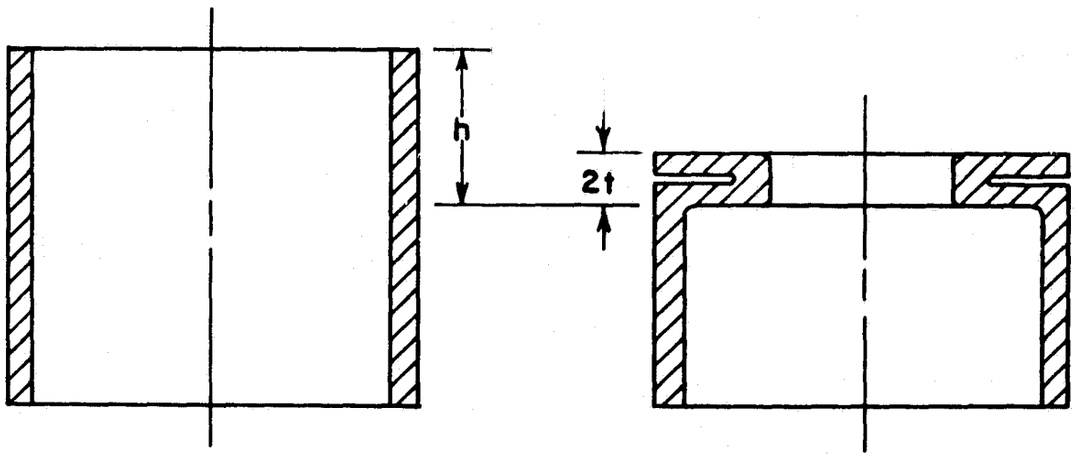

Figure 6.3.2. Local Folds in Collapsing Tube

The energy W absorbed by one fold is therefore F(h - 2t). The weight of a folding section is $\pi\rho hDt$ where ρ is the weight density of the material. Therefore the energy U absorbed per unit pound of deformed material is

$$U = \frac{F(h - 2t)}{\pi\rho hDt} \qquad (6.3.3)$$

The use of (6.3.1) and (6.3.2) in (6.3.3) gives

$$U = \frac{\sigma_y}{\rho D}\left(1.9\sqrt{Dt} - 2t\right) \qquad (6.3.4)$$

after some simplification. The use of a high-strength low density material obviously increases the efficiency of energy absorption.

For practical applications it is important to minimize U under the condition that F remains constant. Constancy of the axial force implies, for a specific material, that

$$t\sqrt{tD} = \frac{F}{6\,\sigma_y} = K = \text{constant} \qquad (6.3.5)$$

when (6.3.1) is noted. Solving for D we obtain

$$D = \frac{K^2}{t^3} \qquad (6.3.6)$$

and therefore (6.3.4) can be written as

$$U = \frac{\sigma_y}{\rho K^2}\,(1.9\,Kt^2 - 2t^4) \qquad (6.3.7)$$

To obtain the condition for maximum U under constant axial load we differentiate (6.3.7) with respect to t and equate to zero. The result is

$$t(3.8K - 8t^2) = 0 \qquad (6.3.8)$$

The two solutions of (6.3.8) are t = 0, which gives a minimum value of U, i.e., U = 0, and

$$t = 0.69\,K^{\frac{1}{2}} \qquad (6.3.9)$$

which is readily shown to maximize U. This value for t gives a ratio of t/D of 0.226, a value which is far too high for the collapse analysis to be valid. However, it does provide an indication that higher values of t/D increase the efficiency of energy absorption. We will provide some experimental verification of this result in the following section.

In dimensioning a tube for a particular application care must be taken that the collapse load in folding is less that the Euler critical load (failure by column instability). The Euler critical load $\underline{P}$ is a minimum when the end conditions are hinged-hinged. For this case

$$\underline{P} = \pi^2\,\frac{EI}{L^2} \qquad (6.3.10)$$

where E is Young's Modulus, L is the length of the tube, and the moment of inertia I of the cross section is approximately

$$I = \frac{\pi}{8} t D^3 \qquad (6.3.11)$$

when t/D is << 1. Since the collapse load is folding F < P, we obtain

$$\left(\frac{L}{D}\right)^2 \left(\frac{t}{D}\right)^{\frac{1}{2}} < 0.65 \frac{E}{\sigma_y} \qquad (6.3.12)$$

as the condition for proper functioning of the device.

To obtain an estimate of the restrictiveness of (6.3.12), consider an aluminum tube with a yield strength of 20,000 psi. Since $E = 10 \times 10^6$ for aluminum, we have

$$\left(\frac{L}{D}\right)^2 \left(\frac{t}{D}\right)^{\frac{1}{2}} < 325 \qquad (6.3.13)$$

from (6.3.12). We expect t/D to be << 0.1. Thus, (6.3.13) can be written

$$\frac{L}{D} < 32 \qquad (6.3.14)$$

when

$$\frac{t}{D} < 0.1 \qquad (6.3.15)$$

The acceptable L/D ratio of 32, under the condition (6.3.15), is quite high. A 16 feet length of 6 inches diameter tubing, for example, would still collapse by folding rather than by column instability.

As a sample design problem let us consider the use of aluminum tubing in an energy absorbing system to protect vehicles from impacting a highway obstacle. We will design for a head-on impact of a 4500 lb car moving at 60 mph, under the constraint that the car deceleration not exceed 20 g's. The stopping distance of the car must therefore be greater than 5-1/2 feet. The total force necessary to decelerate the car at 20 g's is 90,000 lbs, and if we distribute this

over four tubes, each tube must collapse at 22,500 lbs. If 6 inch diameter tubing is used the wall thickness, according to (6.3.3), must be

$$t = \left[\frac{22,500}{6(20,000)\sqrt{6}}\right]^{\frac{2}{3}} = 0.18 \text{ inch}$$

The height of each fold, from (6.3.2), is about 2 inches initially. This will collapse 1.6 inches, so that there will be an 80% reduction in length when the tube is completely folded. If 5.5 feet of stopping distance is to be provided, the original length of the tube must be 6.85 feet. The weight of this length tube is 27.4 lbs. It absorbs 124,000 ft. lb of energy, and therefore

$$U = 4550 \text{ ft-lb/lb}$$

where U is the energy absorbed per pound of device.

c. Experimental Verification

Testing was begun using seamless 3 inch diameter aluminum tubing with wall thicknesses of 0.022 inch and 0.069 inch. The tube material was 3003-H14, chosen because it is virtually nonwork hardening (tensile yield = 20,000 psi; tensile ultimate = 22,000 psi) and is fairly ductile (% elongation = 10). The use of a perfectly plastic material is an aid in proper interpretation of test results, since it insures the constancy of relevant material properties as the tube collapses. Variations in axial load during folding can then be entirely attributed to changes in geometry.

Although the uses of the collapsing tube for energy absorption all involve dynamic load application, testing has included static as well as dynamic loading. Static testing is valuable since it indicates the force level to be expected dynamically (often more reliably than analysis) and enables one to closely follow the details of the deformation process.

Static Testing

i. Thin Walled Tube (t = 0.022)

The static force-displacement curve for the first 1.25 inch of collapse is shown in Figure 6.3.3. Preceding the collapse of the tube there is an initial spike of 1,800 lbs. Once folding begins, the axial

load becomes nearly periodic, varying in magnitude from about 550 lbs to 1050 lbs. The amplitude of the oscillation is 250 lbs. or 31% of the average force of 800 lbs. Each cycle corresponds to the folding of a single section of the tube. A portion of the folding process is shown in the sequence of pictures in Figure 6.3.4. The tube is folding downward from (i) → (iv) such that the cross section of each fold is a square. Each set of folds is rotated 45° from the adjoining set. In (i) the large fold A has been collapsed so that it is nearly flat. Displaced 45° and slightly below it, a new fold B is beginning to form. In (ii) fold A has been flattened as the second fold B becomes well developed. Another fold C, 90° from the second fold, can also be seen forming. In (iii) folds B and C have developed further, flattening and extending internally until their boundaries have intersected. This intersection forms the boundary for a new fold D, which is forming directly under the original fold A. In (iv) B has been flattened and D is now well formed.

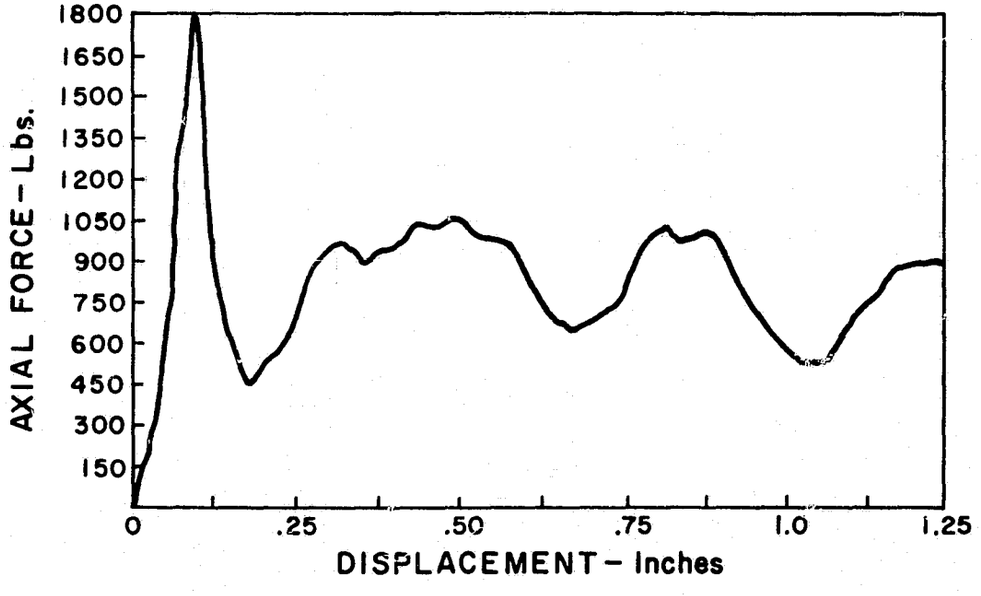

Figure 6.3.3. Static Force-Displacement Curve

The formation and eventual flattening of an individual fold is essentially a bending and shearing process about the edges of the fold. In bending, the edges act as plastic hinges, as indicated in Figure 6.3.5, where a vertical cross section through a fold is shown. As the fold flattens, the moment arm increases and the vertical force needed to

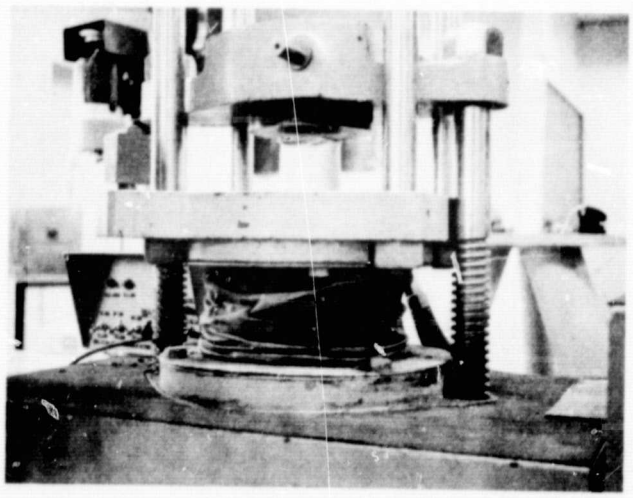

i

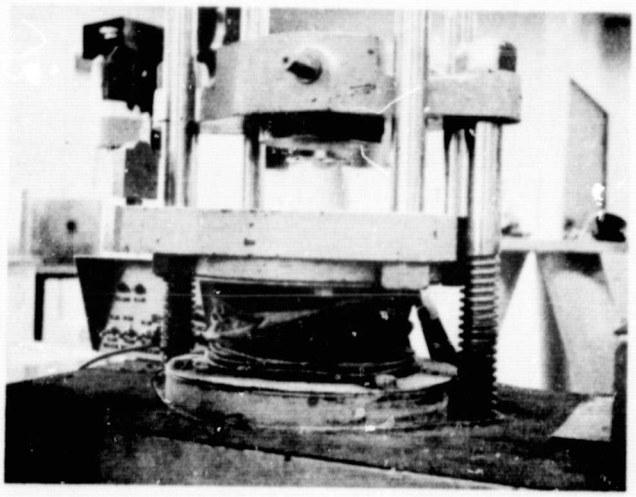

ii

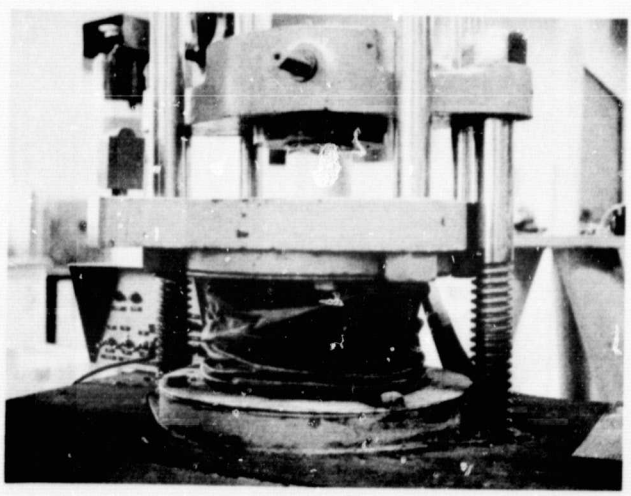

iii

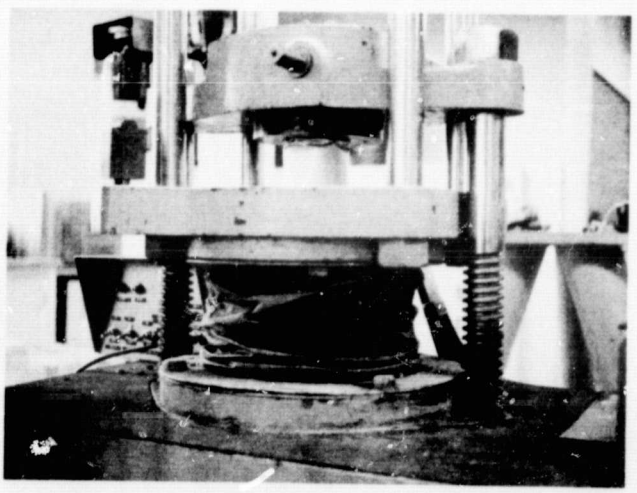

iv

Figure 6.3.4. Collapsing Tube Tests

produce continued yielding at the hinges decreases. This explanation of the folding process is highly simplified since it does not account for the increase in the width of the fold during flattening. However, the rough qualitative picture it provides is of value in explaining the initial peak as well as the periodicity of the axial load. At the onset of loading the tube is essentially straight, and the bending stresses are nearly zero. A bending moment sufficient to initiate plastic instability is not attained until elastic buckling produces lateral motion in the sides of the tube. The elastic buckling load corresponds to the initial peak load in the force-displacement curve. If this description is substantially correct, then an initial end moment on the tube should decrease the height of the spike. As a simple experiment we crimped the end of a tube, as shown in Figure 6.3.6, to provide initial end moment. This procedure reduced the magnitude of the spike from 1800 lbs to 1400 lbs. Additional verification was obtained by unloading a partially folded tube completely and then reloading. The reloading produced no initial spike. The specimens merely continued to fold at the force level at which unloading occurred.

Equation (6.3.1) predicts the average collapse load to be

$$F = 6(20,000)(.022)\sqrt{3(.022)} = 675 \text{ lbs}$$

Although (6.3.1) was derived for thick walled tubes (circular cross sections after buckling) and the tube under consideration is thin walled (polygonal cross sections after buckling), the average collapse load computed above is in reasonably good agreement with the measured mean collapse load of 800 lbs.

ii. Thick Walled Tube (t = 0.069 inch)

The folding cross sections are circular for this case, as can be seen in Figure 6.3.7, a photograph of a partially folded tube. A typical force-displacement curve is shown in Figure (6.3.8). The initial spike of 12,000 lbs is followed by an oscillatory force whose magnitude varies from about 4400 lbs minimum to 7000 lbs maximum on the average. The mean value of the collapse load is 57,000 lbs. The magnitude of the oscillation is 1300 lbs or approximately 23% of the average force.

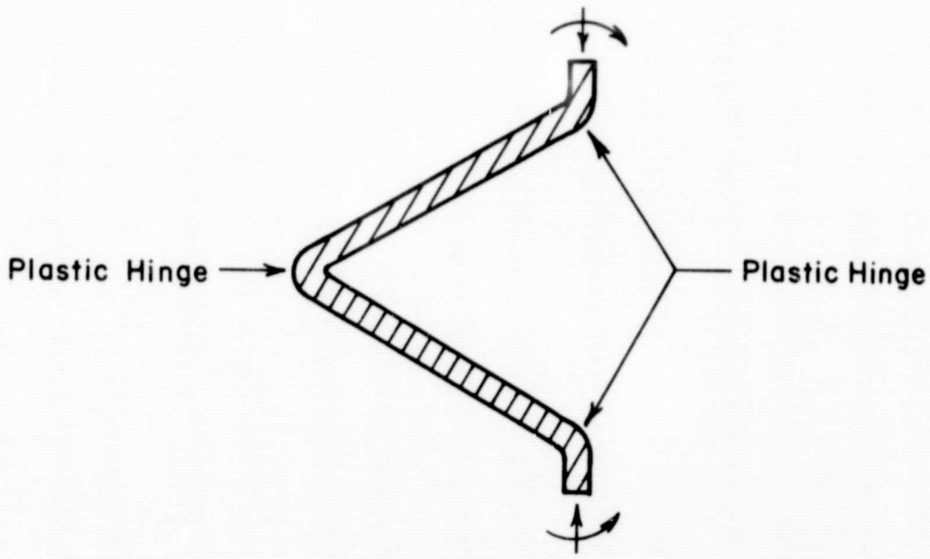

Figure 6.3.5. Free Body of Tube Fold

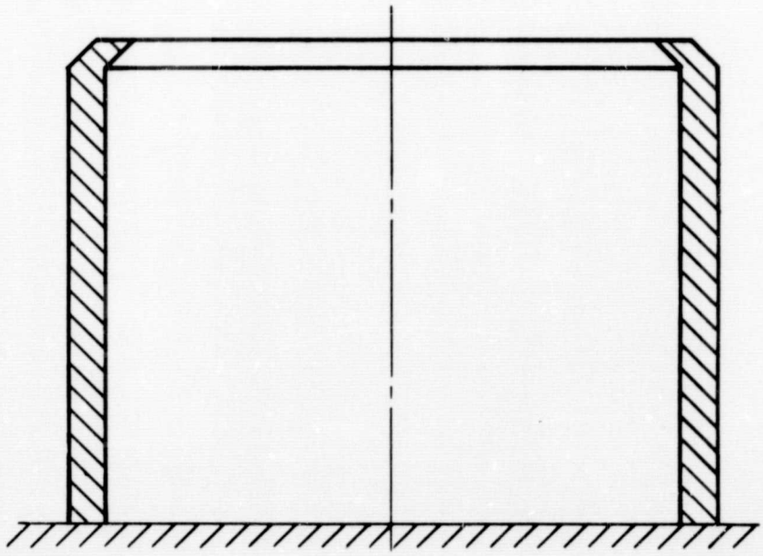

Figure 6.3.6. End Modification of Collapsing Tube

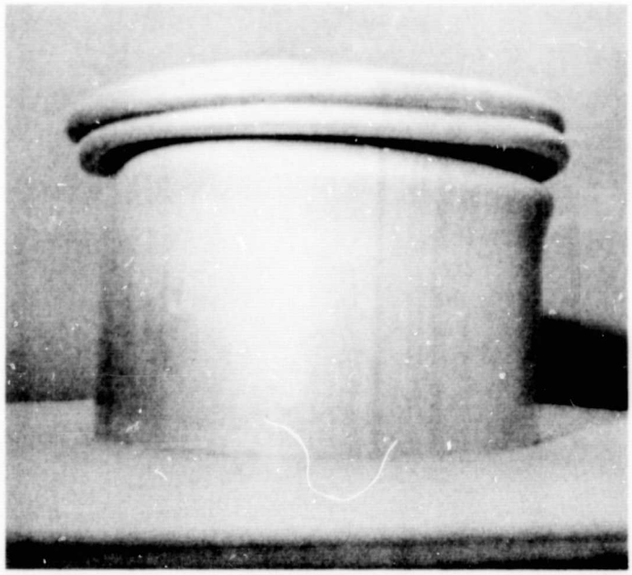

Figure 6.3.7. Partially Folded Thick Walled Tube

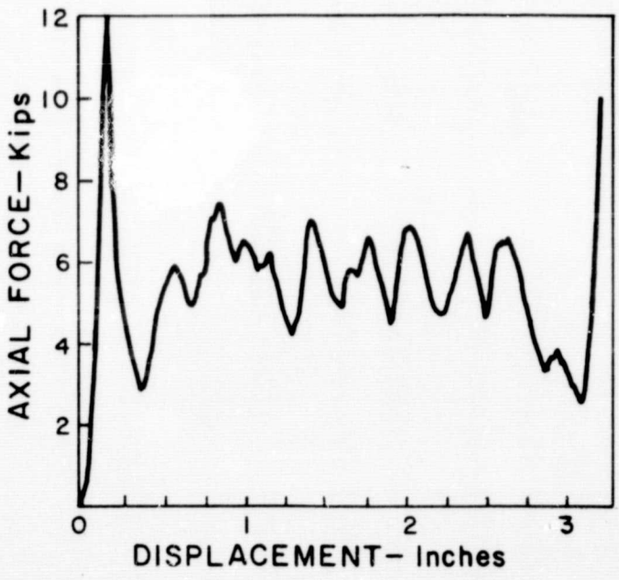

Figure 6.3.8. Force-Displacement Curve for Thick Walled Collapsing Tube

The use of (6.3.1) to predict the average collapse load gives

$$F = 6(20,000)(.069)\sqrt{3(.069)} = 3800 \text{ lbs}$$

which is considerably in error.

iii. Dynamic Testing

At present, only the thin walled tubing has been tested dynamically. The forces necessary to collapse the thick walled tube are beyond the design capability of the dynamic tester. The dynamic force-displacement curve is obtainable from the accelerometer trace shown in Figure 6.3.9. The accelerometer was mounted on the side of the 36.8 lb driving block. Its output, therefore, is directly proportional to the axial load acting on the tube. The vertical force scale in Figure 6.3.9 is approximately 400 lbs/centimeter while the time scale is 5 milliseconds/centimeter.

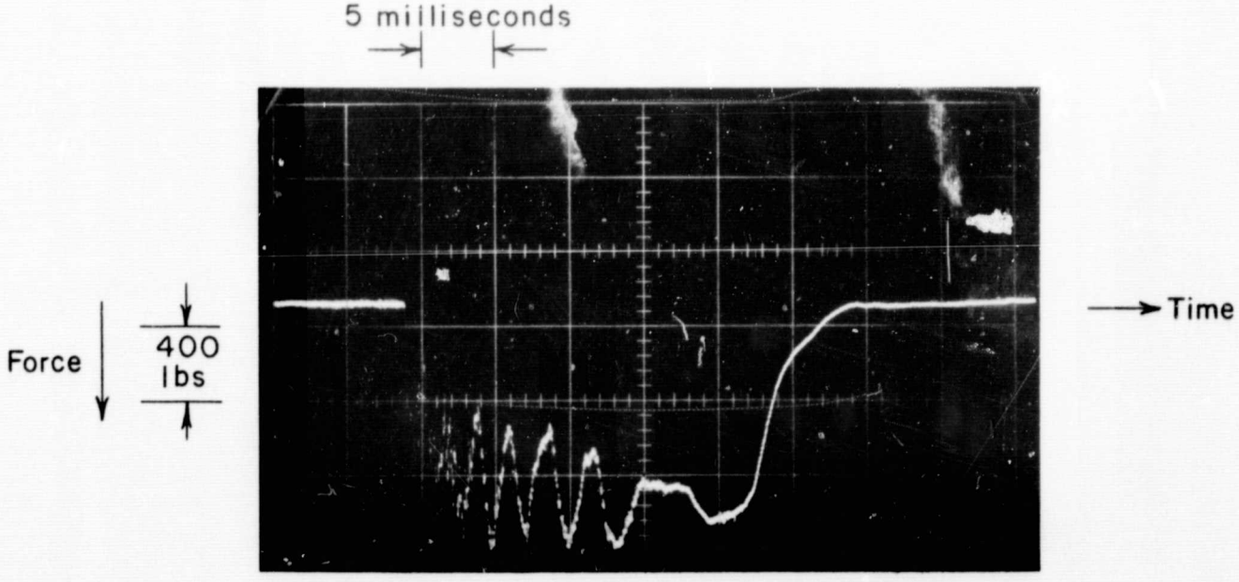

Figure 6.3.9. Force-Time Curve for Dynamic Test of Thin Walled Collapsing Tube

Prior to impact the driving block is moving at 23 fps. At impact (1.8 msec from the left side of the trace) a spike is generated. The magnitude of the spike cannot be determined from Figure 6.3.9 since it went off scale, but traces of other runs indicate that the initial force reaches 3600 lbs. Following the spike the load oscillates between 1300 and 700 lbs on the average. The mean dynamic load is 1000 lbs or 200 lbs greater than the average static collapse load. The collapse mode is identical to the static mode, i.e., the cross sections of the tube fold into squares. The increase in collapse load under dynamic loading is to be expected, since the axial load must now accelerate the tube downward in addition to folding the tube. The folding of the tube under dynamic load is shown by the sequence of pictures in Figure 6.3.10.

c. Remarks

The energy absorption per lb, U, in the two static tests was 3200 ft-lb/lb for the thin walled tube and 4500 ft-lb/lb for the thick walled tube. In the dynamic test the energy absorption was improved to 4000 ft-lb/lb due to the increased force level. Thus U seems to increase with t/D as predicted by the analysis. Apparently, most of the plastic deformation takes place at the plastic hinges. Therefore only a small portion of the entire tube is absorbing significant amounts of energy. Aluminum alloys with higher yield points could be used to increase U to perhaps 10,000 or 15,000 ft-lb/lb. This is still somewhat low. However, it should be recognized that U is only a rough estimate of efficiency. We are actually interested in the amount of energy absorption per dollar of device. No values for this measure of efficiency are available at this point in the program, but it is clear that the collapsing tube will be quite competitive on this basis. It is simply a piece of commercial tubing cut to the desired length. Furthermore, the tube has no additional pieces to add to its cost.*

In many possible applications of energy absorbing devices, e.g., buffering of an existing highway obstacle, one would like to provide the maximum stopping distance in the available space. If, for example, there were 12 feet around a concrete pier for placement of an energy absorber, the collapsing tube would provide nearly 12 feet of stopping distance, while a device such as the rolling torus would provide a maximum of six feet, and more probably only four feet, of stopping distance.

---

* For non-axial impacts some type of restraining device or guide is probably necessary to insure proper functioning. This is true as well for most of the other devices being investigated.

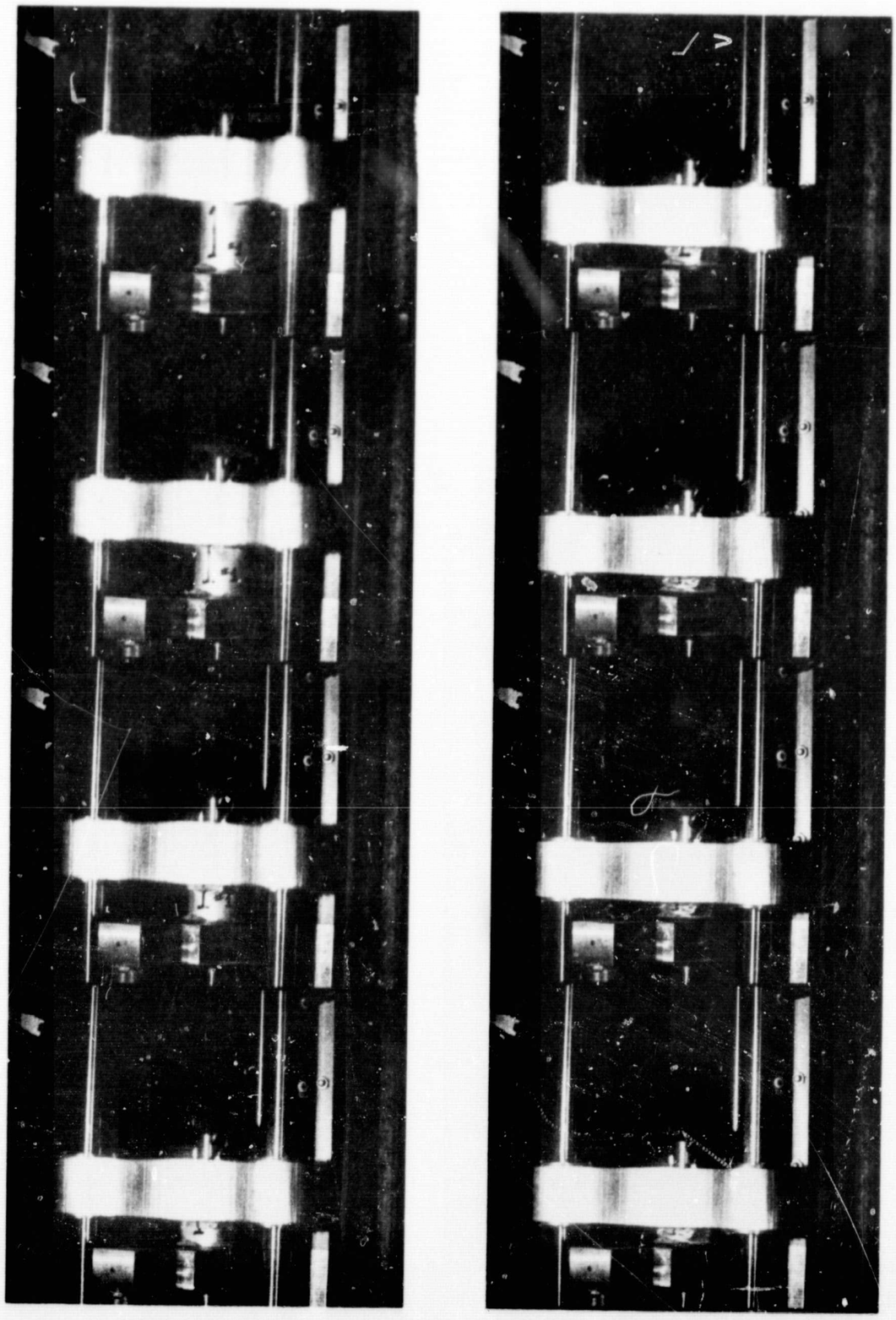

Figure 6.3.10. Speed Photographs of Collapsing Tube Under Impact

The force-displacement response of the tube has two major defects--the initial spike and the oscillatory nature of the collapse load. The initial spike can be removed completely (at least statically) by a slight folding of the tube. The oscillation in the load was produced entirely by changes in geometry, since the material we used was essentially nonwork hardening. The use of a highly work hardening material would, we believe, reduce the magnitude of the oscillation considerably. The increase in material strength as the fold flattened would then partially compensate for the increased ease in bending produced by the changes in configuration. This hypothesis will be examined as part of the test program.

It is clear that the analytical descriptions of tube folding found in the literature are not adequate for design purposes. There is no description of the variation in collapse load as the tube folds. There is no means of predicting the folding mode. Even the existing analysis of the average collapse load may give values which are quite different than those observed experimentally. A detailed description of tube behavior is obtainable at this time only by means of an experimental program.

The character of the force-displacement response for the thin tube was identical under static and dynamic load, while the response amplitude differed by only 20%. This indicates that static testing of significant value in determining the response of energy absorbers which must be designed to operate under dynamic load. Static testing is, in general, less costly than dynamic testing.

4. Metal Tearing and Shearing (Patent No. 3,232,383)

a. Introduction

This analysis was made to determine the suitability of this device as an energy absorber. The device was selected for further study because of its promise in automobile seat harness or seat belt applications; namely, it appears to operate under constant tensile load and should be fairly inexpensive to manufacture.

The essential operating features of the device are depicted in Figure 6.4.1. A piece of sheet metal is held between two guides whose width is slightly less than that of the hole in the stationary block. The sheet metal strip is wider than the hole so that under application of a sufficiently large tensile force, the overlapping sheet metal is sheared

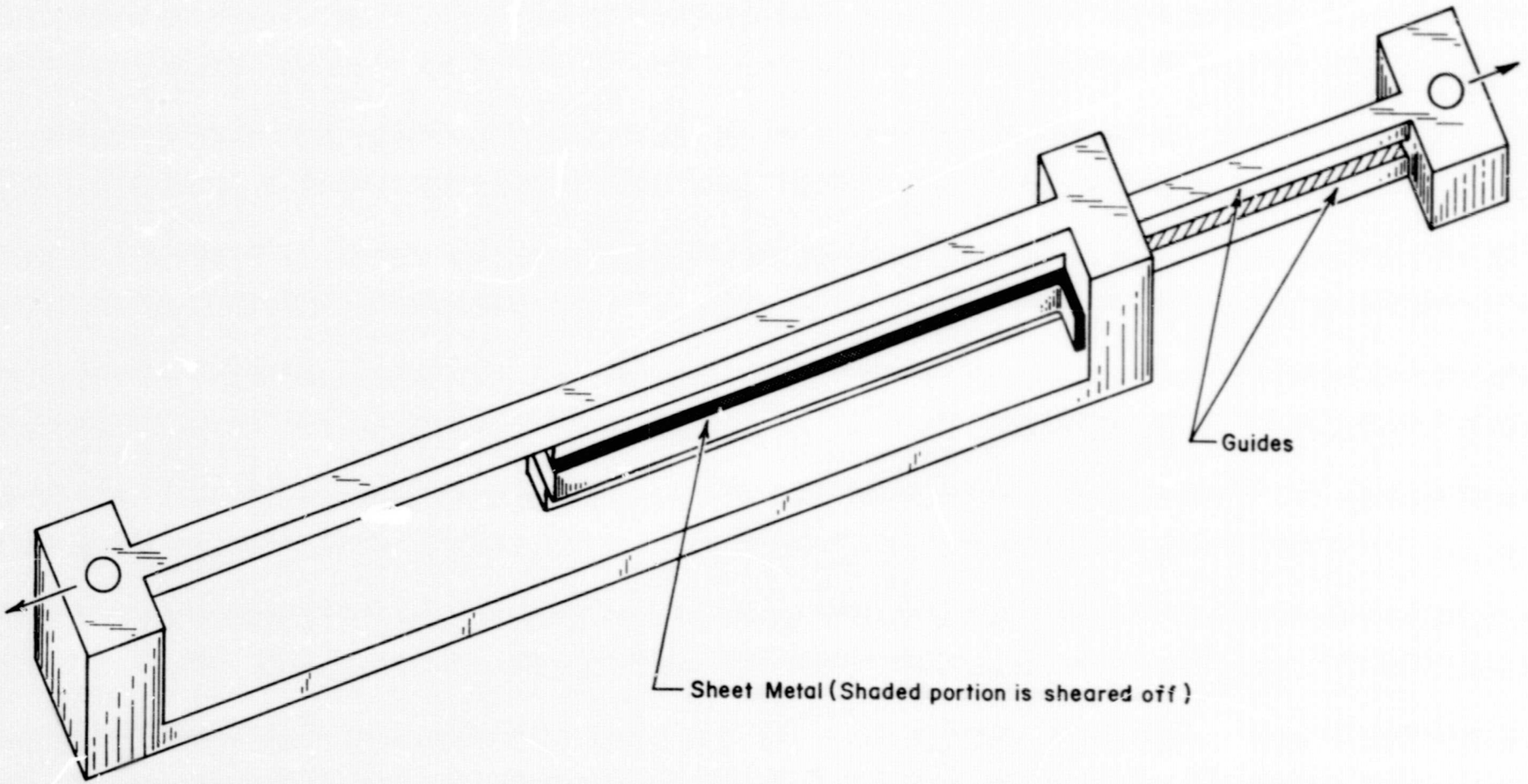

Figure 6.4.1. Sheet Metal Tearing Device

off as the guides pass through the hole. The cutting force F_c is controlled by the amount of overlap and the thickness of the sheet. The total energy absorption capability is the product of F_c and the length of the sheet metal strip.

The device is readily reusable. After each impact situation it is only necessary to insert another piece of sheet metal.

For design purposes, it is necessary to know the cutting force as a function of the width and depth of cut and the material properties of the sheet metal. This relationship is developed in the following section.

b. Analysis

There is no rigorous analysis of metal shearing in the literature. This is understandable, since such an analysis requires the determination of the plastic stress field in the neighborhood of the cutting edge as well as the use of these stresses in a suitable theory of fracture. No such theory, in the opinion of many designers, has yet been developed.

Several papers have been written attempting to analyze the machining of metal, a process which is closely related to the energy absorption problem at hand. The papers of Merchant on this subject[8,9,10] will be used as the basis for our estimation of the cutting force. Merchant's analysis has the advantage of being relatively simple, while providing results which are sufficiently accurate for the design of initial test pieces. In the following we have outlined that part of Merchant's work which is of importance in our study.

Experimental observation indicates that the deformation of metal being machined is confined to a narrow zone in the neighborhood of the edge of the tool. Furthermore, the freshly machined surface near the edge of the tool has little curvature. Based on these observations, Merchant assumes that the deformation consists of a simple shear produced as the material passes through a shear plane inclined at some angle ϕ to the uncut surface (Figure 6.4.2). Thus, the cross hatched rectangle is deformed into the cross hatched parallelogram in Figure 6.4.2.

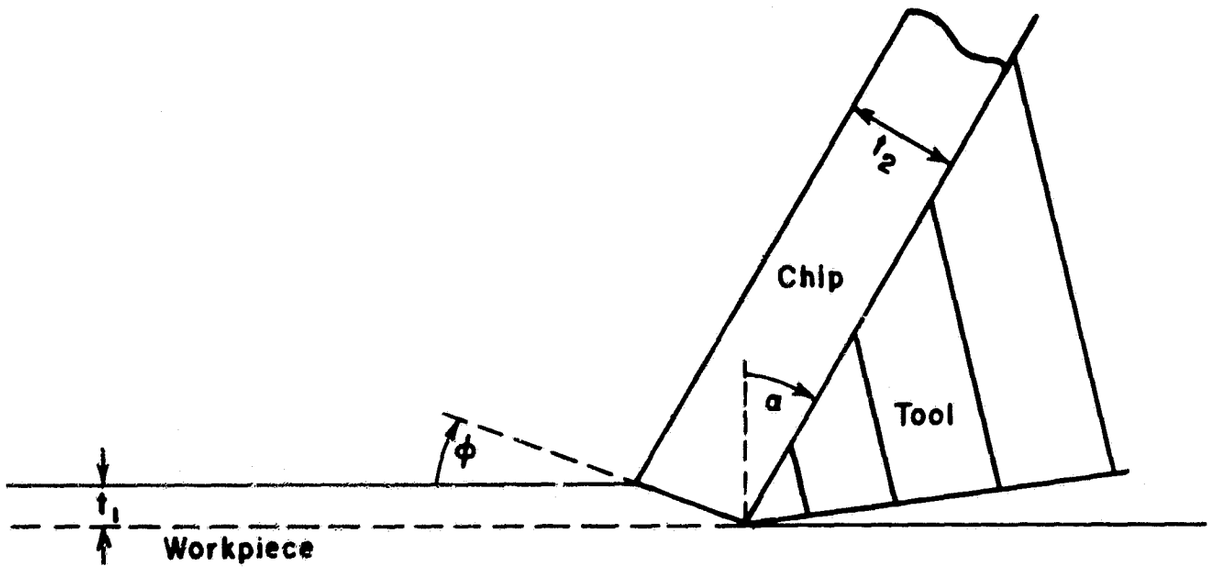

Figure 6.4.2. Mechanism of Metal Cutting

i. Velocity Relations

The cutting velocity V_c is the velocity of the workpiece relative to the tool while V_f is the velocity of the chip relative to the tool. Constancy of volume requires that the magnitudes of V_c and V_f be related by

$$V_c t_1 = V_f t_2 \tag{6.4.1}$$

where t_1 is the depth of cut and t_2 the chip thickness, as indicated in Figure 6.4.2. From geometrical considerations

$$\frac{t_1}{t_2} = \frac{\sin\phi}{\cos(\phi-a)} \tag{6.4.2}$$

where a is the oblique rake angle of the cutting tool (Figure 6.4.2). The substitution of (6.4.2) into (6.4.1) yields

$$V_f = V_c \frac{\sin\phi}{\cos(\phi-a)} \tag{6.4.3}$$

The velocity V_s of the chip relative to the workpiece is simply the vector difference between V_f and V_c (Figure 6.4.3).

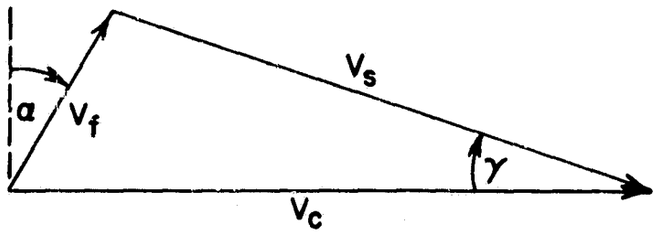

Figure 6.4.3. Velocity Vectors

The included angle γ between V_s and V_c is determinable in terms of ϕ and α in view of (6.4.3) and the fact that the included angle between V_f and V_c is $\pi/2 - \alpha$ (Figure 6.4.3). Carrying out the required calculations it is found that

$$\gamma = \phi \tag{6.4.4}$$

and that

$$V_s = V_c \frac{\cos\alpha}{\cos(\phi-\alpha)} . \tag{6.4.5)}$$

It follows from (6.4.4) that V_s is directed along the shear plane, and for this reason is called the shear velocity.

ii. Force Relations

The necessary force relations are obtained by analyzing the chip as a free body in equilibrium (Figure 6.4.4).

The force R of the workpiece on the chip is conveniently resolved into the shearing force F_s along the shear plane and F_n normal to the shear plane. A resolution of R into the cutting force F_c parallel to the surface of the workpiece and the thrust force F_t is also necessary. The force R' exerted by the tool on the chip is resolved in Figure 6.4.4 into the friction force F_f and normal force N. Since the chip is in equilibrium R = R' and the following relationships between the different components of force can then be derived from the geometry.

$$F_c = F_s \frac{\cos(\tau - \alpha)}{\cos(\phi + \tau - \alpha)} \qquad (6.4.6)$$

$$F_c = F_f \frac{\cos(\tau - \alpha)}{\sin\tau} \qquad (6.4.7)$$

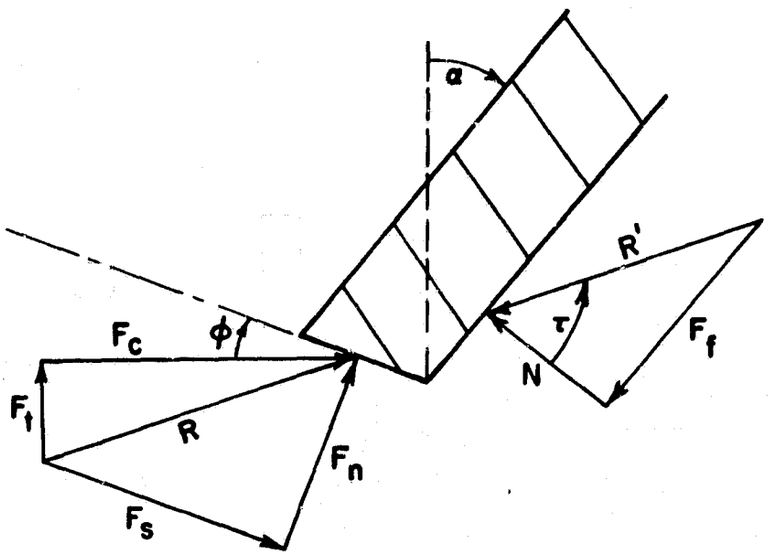

Figure 6.4.4. Force Vectors

In the above equations, as shown in Figure 6.4.4, τ is the friction angle, i.e.,

$$\tau = \tan^{-1} \frac{F_f}{N} = \tan^{-1} \mu \qquad (6.4.8)$$

where μ is the coefficient of friction between the tool and chip.

iii. Work Relations

The work W_c of removing a unit volume of metal is simply

$$W_c = \frac{F_c V_c}{A_o V_c} \qquad (6.4.9)$$

where A_o is the cross sectional area of the chip prior to removal. With the use of (6.4.3), (6.4.5), (6.4.6) and (6.4.7), it is possible to demonstrate that W_c can be expressed as the sum of the shear work W_s per unit volume (of metal removed) and the frictional work W_f per unit volume. Thus

$$W_c = W_s + W_f, \tag{6.4.10}$$

where

$$W_s = \frac{F_s V_s}{A_o V_c} \tag{6.4.11}$$

and

$$W_f = \frac{F_f V_f}{A_o V_c} \quad . \tag{6.4.12}$$

The cross sectional area A_s of the shear plane is related to A_o by

$$A_o = A_s \sin\phi. \tag{6.4.13}$$

Recognizing that F_s/A_s is the mean shear stress S_s over the shear plane, (6.4.11) can be written as

$$W_s = S_s \frac{\cos\alpha}{\sin\phi \cos(\phi - \alpha)} \tag{6.4.14}$$

when (6.4.5) and (6.4.13) are used. When (6.4.3) is used in (6.4.12) and the result is added to (6.4.14) we obtain

$$W_c = S_s \frac{\cos\alpha}{\sin\phi \cos(\phi-\alpha)} + \frac{F_f \sin\phi}{A_o \cos(\phi-\alpha)} \tag{6.4.15}$$

in view of (6.4.10).

iv. Determination of S_s and ϕ

Under normal circumstances, the depth of cut t_1 and the oblique rake angle α are known and the coefficient of friction μ can be reasonably estimated. No analytic solution is obtainable, however, until both S_s and ϕ are also specified. Merchant arrives at values for S_s and ϕ by assuming that S_s is equal to the shear strength of the material being machined while the value of ϕ is such as to minimize the cutting work or, equivalently, the cutting force F_c.

In the simplest application of his theory, Merchant assumes the shear strength to be constant and thus

$$S_s = b = \text{const.} \tag{6.4.16}$$

The use of (6.4.6) together with (6.4.13), (6.4.16), and the definition of S_s, leads to the following expression for the cutting force.

$$F_c = b A_o \frac{\cos(\tau - \alpha)}{\sin\phi \cos(\phi + \tau - \alpha)} \tag{6.4.17}$$

Differentiating (6.4.17) with respect to ϕ and equating the resulting expression to zero yields the result that F_c is minimized when

$$2\phi = \frac{\pi}{2} + \alpha - \tau. \tag{6.4.18}$$

Merchant's experiments on polycrystalline metals indicate that this formula overestimates ϕ by 20 to 40 percent.

A better estimate of ϕ is obtained by Merchant when he accounts for the effect of normal stress on shear strength. The average normal stress on the shear plane S_n is related to the average shear stress by

$$S_n = S_s \tan(\phi + \tau - \alpha). \tag{6.4.19}$$

Following Bridgeman's experimental results on drill rods, Merchant assumes the material shear strength to vary linearly with normal pressure, i.e.,

$$S_s = S_o + k S_n \tag{6.4.20}$$

where k and S_o are material constants. Proceeding in the same way as before it is found that the cutting force is minimized when

$$2\phi = C + \alpha - \tau \tag{6.4.21}$$

where

$$C = \cot^{-1} k. \tag{6.4.22}$$

With the use of (6.4.21), Merchant is able to obtain a good fit of his experimental data. Although (6.4.21) is more accurate than (6.4.18), it cannot be used for initial design. The nature of the dependency of shear strength on normal stress is not known for most materials, and thus k cannot be determined until after the test program has begun. We shall, therefore, use (6.4.18) to obtain initial estimates of F_c.

v. Application to Energy Absorber

In the energy absorber under consideration the oblique rake angle of the "cutting tool" (stationary block) is zero and the equation of particular interest, namely (6.4.17) reduces to

$$F_c = 2A_o b \frac{\cos \tau}{1 - \sin \tau} \qquad (6.4.23)$$

when Eq. (6.4.18) and the trigonometric formulas for sum and differences of angles are used. Equation (6.4.23) which will be used for initial design purposes, gives the cutting force as a function of the cross sectional area of the cut, the shear strength of the material, and the friction angle.

An estimate of the necessary cross sectional area of sheet metal depends of course on the particular application. In a seat belt application where the weight of the passenger is 200 pounds and it is desired to limit deceleration to 20g's, the cutting force must be

$$F_c = 20 \times 2000 = 4000 \text{ lbs.}$$

With an aluminum sheet (2024-T3) whose shear strength is 41,000 psi and a coefficient of friction of 0.75, the cross sectional area necessary to provide 4000 pounds of cutting force is found from (6.4.25) to be

$$A_o = .025 \text{ in}^2.$$

For a 1/8 inch sheet a total overlap of 0.2 inch is necessary, or an overlap of 0.1 inch on each side of the block. We estimate the width of the hole in the device to be tested at 1/4 inch and the length of sheet at 6 inches. Initially then, the sheet is .125 inch × .45 inch × 6 inches and has a weight of 0.034 lbs. The total energy absorption capability is 4000 × 6 in-lb or 2000 ft-lb. The total weight of the device was 0.688 lbs. A measure of the efficiency U of energy absorption is energy absorption per pound of deformed material. In this case we have

$$U = \frac{2000}{0.688} = 2930 \text{ ft-lb/lb.}$$

If the coefficient of friction were to vanish through the use of lubricants, we would obtain a minimum value of U. In the example under consideration U would be reduced to 1460 ft-lb/lb.

c. Remarks

The analysis shows the cutting force to be somewhat more dependent on friction than was originally anticipated. This dependence is shown in the plot of $F_c/2A_ob$ versus the coefficient of friction μ in Figure 6.4.5. The cutting edge for this device will be steel while the sheet metal will probably be either steel or aluminum. Thus the value of coefficient of friction during cutting will, with no lubrication, most likely fall between 0.5 and 1.0. In this range the effects of shearing and friction on the magnitude of the cutting force are about equal. It follows that about half of the total energy absorption will be provided by friction when no lubrication is provided.

Energy dissipation by means of friction is felt to be unreliable in view of the dependency of the coefficient of friction on the normal pressure, rubbing velocity, and condition of the rubbing surfaces. Each of these parameters is difficult to control. The initial rubbing velocity, for example, depends on the velocity of impact, an unknown variable. Moreover, the rubbing velocity is continually changing during the shearing process. V_f reaches a final value of zero when the total initial energy has been dissipated. The average normal pressure is related to the rate at which the chip curls away from the "cutting tool." The dependency of chip curling on other parameters involved in metal shearing is not known. Finally, the condition of the rubbing surfaces may be altered by the formation of oxides, inadvertent contact with foreign material, or even by the cutting process itself. The variation of μ during cutting is undesirable since it produces a variation in the cutting force and a deviation from the goal of a flat force-displacement diagram.

The effects of friction will be established during the early stages of our test program of this device. If reliability or force variation during shearing are problems, we shall attempt to drastically reduce the coefficient of friction by the use of a suitable lubricant, e.g., molybdenum disulfide which can withstand pressures of 400,000 psi

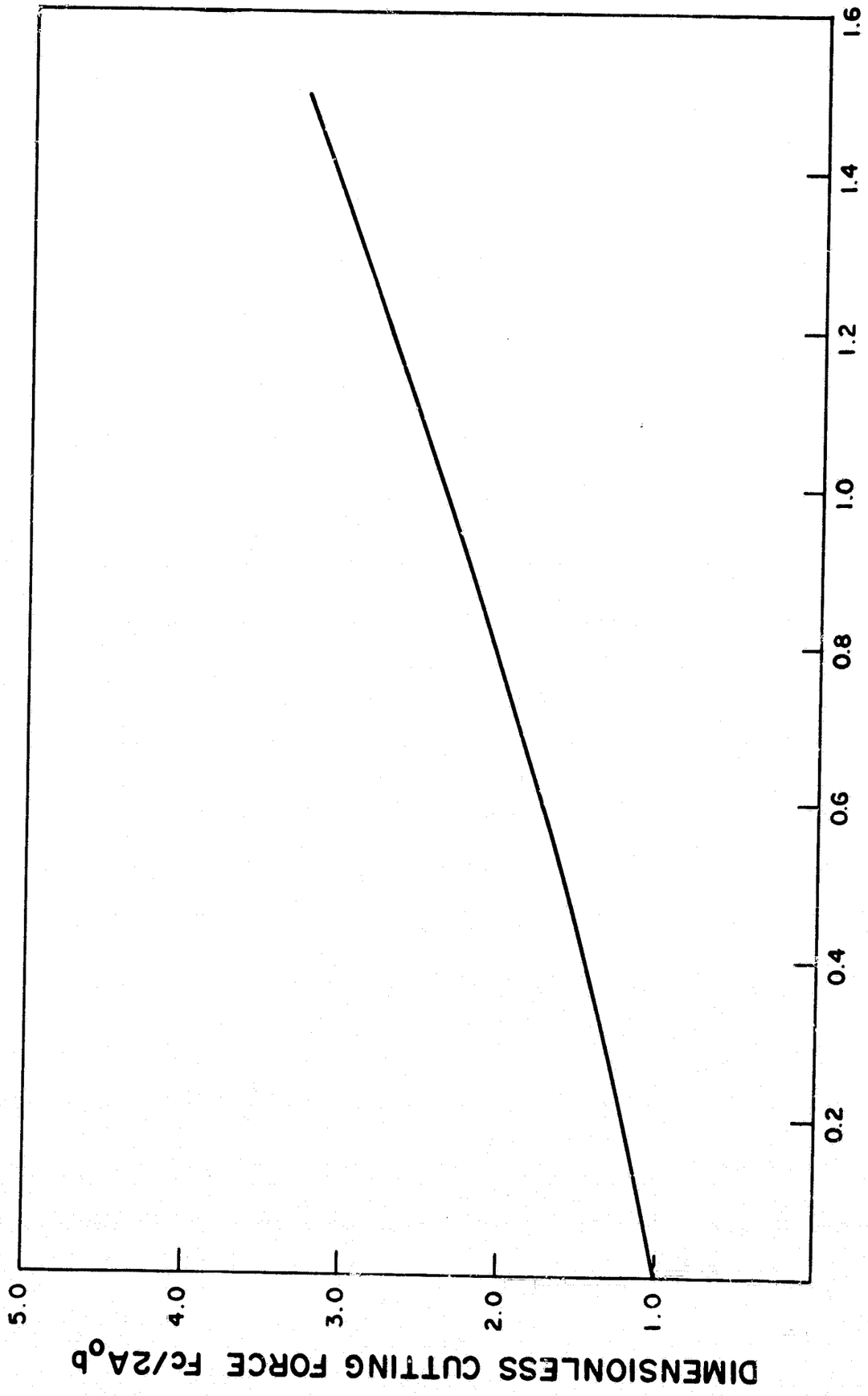

Figure 6.4.5. Coefficient of Friction μ

without being "squeezed out." If the friction force can be reduced so that $F_f << F_s$, then large percentage changes in μ will have little effect on the cutting force F_c.

The primary difference between normal machining of metal and the cutting action of the energy absorber is in the depth of cut. The considerable increase we will have in chip thickness will probably result in decrease in the curvature of the surface of the chip in the neighborhood of the workpiece, indicating that the shear stress distribution across the shear plane is not constant, but decreases as we move away from the point of the cutting tool. This will decrease the shearing work below that predicted by Merchant.

A discussion of the merits of the device is premature until testing has been completed. However, the analysis indicates that the device will provide a constant or near constant force (assuming that friction can be controlled or essentially eliminated) and a high value of energy absorption per pound of sheet metal.

5. Analysis of Extrusion Device (Patent No. 3,380,557)

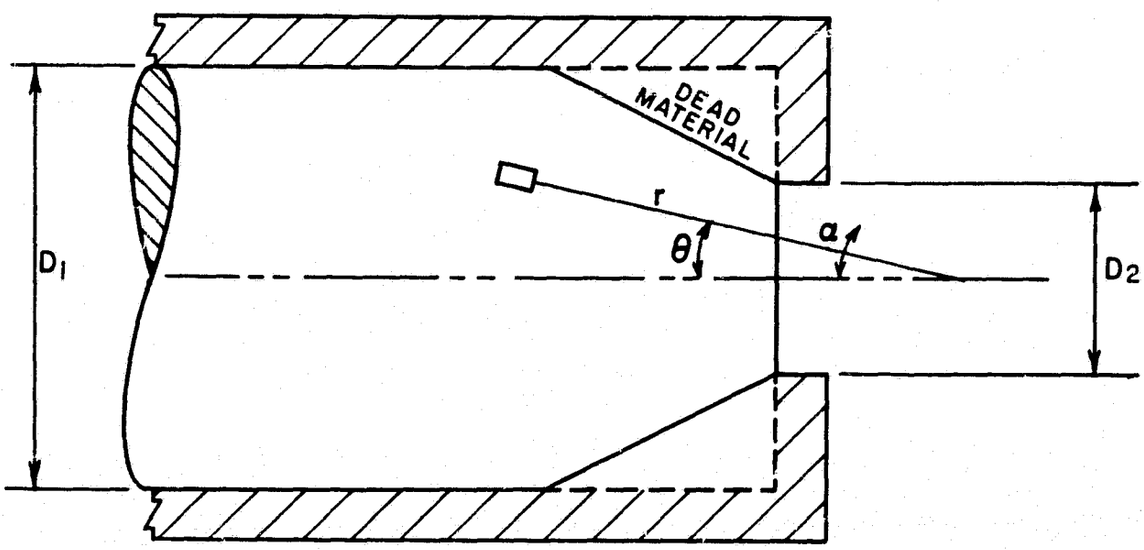

Figure 6.5.1. Extrusion Device

The analysis of this patent can be made based on Shield's theory of plastic flow in a conical channel.[11]

In spherical coordinates the nonzero stress components are given by σ_{rr}, σ_{ϕ}, $\sigma_{\theta\theta}$ and $\sigma_{r\theta}$. It is assumed that $\sigma_{\phi} = \sigma_{\theta\theta}$ and $\sigma_{r\theta}$ is a function of θ only. Under these assumptions the equilibrium equations become

$$\frac{\partial \sigma_{rr}}{\partial r} + \frac{1}{r}\frac{\partial \sigma_{r\theta}}{\partial \theta} + \frac{1}{r}\{2\sigma_{rr} - 2\sigma_{\theta\theta} + \sigma_{r\theta}\cot\theta\} = 0$$

$$\frac{\partial \sigma_{\theta\theta}}{\partial \theta} + 3\sigma_{r\theta} = 0 \qquad (6.5.1)$$

The Von Mises yield criteria is used.

$$\frac{1}{3}(\sigma_r - \sigma_\theta)^2 + \sigma_{r\theta}^2 = k^2 \qquad (6.5.2)$$

k is the yield in simple shear. Define a new variable τ by

$$\tau = \frac{\sigma_{r\theta}}{k}$$

These equations lead to an equation for τ.

$$\frac{d\tau}{d\theta} + 2\sqrt{3(1-\tau^2)} + \tau\cot\theta = c \qquad (6.5.3)$$

where c is a constant. If the value of τ prescribed at the boundary is given by m then the boundary conditions for τ are

$$\tau = 0 \quad \text{at} \quad \theta = 0$$
$$\tau = m \quad \text{at} \quad \theta = a \qquad (6.5.4)$$

The extrusion force can be shown to be

$$P = \frac{\pi D_2^2}{8} k c \ln \frac{D_1^2}{D_2^2} \qquad (6.5.5)$$

Our problem now reduces to integrating equation (6.5.3). If α and m are small $(1 - \tau^2) \approx 1$ and $\cot\theta \approx 1/\theta$. For this case, (6.5.3) can be solved exactly and gives

$$\tau = \frac{m\theta}{\alpha} \tag{6.5.6}$$

For our case, however, m and θ cannot be considered to be small since optimum energy absorption is desired. Consequently (6.5.3) can in general be solved only approximately. We would now like to derive an approximate formula for τ for large m and θ based on finite differences and a mesh size of two. Let the center nodal point be located at $\theta = \alpha/2$. Let t denote the value of τ at this point. The appropriate equations are

$$\begin{aligned} &\frac{m - t}{\alpha - \frac{\alpha}{2}} + 2\sqrt{3(1-m^2)} + m\cot\alpha = c \\ &\frac{t - 0}{\frac{\alpha}{2} - 0} + 2\sqrt{3(1-t^2)} + t\cot\frac{\alpha}{2} = c \end{aligned} \tag{6.5.7}$$

Equating equations (6.5.7) results in a second order equation for t.

$$t^2[b^2 + 12] + t[-2ab] + [a^2 - 12] = 0 \tag{6.5.8}$$

where

$$a = 2\sqrt{3(1-m^2)} + m\cot\alpha + \frac{2m}{\alpha}$$

$$b = \frac{4}{\alpha} + \cot\frac{\alpha}{2}$$

Solving for t gives

$$t = \frac{ab + 2\sqrt{36 - 3(a^2 - b^2)}}{b^2 + 12} \tag{6.5.9}$$

Once t is known c can be calculated from the first of equation (6.5.7).

Consider now the case wh e $\alpha = \pi/4$ and there is a perfect bond between the case and extrusion material (m = 1). For this case

$$t = 0.767$$

$$c = 1.592$$

If the more simplified equation (6.5.6) is used

$$c = 6.01$$

The great difference in the values of c points out the dangers of using (6.5.6) for this problem.

The following graph illustrates the variation of t with α for m = 1. This can be used for design purposes.

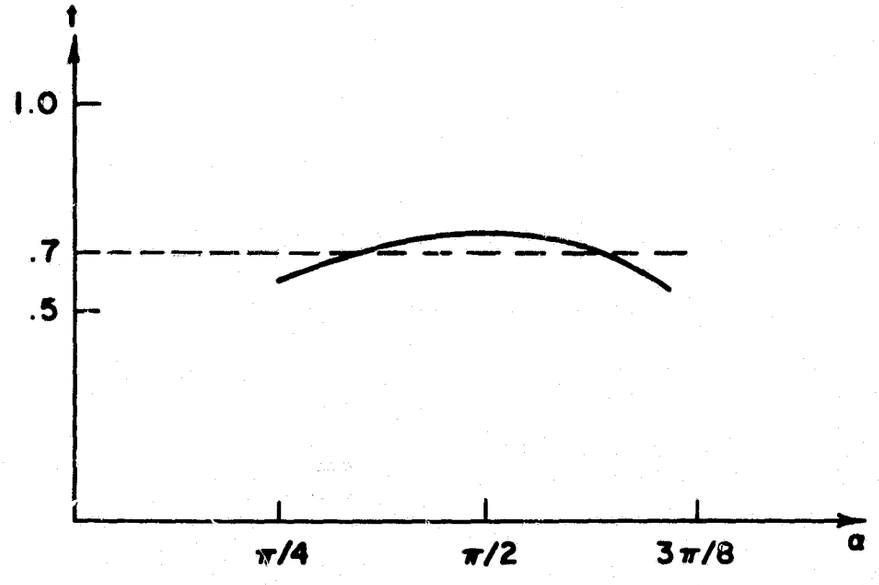

Figure 6.5.2. Variation of t with α

This graph shows that the variation is nearly linear. Hence an approximate value for t will be used.

$$t = 0.7 \qquad (6.5.10)$$

for m = 1

Using equation (6.5.7) an approximate equation for c is obtained for m = 1.

$$c = \cot \alpha + \frac{0.6}{\alpha} \qquad (6.5.11)$$

If $\alpha = \pi/4$ then the extruding force is given by

$$P = \pi \frac{D_2^2}{5.02} k \ln \frac{D_1^2}{D_2^2} \qquad (6.5.12)$$

Consider the following example

$$\frac{D_1}{D_2} = 2.0$$

$$D_2 = 0.5 \text{ inch}$$

$$k = 1,000 \text{ psi.}$$

Using equation (6.5.12), we obtain a value for P.

$$P = 217 \text{ lb}$$

For m = 0

$$P = 186 \text{ lb}$$

Note that frictional forces on the horizontal sides of the tube Figure 6.5.1 were neglected. For maximum reliability the sides should be lubricated or some gap left between the material and case on this portion.

In this analysis it is important to point out that for a conical shaped nozzle the value of m is somewhat arbitrary depending on the material and the amount of lubrication. For a flat ended tube Figure 6.5.1 we may consider part of the material to be dead. For this case, m and α both are somewhat arbitrary and the best approach would be to examine experimental results such as a cross-section of the material that had been partically extruded. It should then be possible to get an idea of about what m and α should be. Making certain assumptions it is possible, however, to obtain an approximate relation between m and α for this case. To do this, we assume a homogeneous

state of stress in the dead material and no shear stresses on the vertical and horizontal sides.

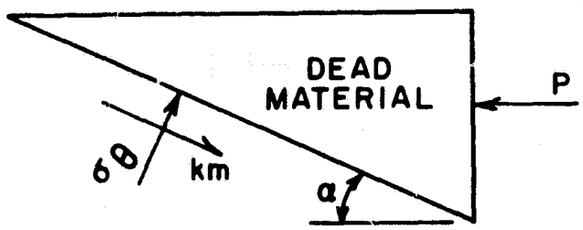

Figure 6.5.3. Free Body of Dead Material

Equilibrium requires

$$\sigma_\theta \sin \alpha + mk = p \cos \alpha. \qquad (6.5.13)$$

If σ_r is assumed zero, the yield condition gives

$$\frac{1}{3} \sigma_\theta^2 + (mk)^2 = k^2 \qquad (6.5.14)$$

combining (6.5.13) and (6.5.14) and solving for p gives

$$p = k\sqrt{3(1-m^2)} \tan \alpha + mk \sec \alpha . \qquad (6.5.15)$$

The actual slip surface will be the one that minimizes p.

That is

$$\frac{\partial p}{\partial \alpha} = 0 \qquad (6.5.16)$$

The consequence of this condition is the desired equation.

$$m = \sqrt{\frac{3}{\sin^2 \alpha + 3}} \qquad (6.5.17)$$

For $\alpha = \pi/4$

$m = 0.9$

Analysis for Flat-Ended Tubes

Experiments were carried out with household wax used as the extruding material. It was obvious after a few tests on flat-ended tubes that the previous analysis gave very poor answers for this situation. It is necessary for this situation to construct a slip line field for the region near the extruding end.

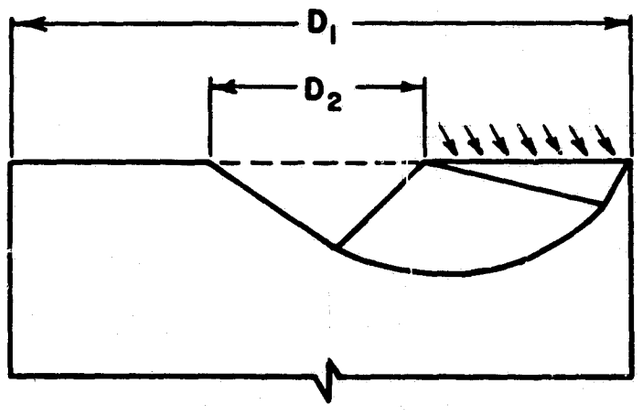

Figure 6.5.4. Slip Line Field

The analysis for such slipline fields are well known (see Sokolovski, "Statics of Soil Media"). Assume on the flat end that the relation between normal stress and shear stress is given by

$$\tau_{xy} = (p + H) \tan \delta \qquad (6.5.18)$$

where

$H = k \cot \rho$

ρ = angle of internal friction

$\delta \leq \rho$

Assuming uniform pressure on the face of tube and δ_1 constant, the pressure can be shown to be given by

$$p = H \cos\delta \frac{[\cos\delta + (\sin^2\rho - \sin^2\delta)^{\frac{1}{2}}]}{[1+\sin\rho]} \times \exp\left\{\left(\pi + \delta + \arcsin\frac{\sin\delta}{\sin\rho}\right)\tan\rho\right\} - H \tag{6.5.19}$$

The extruding force is then given by

$$P = \frac{\pi}{4} p (D_1^2 - D_2^2) \tag{6.5.20}$$

If perfect bond between the case and material is assumed (i.e., $\rho = \delta$) (6.5.19) reduces to

$$p = H \frac{\cos^2\rho}{[1-\sin\rho]} \exp\left\{\left(\frac{3\pi}{2} + \rho\right)\tan\rho\right\} - H \tag{6.5.21}$$

Strictly speaking, the stress field constructed will hold for only one D_2/D_1 ratio. This ratio is determined by

$$\frac{2}{[1 - D_2/D_1]} = \frac{\sin\left(\frac{3\pi}{4} - \frac{\rho}{2} - \frac{\delta}{2} - \frac{\sin^{-1}\left(\frac{\sin\delta}{\sin\rho}\right)}{2}\right)}{\sin\left(\frac{\pi}{4} - \frac{\rho}{2}\right)} \times \exp\left(\tan\rho\left[\frac{\pi}{2} + \frac{\delta}{2} + \sin^{-1}\left(\frac{\sin\delta}{\sin\rho}\right)\right]\right) \tag{6.5.22}$$

For $\rho = \delta$

$$\frac{D_2}{D_1} = 0.23$$

If D_2/D_1 is not far from that given by (6.5.22), then (6.5.19) and (6.5.21) can be used as an approximation.

In order to compare the theory to experiments, consider the following case for household wax.

$\delta = \rho$ $\qquad$ $k = 100$ psi

$\rho = 10°$

k was determined easily by testing a sample of Enco household wax. It was found to have a yield in shear of 100 psi under a normal stress of 50 psi. A modest value of ρ was assumed. Further tests will be necessary to determine what ρ actually is for wax. For this case (6.5.21) yields

$$p = 920 \text{ psi}$$

The extruding force is

$$P = 725 \ (D_1^2 - D_2^2)$$

Three experiments were run with $D_1 = 1$ inch and three different values of D_2. The results are plotted on the following graph.

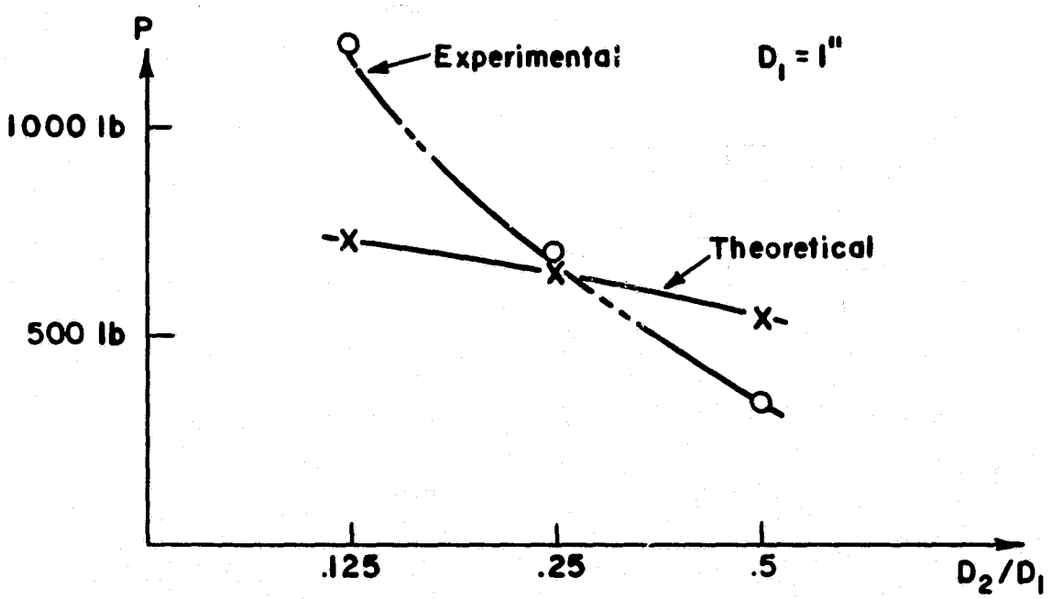

Figure 6.5.5. Curve of P vs. D_2/D_1

The slip field was calculated for a value of D_2/D_1 of 0.23. For this region theory and experiment are remarkably close. For very

small and very large holes caution must be used as indicated by the graph. The discrepancies are probably due to the following factors:

1. inadequate slip line field
2. nonuniform pressure on end of tube
3. inaccurate value of δ
4. inaccurate value of ρ

More analytical and experimental work is needed before reliable data on mechanical efficiency can be obtained. The unfavorable ratio of length to stroke (see Figure 6.5.1) for this device, however, discourages a much more detailed consideration.

6. Friction Devices (Patent No. 3, 164, 222)

a. Introduction

This report contains the results of a study to evaluate Patent No. 3, 164, 222, a device which dissipates energy through frictional work. The device (Figure 6. 6. 1) consists of two partially overlapping sheets which have been wrapped over a cylindrical core (Figure 6. 6. 2). During wrapping, the sheets are in lateral tension. The sheets contract when the lateral load is removed producing a radial compressive stress between the overlapping surfaces. The existance of this stress is necessary for proper functioning of the device, for without a normal force between the sheets there would be no friction force and hence no energy absorption.

Frictional devices are generally felt to be unreliable because of the variation of the coefficient of friction μ with normal pressure, rubbing velocity, and the nature of the rubbing surfaces. However, it was felt that one such device should be examined in some detail to determine its efficiency U of energy absorption. If the device had an extremely high value of U compared to the other devices then an investigation of the reliability problem would be warranted. In conducting the analysis, the major assumptions which are made will tend to increase U. If the device is not highly competitive under these favorable conditions, it must be rejected.

b. Analysis

A highly refined estimate of the energy absorption capabilities of the friction device is not of interest at this time. In light of this and the expectation that the diameter of the cylindrical wrapping core will be many times larger than the thickness of an individual sheet, we will make the following assumptions:

A1. The stress field in a single wrap of sheet ($n\pi \leq \theta \leq (n+2)\pi$) is identical with the stress field in a cylindrical shell of the same diameter and wall thickness.

A2. The tension during wrapping can be controlled to produce any desired value of compressive radial stress.

A3. The sheets shall be of sufficient thickness to prevent local collapse as cylindrical shells.

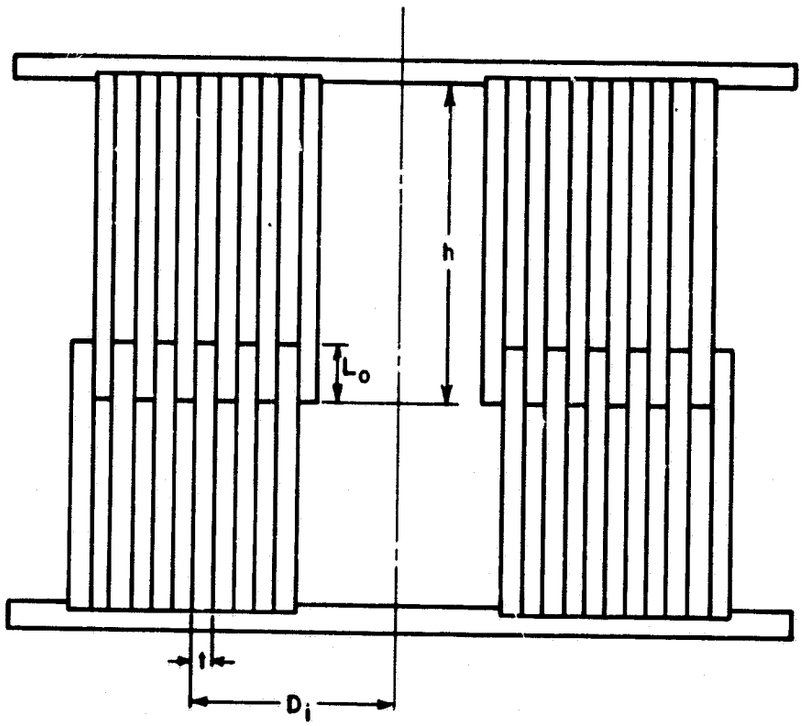

Figure 6.6.1. General Arrangement

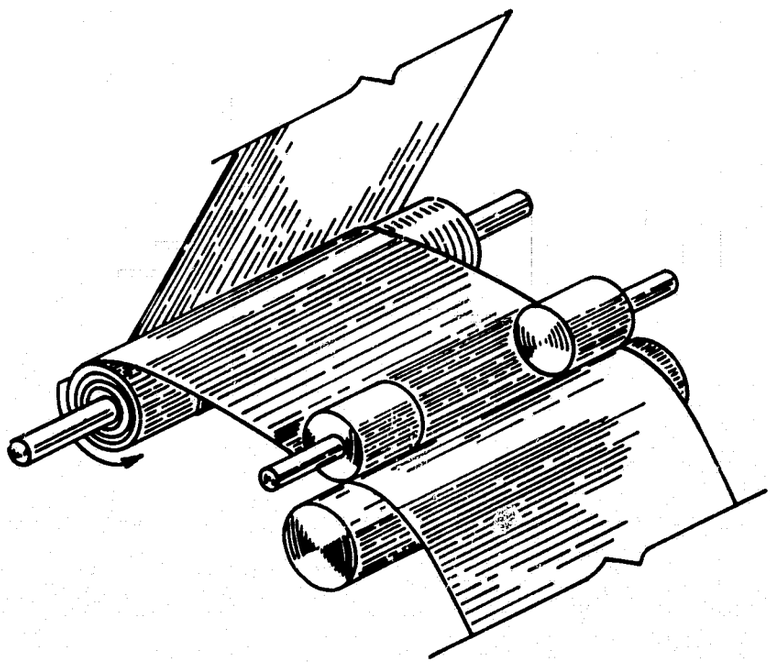

Figure 6.6.2. Pictorial View

The total axial force F necessary to produce axial motion is

$$F = \mu A \sigma = \sum_{i=1}^{N} R_i \qquad (6.6.1)$$

where μ is the coefficient of friction, A is the contact area between the upper and lower sheets, the average radial compressive stress is σ, and R_i is the axial force acting on the i^{th} of N wraps. The weight of a single wrap of mean diameter D_i is approximately $\pi \rho h D_i t$, where ρ, h, and t are respectively the sheet density, width, and thickness (Figure 6.6.1). The energy U dissipated per pound of wrapping is therefore

$$U = \frac{\sum_{i=1}^{N} \int_{L_o}^{h} R_i \, dL}{2\pi \rho h t \sum_{i=1}^{N} D_i} \qquad (6.6.2)$$

where L_o is the initial length of overlap between the sheets and L is the axial length of contact at some later time.

The design problem is to maximize U under the constraint that there be no column instability or axial folding of the sheets. From the work on the folding tube, it appears that the axial folding load for this type of configuration is lower than the Euler critical load so that our stability condition will be

$$R_i < 6 \sigma_y t^{3/2} D_i^{1/2} \qquad (6.6.3)$$

where σ_y is the tensile yield strength of the material.

Minimization of (6.6.2) under the constraint (6.6.3) would be rather tedious in view of the number of independent variables. For our purposes it is sufficient to note from (6.6.2) and (6.6.3) that increasing R_i by thickening the sheet increases U, i.e., a small number of thicker sheets carrying high load is more efficient than a large number of low load bearing thin sheets. As an obvious example, we could have an

infinite number of sheets of zero thickness, each of which could carry no axial load. The efficiency of the device would be zero, since it could not absorb energy in its design mode.

There is a limit to the efficiency which can be gained through the use of thicker sheets. The pressure between the sheets and hence the friction force cannot be increased without limit, for at sufficiently high pressures yielding of the material occurs. Beyond this point, extremely large changes in strain are necessary to produce relatively small pressure changes. Therefore, we shall design our device such that the inner and outer surfaces of the sheets in contact are at the yield point of the material. It is doubtful that wrapping the sheets under tension could produce this high a contact pressure, so that our estimates of energy absorption will be high.

In order to determine the conditions for yielding, the stress field on the surface of the sheet must be determined. Each sheet is subjected to radial stresses σ_r and shear stresses σ_{rz} (assuming the z axis to be the center line of the cylinder). According to A1, we may consider each wrap as a circular cylinder, subjected to pressure and axial shear stresses on both the inner and outer faces. The stress field produced by the pressure acting alone was determined by Lame in 1852. It has the non-vanishing components

$$\sigma_r = - \frac{a^2 b^2 (p_i - p_o)}{r^2 (b^2 - a^2)} + \frac{a^2 p_i - b^2 p_o}{b^2 - a^2} \tag{6.6.4}$$

$$\sigma_\theta = \frac{a^2 b^2 (p_i - p_o)}{r^2 (b^2 - a^2)} + \frac{a^2 p_i - b^2 p_o}{b^2 - a^2} \tag{6.6.5}$$

where a and b are the inner and outer radii of the cylinder, p_i and p_o are the internal and external pressures, and r is the radial position of a point in the cylinder. In particular, at the inner radius

$$(\sigma_r)_{r=a} = - p_i; \; (\sigma_\theta)_{r=a} = \frac{- 2b^2 p_o + p_i (a^2 + b^2)}{b^2 - a^2} \tag{6.6.6}$$

while at the outer radius

$$(\sigma_r)_{r=b} = - p_o; \; (\sigma_\theta)_{r=b} = \frac{2a^2 p_i - p_o (b^2 + a^2)}{b^2 - a^2} \tag{6.6.7}$$

The shear stresses at the surface are produced by friction. Thus

$$(\sigma_{rz})_{r=a} = -\mu p_i \tag{6.6.8}$$

and

$$(\sigma_{rz})_{r=b} = \mu p_o. \tag{6.6.9}$$

Since $t/D << 1$ we can assume that σ_{rz} varies linearly in the radial direction, i.e.,

$$\sigma_{rz} = \frac{\mu}{t} [r(p_o + p_i) - ap_o - bp_i] \tag{6.6.10}$$

The axial stress σ_z can be obtained by integrating the equation of equilibrium

$$\frac{\partial \sigma_z}{\partial z} + \frac{\partial \sigma_{rz}}{\partial r} + \frac{\sigma_{rz}}{r} = 0 \tag{6.6.11}$$

with the use of (6.6.10).

The result is

$$\sigma_z = -\frac{\mu z}{t} \quad 2(p_o + p_i) - \frac{1}{r}(ap_o + bp_i) \ . \tag{6.6.12}$$

At the inner surface, $r = a$, the axial stress is

$$(\sigma_z)_{r=a} = -\frac{\mu z}{t} \left[p_i + p_o - \frac{t}{a} p_i\right] \tag{6.6.13}$$

while at the outer surface

$$(\sigma_z)_{r=b} = -\frac{\mu z}{t} \left[p_i + p_o + \frac{t}{b} p_o\right] \tag{6.6.14}$$

Since t/a and t/b are << 1, we shall approximate these expressions by

$$(\sigma_z)_{r=a} = (\sigma_z)_{r=b} = -\frac{\mu z}{t}(p_i + p_o) \qquad (6.6.15)$$

The stress field at the inner and outer surfaces is given by (6.6.6), (6.6.7), (6.6.8), (6.6.9), and (6.6.15). The principle stresses $\sigma_1 \geq \sigma_2 \geq \sigma_3$ must now be found in order to apply the Tresca yield condition,

$$|\sigma_1 - \sigma_3| = \sigma_y \qquad (6.6.16)$$

where σ_y is the tensile yield stress of the material.

Before computing σ_1, σ_2, and σ_3 we can make some additional simplifications. Certainly the variation in pressure across a single thickness of sheet will be small compared to the pressure itself, i.e.,

$$\frac{p_i}{p_o} \doteq 1 \qquad (6.6.17)$$

It follows from (6.6.6) and (6.6.7) that the tangential and radial stresses at the inner and outer surface are nearly equal. Note that σ_r and σ_θ are both compressive. The axial stress σ_z varies linearly with z and is a maximum when the entire width of sheet is in contact. For this case z = h and (6.6.15) becomes

$$(\sigma_z)_{max} = -\frac{\mu h}{t}(p_i + p_o) \qquad (6.6.18)$$

Since we expect h/t << 1, it can be seen from (6.6.8) and (6.6.18) that $(\sigma_z)_{max} >> \sigma_{rz}$. Therefore, we can disregard σ_{rz} in determining the principle stresses. As a consequence of these considerations, the maximum and minimum principle stresses at r=a are

$$\sigma_1 = -p_i; \quad \sigma_3 = -\frac{\mu h}{t}(p_i + p_o) \qquad (6.6.19)$$

Similarly at r=b

$$\sigma_1 = -p_o; \quad \sigma_3 = -\frac{\mu h}{t}(p_i + p_o) \qquad (6.6.20)$$

The use of (6.6.19) and (6.6.20) in the yield condition (6.6.16) shows that yielding occurs simultaneously at the inner and outer surfaces when

$$p_i = p_o = p \tag{6.6.21}$$

where

$$p = \frac{\sigma_y t}{2\mu h + t} \doteq \frac{\sigma_y t}{2\mu h} . \tag{6.6.22}$$

The approximate form of (6.6.22) is written by noting that $\mu h >> t$. In the remainder of the analysis we shall assume that the tension during the wrapping process has been controlled so that the compressive stress between the sheets is given by (6.6.22). Then, according to our previous discussion, the friction device should be operating near its maximum efficiency.

The frictional (shear) stress is found to be

$$(\sigma_{rz})_{r=b} = -(\sigma_{rz})_{r=a} = \frac{\sigma_y t}{2h} \tag{6.6.23}$$

when (6.6.21) and (6.6.22) are used in (6.6.8) and (6.6.9). The axial force on a single wrap is

$$R_i = \pi \sigma_y t L \frac{(b + a)}{h} \tag{6.6.24}$$

or

$$R_i = \frac{\pi}{h} \sigma_y t L D_i \tag{6.6.25}$$

where D_i is the mean diameter of the wrap. The energy W_i dissipated by a single wrap is

$$W_i = \int_{L_o}^{h} R_i \, dL = \frac{\pi}{2h} \sigma_y t D_i (h^2 - L_o^2). \tag{6.6.26}$$

For purposes of maximizing energy dissipation, we shall assume L_o to be zero in (6.6.26). Physically, of course, this is impossible since

there must be some initial overlap of the two sheets in order for the device to properly function. The energy dissipated per pound of wrap is therefore*

$$U_i = \frac{Y}{4\rho} . \qquad (6.6.27)$$

Equation (6.6.27) indicates that U_i is only a function of σ_y/ρ. It is independent of sheet thickness, diameter of wrap, sheet width and coefficient of friction μ.** These conclusions are, of course, only approximations to the actual operating efficiency of the device under the initial compressive stress state given by (6.6.21) and (6.6.22).

As an indication of the efficiency predicted by (6.6.27), consider the use of aluminum sheets with 20,000 psi yield strength. For this case

$$U_i = 4150 \text{ ft-lb/lb.}$$

Remarks

The force necessary to produce axial displacement of the device does not remain constant. As can be seen from (6.6.25) it varies linearly with displacement. The initial force is proportional to the amount of overlap L_o between the upper and lower sheets, while the maximum force is dependent on the width h of the sheets. The percentage variation in force is $1 - h/L_o$. Constancy of force can only be approached, therefore, when $h \doteq L_o$. But if $h \doteq L_o$ the "stroke" of the device becomes small, resulting in low energy dissipation (see (6.6.24)) and extremely low efficiency.

Another poor design feature of the device is that the stroke is at most only half the total length of the device. Considering that end plates are necessary and that the initial overlap cannot be zero, a stroke/length ratio of 1/3 is probably realistic. Thus if 12 feet of

---

* In computing the weight we must include the weight of both a lower and an upper wrap.

** The independence of efficiency on the coefficient of friction at first seems surprising. However, we must remember that since the contact pressure p is inversely proportional to μ (see (6.6.22)) the axial force does not depend on the friction coefficient.

space were available for placement of an energy absorber around a highway obstacle, only 4 feet could be used for controlled energy absorption.

The efficiency of energy absorption of the device is low compared to most of the other devices under consideration. The device, therefore, has literally nothing to recommend it. It has low efficiency, low stroke/length ratio, variable force-displacement characteristics, and is probably unreliable in view of its dependency on friction. It shall not be considered for further study.

VII. FABRICATION

Part of the research effort to establish economic feasibility of a patent of an energy absorbing device is the determination of the most economical method of fabrication. In order to establish fabrication costs both for a single item as well as for a high production level, we have enlisted the services of a local metal fabrication company, the Silver Engineering Company, which is a division of the Colorado Fuel and Iron Corporation. The most reliable method of cost determination is to build a specimen. Economy can be achieved by building one-fifth scale model specimens, to correspond to our one-fifth scale model impact tester. The cost can then be extrapolated both to full scale and high production rates.

Our earlier plans were to build these models in the University machine shop. While this is perfectly feasible, our machine shop does not have on its staff experienced manufacturing engineers who can extrapolate costs from a single scale model to both full scale and high production rates.

Our present plans are therefore to build models in each of the five categories of energy absorbing devices with the Silver Engineering Company in Denver. Because of our past association with them, they have agreed to make available to us their methods of cost determination and cost extrapolation.

Devices being fabricated at the present time are the following:

Category	Patent No.
Tube and Mandrel	3,143,321 (NASA)
Collapsing Tube	2,870,871
Cyclic Bending (Metal through Offset Pins)	3,211,260
Metal Shearing	3,232,383
Extrusion	3,380,557

VIII. TESTING PROGRAM

Testing of the energy absorbing devices was undertaken using the static testing facilities in the Civil Engineering Materials Laboratory and a dynamic tester which was built and installed in the Mechanical Engineering Laboratory. Since many tests are required in the development and optimization of devices such as these, it was considered desirable to conduct most of the tests on laboratory scale models. It was also anticipated that specific devices would require full scale testing in the actual application.

Since the major field of interest of this program is the application of energy absorbing devices in auto safety, a dynamic tester was desired which would simulate, at 1/5 scale, a 4500 lb. auto traveling at 60 mph (88fps). The analysis of the scaling law and similitude requirements is given in Appendix 2.

At 1/5 scale the volume of the model would be 1/125 that of the full size auto. Since the density of the materials used in the scale model will be the same as those used in the full scale, the weight of the 1/5 scale auto would be

$$W_m = \frac{1}{125} W_p$$

where W_m is the weight of the model and W_p is the weight of the full size auto. If the full size auto weights 4500 lb. then the weight of the model would be 36 lb.

The deviation of the scale factor for velocity is given in Appendix 2, where it is shown that the velocity of the 1/5 scale simulator should be the same as the full scale prototype. This has been chosen as 60 mph.

a. Dynamic Tester

The dynamic testing machine is shown in Figure 8.1, while Figure 8.2 is a schematic diagram showing the general features of the machine. Bearings in the ram (a) follow three guide rods which insure directional control. The motivating force for the ram is provided by a specially designed pneumatic cylinder (b) which has a light weight piston and rod (nylon piston and tubular steel rod). A specially designed hydraulic shock absorber (c) is positioned to stop

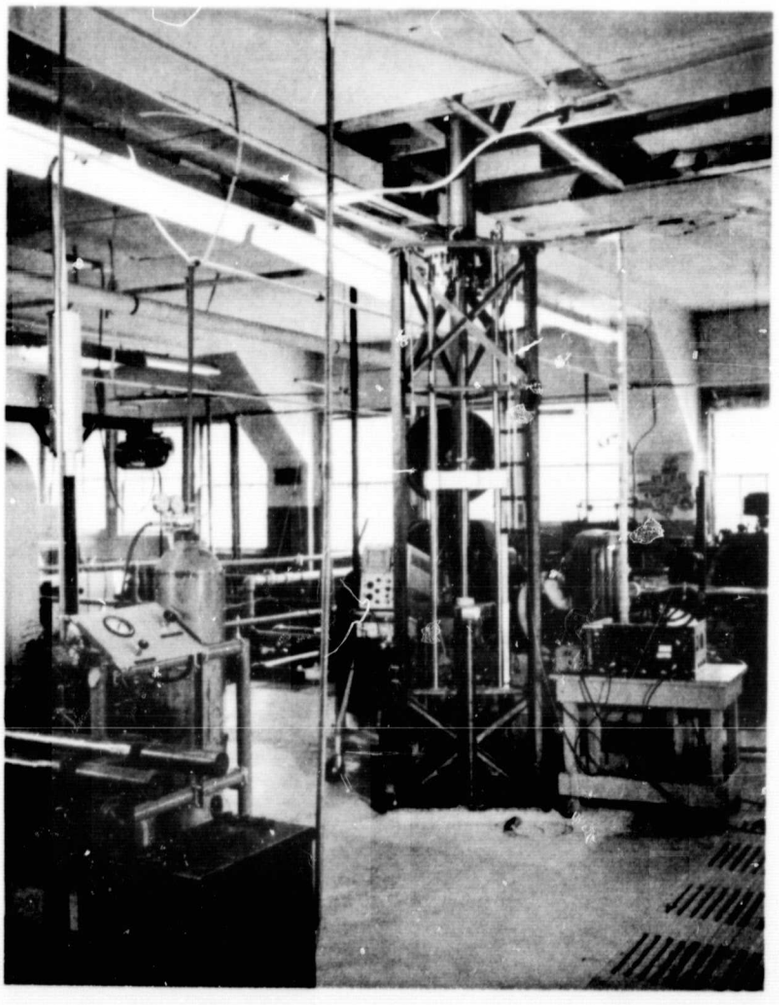

Figure 8.1. One-Fifth Scale Model Impact Tester

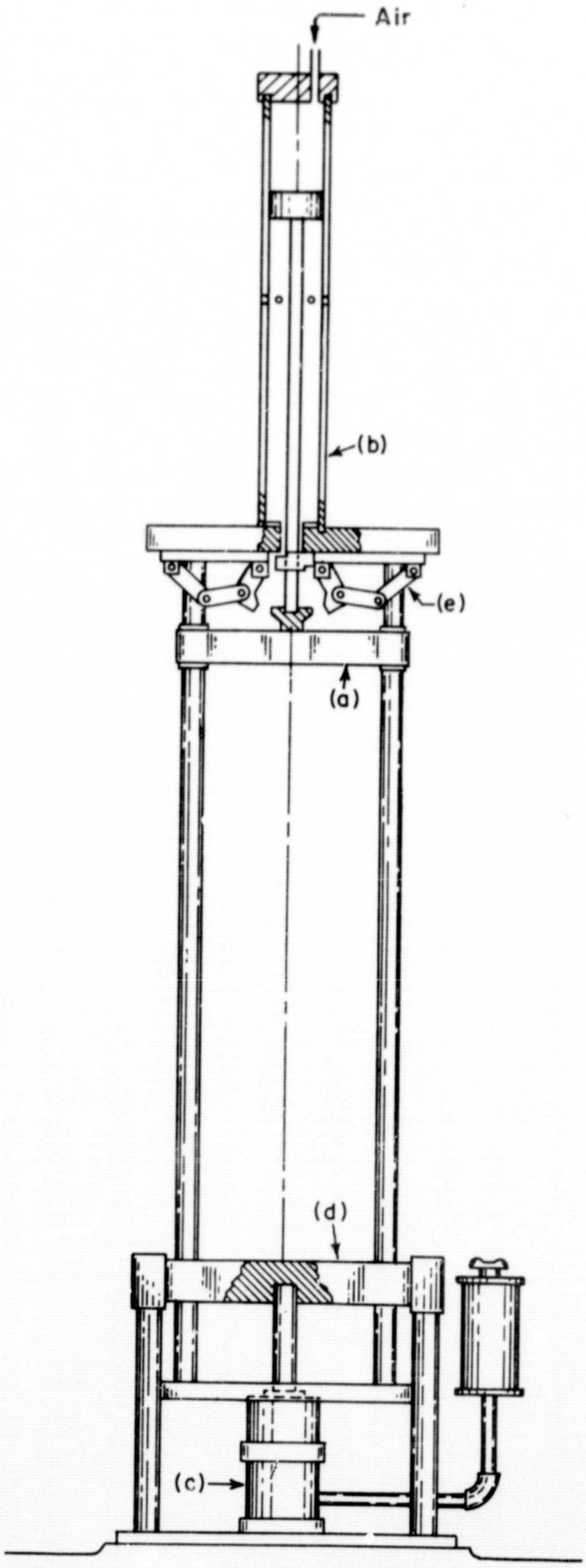

Figure 8.2. General Features of Impact Tester

the ram at the end of its travel. This shock absorber stops the ram when it is fired for calibration and check-out and operates as a back-up system during the energy absorber tests. The specimen holding table (d) is held in place by shear pins on its three support columns. In the event of an overload, the shear pins are sheared and the shock absorber stops the ram, specimen, and support plate.

The ram is held in place by a release mechanism (e) prior to launch while the clearance volume in the cylinder above the piston is pressurized with air from a compressed air bottle. After the release mechanism is operated, the pneumatic cylinder drives the ram downward, accelerating it to speeds ranging from 20 to 88 fps.

In addition to the ram shown in Figure 8.2, which is used for testing compression specimens, a second ram has been constructed for use in the testing of tension specimens. The tension testing ram is shown in Figure 8.3. In this ram the specimen (a) is held between the top flange (b) and the bottom bearing plate (c). Stop rods (d) imbedded in the specimen holding table (used also for the compression specimens) stop the top flange, causing the specimen to be acted on by the kinetic energy in the other parts of the ram.

b. Dynamic Tester Design

In a design problem such as this, the solution is arrived at through an iterative process, which starts with the requirements which must be satisfied, and ends with the finished design. Due to the nature of the design process, it is not possible to give a step-by-step account of how the design was arrived at; rather, it will suffice to describe the elements of the finished design and their justification. The first step in the design process is the formulation of a design concept based on the design requirements. As in most design problems, several concepts were generated. The concept chosen for the tester design consists of an aluminum ram which operates on three guides and is launched by the rod of a specially designed pneumatic cylinder. The ram is stopped by a specially designed hydraulic cylinder when the specimen and specimen support are not in place. This cylinder also functions as a back-up system to stop the ram, specimen, and specimen support when the shear pins holding the specimen support are sheared by an overload in the device under test.

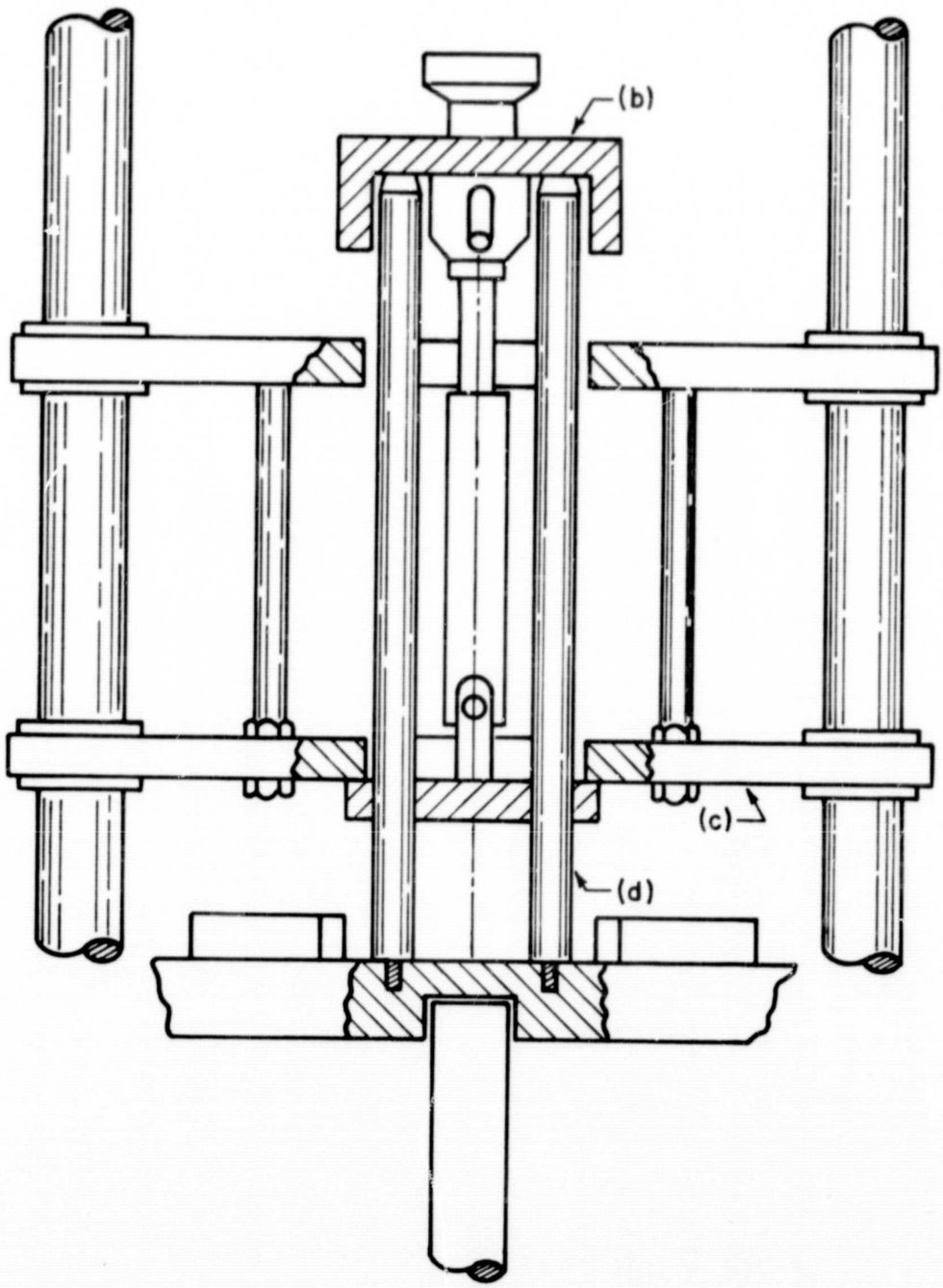

Figure 8.3. Tension Testing Ram

i. Instrumentation

Measurements are taken of the velocity of the ram prior to engagement of the specimen and the acceleration of the ram during the energy absorption process. The velocity measurement is made in one of two ways. The first of these velocity determinations is made using a measurement of the time elapsed between the interruption of two light beams by a small pin extending out from the side of the ram. This pin interrupts beams of light which are directed at photo transistors. The electrical pulses from these transistors are amplified and used to start and stop digital electronic timer which gives the time to 6 decimal places.

The second velocity measuring system designed by a group of students consists of a series of small coils which are passed by a small magnet mounted on the top edge of the ram. As the magnet passes the coils, and electrical EMF which reverses polarity is generated. The EMF reverses polarity when the magnet passes the center of each coil. These pulses are displayed on an oscilloscope with a trace saver. The time taken for the ram to traverse the distance between the coils is read from the trace and then used to compute the velocity. This system consists of seven coils spaced 4.5 inches apart so it can also be used to determine windage and friction losses in the traveling ram.

The acceleration measurement is taken with an accelerometer mounted on top of the ram. The accelerometer output is displayed by a Tektronics Model 555 oscilloscope with a type E preamplifier which is triggered by a pulse from one of the photo transistors in the velocity measuring system. A permanent record is made of the trace with a Polaroid equipped scope camera.

In addition to the above mentioned measurements, a load cell measurement will be taken of the force on the energy absorbers as a function of time. The load cell, consisting of a short, thin walled aluminum tube with strain gages attached to it, is being built as a student project. The strain data will be taken using a Tektronics Model 547 Oscilloscope with a type Q preamplifier.

High speed movies have also been made of the energy absorbing devices during impact. Cameras, which are available for use on this program, are capable of speeds up to 3500 frames per second.

c. Design of Tester Components

The tester was designed with the help of some of the undergraduate Mechanical Engineering Students. The students were assigned to groups which directed their efforts toward the solution of specific problems which were defined by the chosen tester concept. The problems worked on by the students included (1) the release mechanism, (2) safety procedures and design, (3) tester operation manual, (4) thermodynamic considerations in the operation of the driving cylinder.

i. Release Mechanism

The release mechanism, Figure 8.2 part (e), holds the ram up against the force of the driving cylinder piston rod while the cylinder is pressurized and until the mechanism is activated by a hand operated pull cable. Figure 8.4 (a) is a photo of the release mechanism in the engaged position holding the hub of the ram, while Figure 8.4 (b) shows the mechanism in the open position. This unique mechanism has an overall mechanical advantage of 1850 which allows the ram to be released under a force of 7000 lb. with a pull on the release cable of less than 5 lb.

A schematic diagram of the mechanism is shown in Figure 8.5. The hub (a) is held by the release jaws (b) which are positioned by links (c). The links are held in nearly a straight line by positioning stops (d) above, and the release pawls (e) below. Since the links are in nearly a straight line, only a small force is required by the release pawl to keep the jaws closed on the hub. Figure 8.5 also shows free body diagrams of the release jaw, the linkage pair, and the link which connects to the jaw.

Due to the geometry of the jaw, the force in the first link is $0.71\ P_o$. The linkage is adjusted for a small angle γ to insure that when the release pawl, P_2 is rotated out of the way the jaws will open under the force of the driving cylinder rod. As shown in equation below

$$P_2 = 0.71\ P \sin\gamma$$

A γ of 2° was found suitable for good operation.

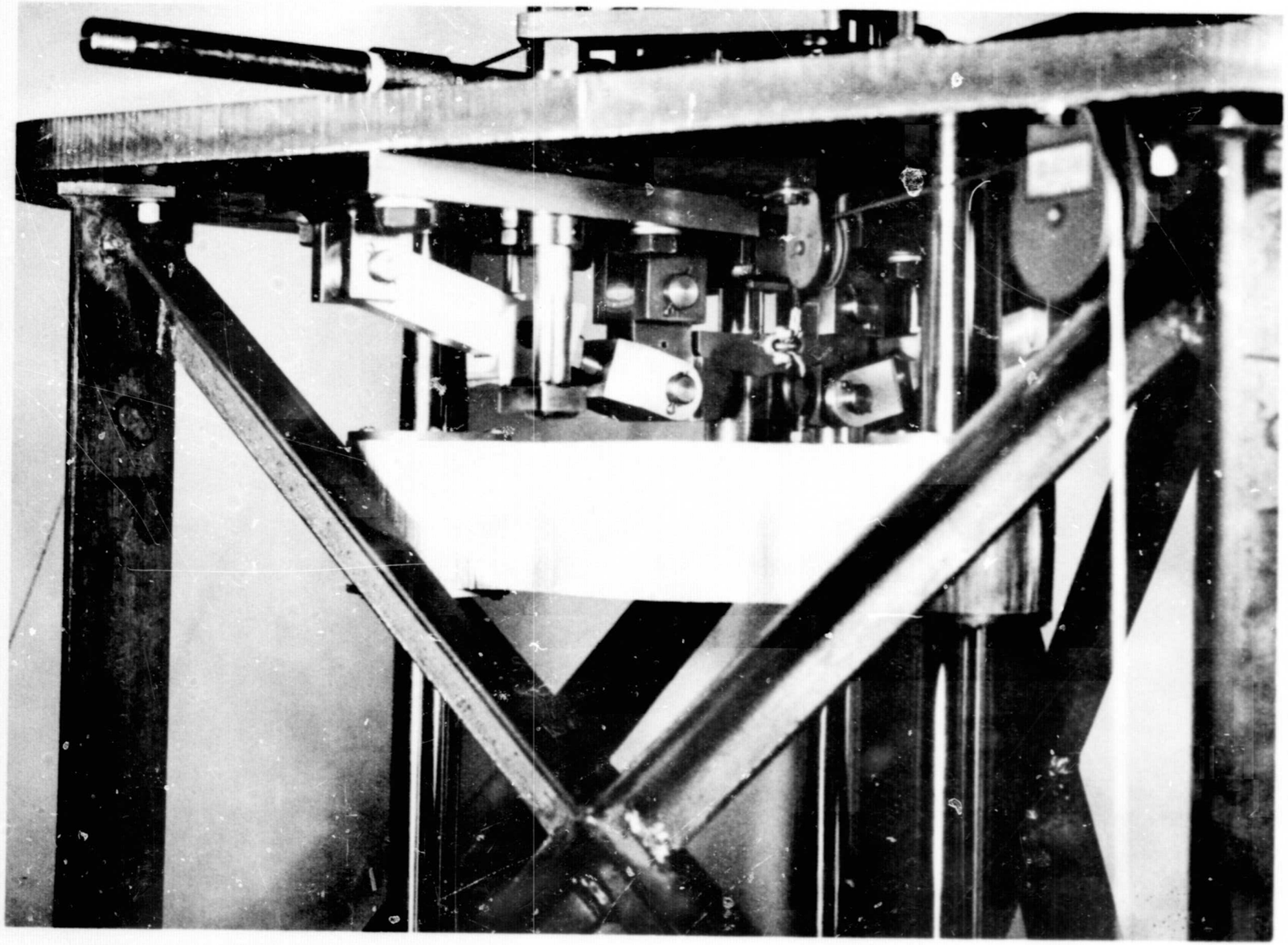

Figure 8.4.a. Release Mechanism in Engaged Position

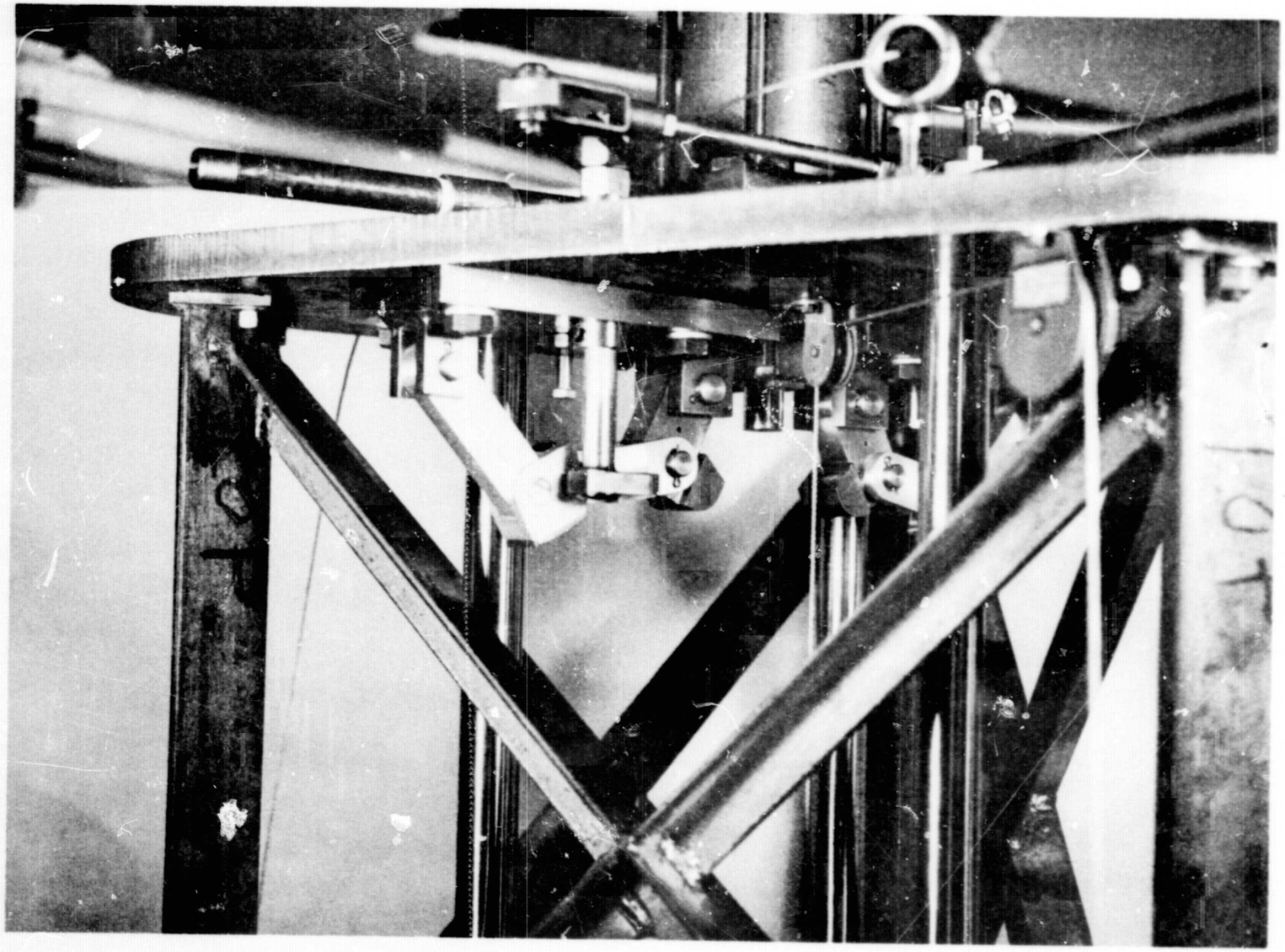

Figure 8.4.b. Release Mechanism Open Condition

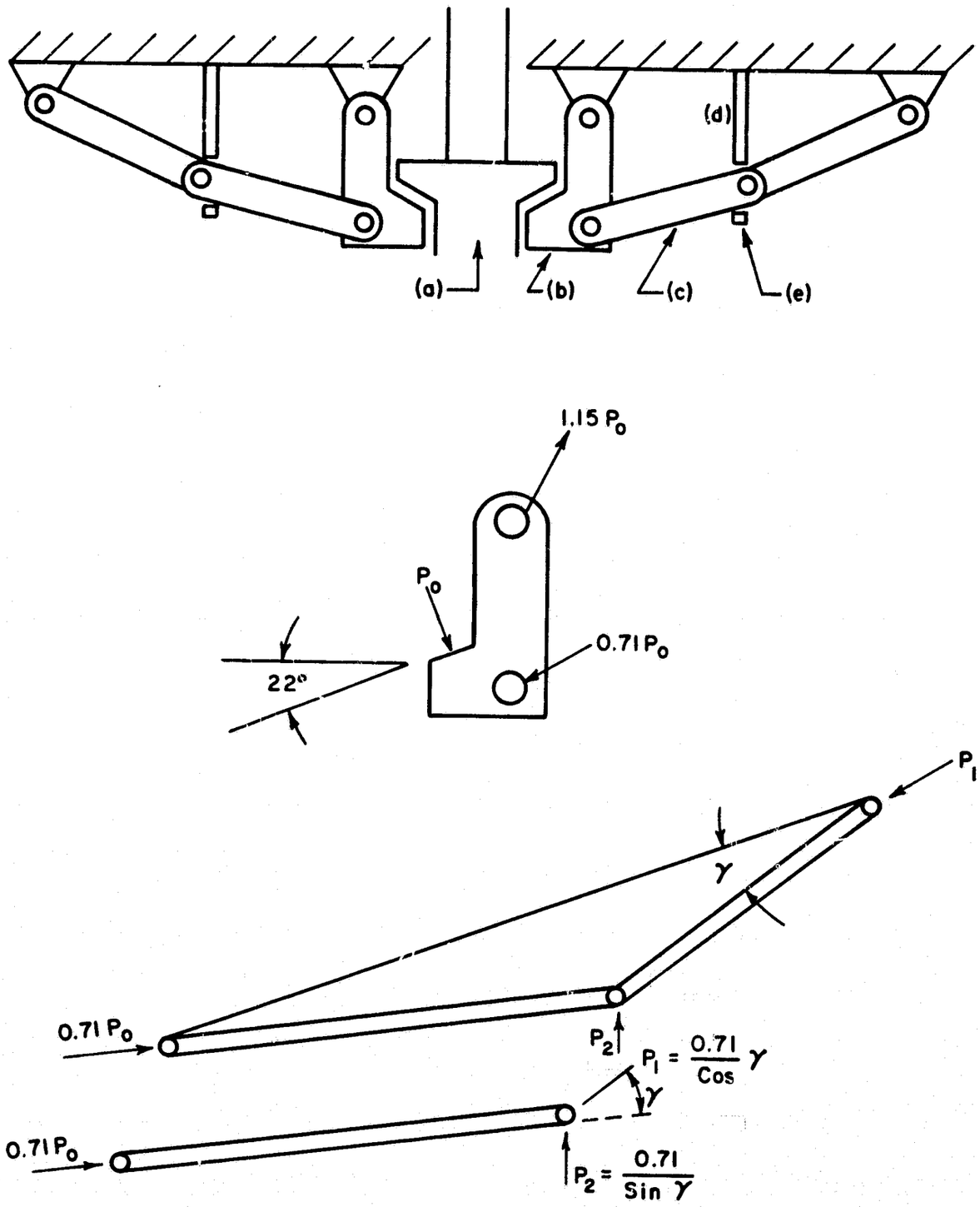

Figure 8.5. Release Mechanism

The ratio of driving and release pawl forces are then

$$\frac{P_o \cos 22^\circ}{P_o \sin 2^\circ} = 37$$

This is the mechanical advantage of the linkage. In addition to this mechanical advantage, the release pawl mechanism has a mechanical advantage of 50. This arises from a 10/1 ratio of the moment arms (release arm length/release pawl length) and a friction coefficient between the pawl and the wear plate on the link of 0.2. The total mechanical advantage of the mechanism is

$$MA = (37)\ (50) = 1850.$$

d. Driving Cylinder

The force which accelerates the ram up to speed is supplied by the driving cylinder, part (b) in Figure 8.2. This pneumatic cylinder consists of a 4 inches I.D. steel tube fitted with a nylon piston and a tubular steel rod and operated by bottled, compressed air.

The selection of a pneumatic cylinder using compressed air was motivated by the following considerations. The kinetic energy in the 36 lb. ram at 88 fps is given by

$$KE = MV^2/2 = (36)\ (88)^2/(2)\ (32.2) = 4320 \text{ ft lb.}$$

The energy must be derived from the work done on the ram by the driving force F, acting through a distance y. If the force F is a function of y then

$$KE = F(y)dy.$$

In terms of the average force $\overline{F}$, this can be written

$$KE = \overline{F}\, dy = \overline{F}(y_2 - y_1) = 4320 \text{ lb.}$$

The average force is then given by

$$\overline{F} = 4320/(y_2 - y_1).$$

Due to laboratory space requirements, the ram must be brought to speed in a distance of one to two feet. If the ram is accelerated to

speed in 2 feet, the average driving force is 2100 lb. The horsepower required to accelerate the ram to 88 fps is

$$HP = KE/550\ t,$$

where t = the time required to accelerate the ram.

Then

$$t = (y_2 - y_1)/\overline{V},$$

where $\overline{V}$ = the average velocity.

$$t = 2/44 = 0.045 \text{ sec.}$$

The average horsepower supplied during this period is then

$$HP = 4320/(0.045)\ (550) = 175 \text{ hp.}$$

The power requirement is high but the power is needed only for a short period of time. This suggested a power source in which energy could be stored, for use in a short period of time, such as a spring.

To fit these energy requirements, a unique pneumatic cylinder was designed. This cylinder is operated by the expansion of compressed air which is charged into the large clearance volume on the piston end. The motion of the piston and rod is prevented during the time the cylinder is being charged and until the ram is released by the release mechanism. When the ram is released, the force on the piston rod accelerates it. After the piston has traveled a distance of 12 inches, it uncovers exhaust ports in the cylinder wall. When these ports are exposed, the driving pressure is exhausted and the piston begins to compress the room air trapped in the rod end of the cylinder. The compression of this air brings the piston and rod to a smooth stop while the ram continues on to impact the energy absorber. Violent rebound of the rod and piston are prevented by a mechanical brake on the rod which is applied by the friction force when the rod moves in the return direction.

Since the piston and rod require energy to become accelerated and also must be stopped after the power stroke, they were made as light as possible. The piston, made of nylon, and the rod, made from steel tubing, have a total weight of 7 lb.

The acceleration of the ram by the driving cylinder can be described mathematically as follows:

The acceleration, a, is given by

$$a = \frac{PA}{M}$$

where M is the mass of the ram, piston, and rod, P is the air pressure, and A the piston area. The pressure on the underside of the piston is small compared to P and is neglected. The gravitational force is also neglected. The acceleration can be written in terms of the velocity, u,

$$\frac{udu}{dy} = \frac{PA}{M}$$

As the piston moves, the air gives up its energy by expanding. This expansion process can be approximated by the adiabatic expansion of a perfect gas which is given by

$$PV^{\gamma} = P_o V_o^{\gamma}$$

where the o's denote the initial conditions and V is the volume. γ is the ratio of the specific heats ($\gamma = 1.40$ for air). The pressure can be written

$$P = \frac{P_o V_o^{\gamma}}{V^{\gamma}} = \frac{P_o y_o^{\gamma}}{y^{\gamma}}$$

where V has been replaced by (A) (y). The equation of motion can then be written

$$\int udu = \frac{AP_o y_o^{\gamma}}{M} \int y^{-\gamma} dy$$

This equation can then be integrated to obtain

$$\frac{u^2}{2} = \frac{AP_o y_o^{\gamma} y^{1-\gamma}}{M(1 - \gamma)} + C$$

where C is the constant of integration. C can be determined by using the initial conditions, $y = y_o$ when $u = 0$.

$$C = - \frac{AP_o y_o}{M(1 - \gamma)}$$

The equation of motion is then

$$u = \left\{ \frac{2AP_o y_o}{M(\gamma - 1)} \left[1 - \left(\frac{y_o}{y} \right)^{\gamma - 1} \right] \right\}^{\frac{1}{2}}$$

This equation gives a velocity of 85.5 fps for a 44 lb. mass (ram, piston, and rod) using an initial pressure of 500 psi and a power stroke of 12 inches. The pressure on the under side of the piston has been neglected since it is quite small compared to the driving pressure.

After the piston passes the exhaust ports it begins to compress the room air trapped in the rod end of the cylinder. The energy relation can be written

$$\frac{M_p u^2}{2} = \int PAdy = AP_o y_o \int y^{-\gamma} dy$$

Where M_p is the mass of the piston and rod, P_o is the initial pressure on the rod side of the piston and y is the distance from the underside of the piston to the end of the cylinder. Intergration gives

$$\frac{M_p u^2}{2} = \frac{AP_o y_o y^{1-\gamma}}{1 - \gamma} + C$$

where C is the constant of integration. C is evaluated from the boundary conditions, $y = y_o$ when $u^2 = u^2$ max.

$$C = \frac{M_p u^2 max}{2} - \frac{AP_o y_o}{1 - \gamma}$$

The equation of motion can then be written

$$\frac{M_p u^2}{2} = AP_o y_o^{\gamma} y^{1-\gamma} + \frac{M_p u^2 max}{2} - \frac{AP_o y_o}{1 - \gamma}$$

The distance from the piston to the end of the stroke is then written as

$$y = \left\{ \frac{1 - \gamma}{AP_o y_o^{\gamma}} \left[\frac{M_p}{2} (u^2 - u^2 max) + \frac{AP_o y_o}{1 - \gamma} \right] \right\}^{\frac{1}{1 - \gamma}}$$

For $U^2 = 0$, $y = y\ min.$

$$y_{min} = \left\{ y_o^{1-\gamma} + \frac{(\gamma - 1) M_p u^2 max}{2AP_o y^{\gamma}} \right\}^{\frac{1}{1 - \gamma}}$$

The stopping distance is then

$$y_s = y_o - \left\{ y_o^{1-\gamma} + \frac{(\gamma - 1) M_p u^2 max}{2AP_o y^{\gamma}} \right\}^{\frac{1}{1 - \gamma}}$$

In development of the above relationships for the ram velocity and the piston stopping distance it has been assumed that the driving pressure drops to atmospheric instantaneously when the exhaust ports are opened. In reality, it takes a finite time for the gas to exhaust. It is impossible, however, to obtain a closed form solution for the pressure on the piston during exhaust since the pressure is a function of both volume and velocity, giving rise to nonlinear terms. The error due to neglecting the additional work performed by the air during the exhaust stroke tends to balance the error incurred by neglecting the friction in the system and the pressure on the under side of the piston during the power stroke.

Figure 8.6 gives the predicted and actual velocities obtained with a 36.78 lb. ram being accelerated with a 12 inch power stroke. Except for the low pressure end where gravitational forces on the ram are large compared to the driving force, the actual velocity is closed to the predicted. The equation for the stopping distance predicts a stopping distance of 23 inches for umax = 78 fps and y_o = 33 if it is assumed that a negligible amount of air flows out of the rod end of the cylinder during the power stroke. This compares to a measured stopping distance of 27 inches.

e. Ram Bearing Design

The ram, upon impact with the energy absorber, is subject to impulsive forces and moments. The mountings for the bearings were

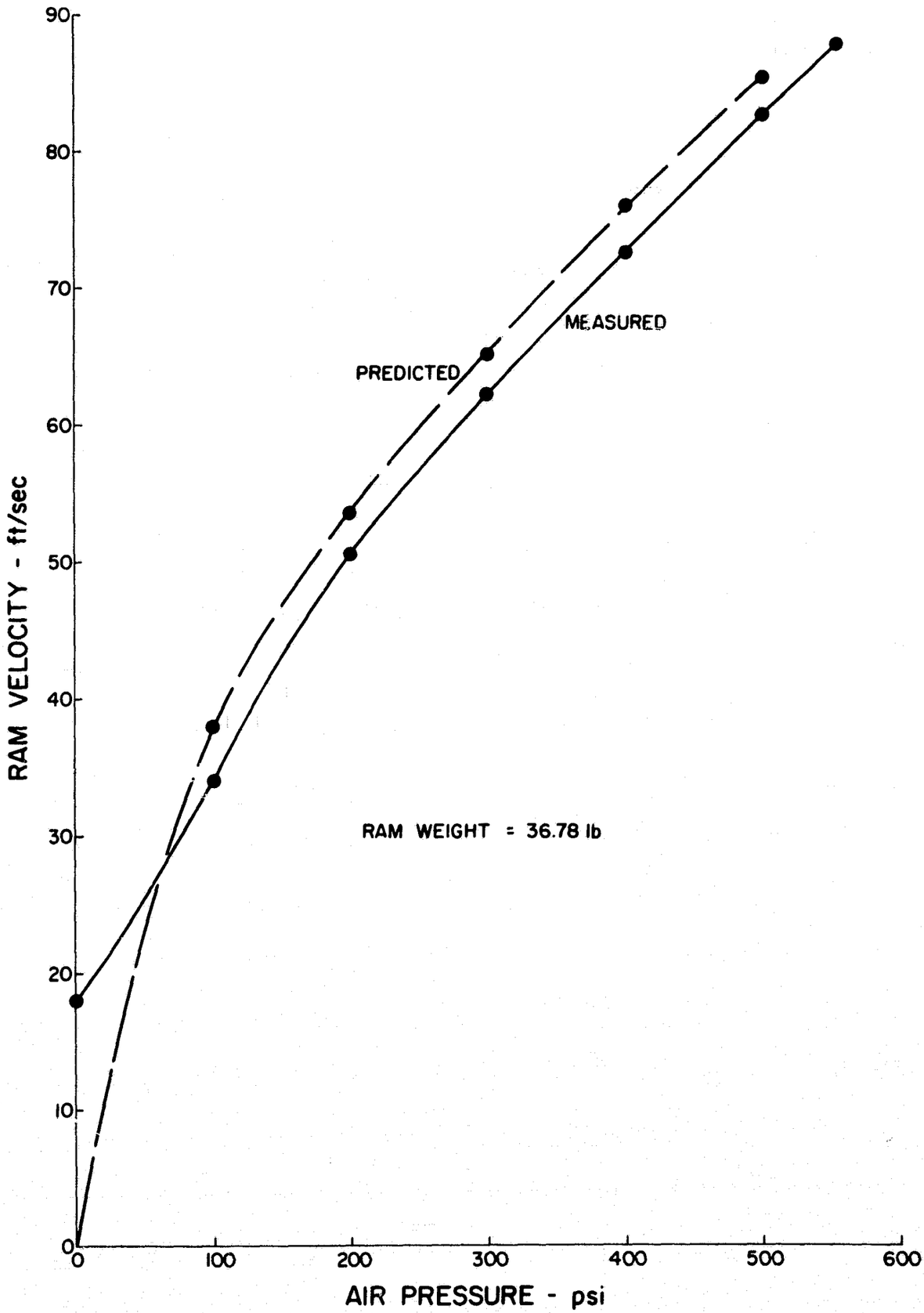

Figure 8.6. Comparison of Predicted and Measured Ram Velocities

designed to minimize the transfer of these loads to the bearings. Figure 8.7 is a photo of the compression testing ram showing the rods and the bearing retainer plates. Figure 8.8 is a drawing which shows how the bearings are mounted. The rubber mounting in the center of the bearing reduces the amplitudes of the impulsive loads transmitted from the ram into the bearings. Also the configuration allows the bearing to rotate in the mounting; this reduces the twisting loads on the bearing. When the ram rotates under the influence of a moment, the mounting rubber is compressed on the outboard side of the bearing causing a restoring force to be developed which tends to restore the ram to the horizontal attitude.

f. Piston Rod Brake

The rebound of the piston rod is controlled by the rebound brake. The brake shown in Figure 8.9 consists of two shoes, contoured to fit the rod, mounted in a cage which is free to rotate about a pivot pin in the mounting bracket. A small spring insures that the shoes remain in contact with the rod by applying a force which tends to rotate the cage counterclockwise. The diagram in the lower portion of the figure shows the geometry of the brake. A counterclockwise rotation of the brake cage about the pivot pin tends to close the distance between the two shoes while a clockwise rotation tends to open it. On the power stroke the friction of the brake shoes against the rod tends to rotate the cage clockwise and disengage it while on the return stroke the friction tends to rotate the cage counterclockwise and apply the brake. The pivot is free to move laterally a small amount to equalize the brake forces.

In operation, the break is adjusted so that the rod is allowed to return rapidly but is brought to a stop with the piston just above the exhaust ports.

g. Specimen Mounting Table and Back Up System

Figure 8.10 is a photo of the bottom part of the dynamic tester showing the specimen support table and the hydraulic shock absorber which serves as a back up system. The specimen support table is seen at the top of the picture. It is supported on three columns; one of these is seen in the center foreground of the picture. The coupling between the table and the columns is provided by shear pins. If the tester is overloaded the shear pins fail allowing the hydraulic shock absorber to pick up the load.

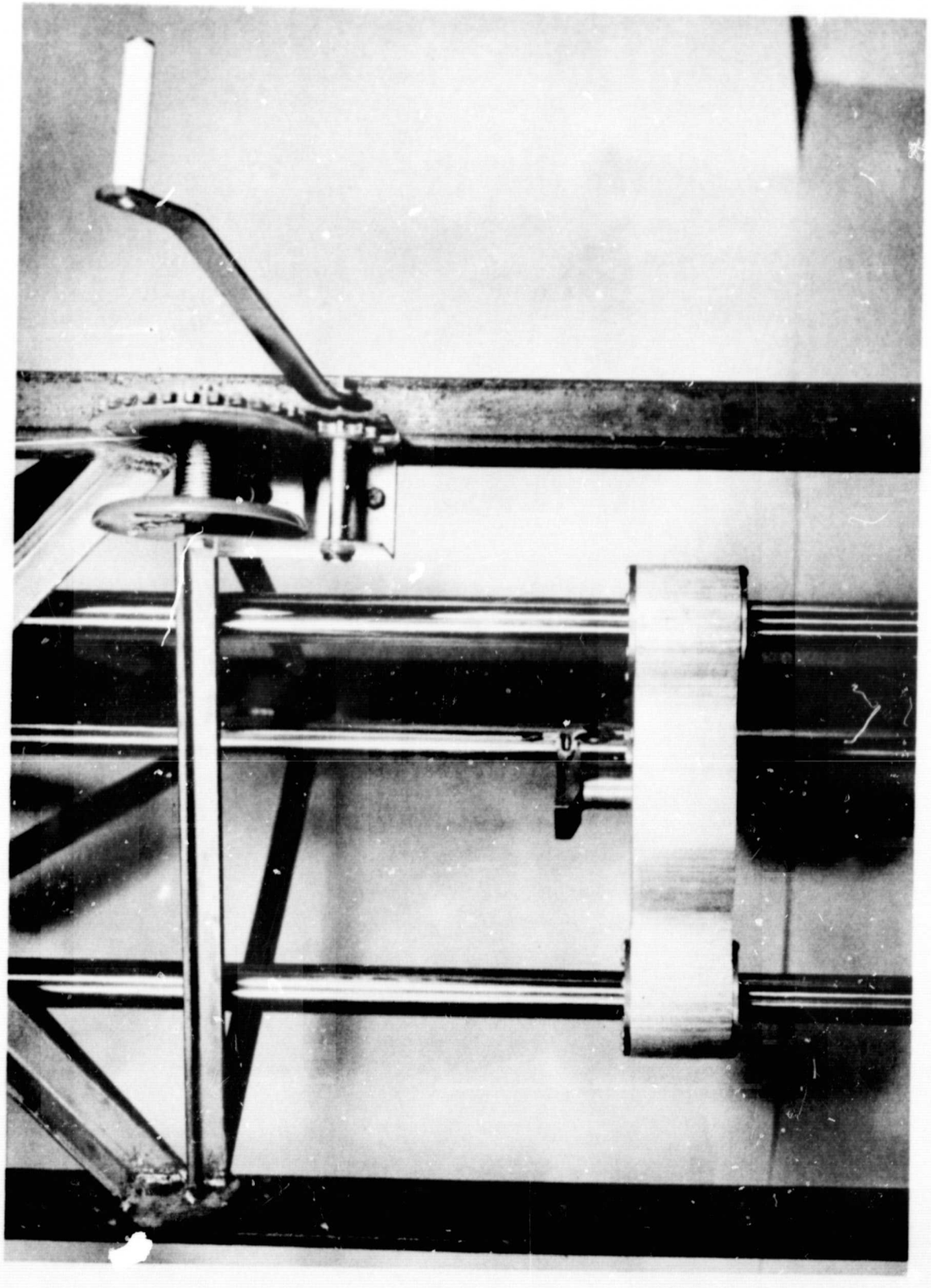

Figure 8.7. Compression Testing Run

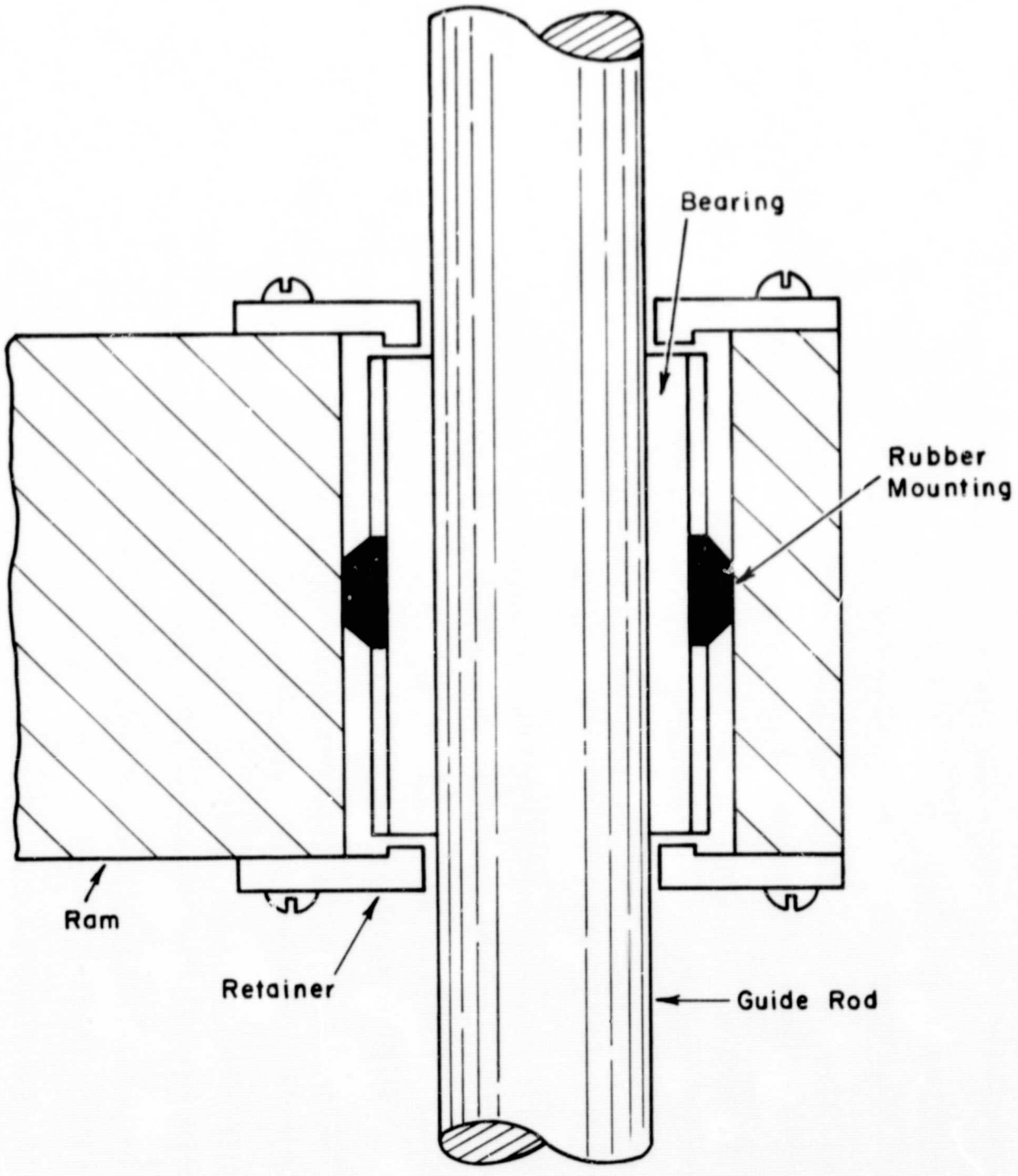

Figure 8.8. Bearing Details

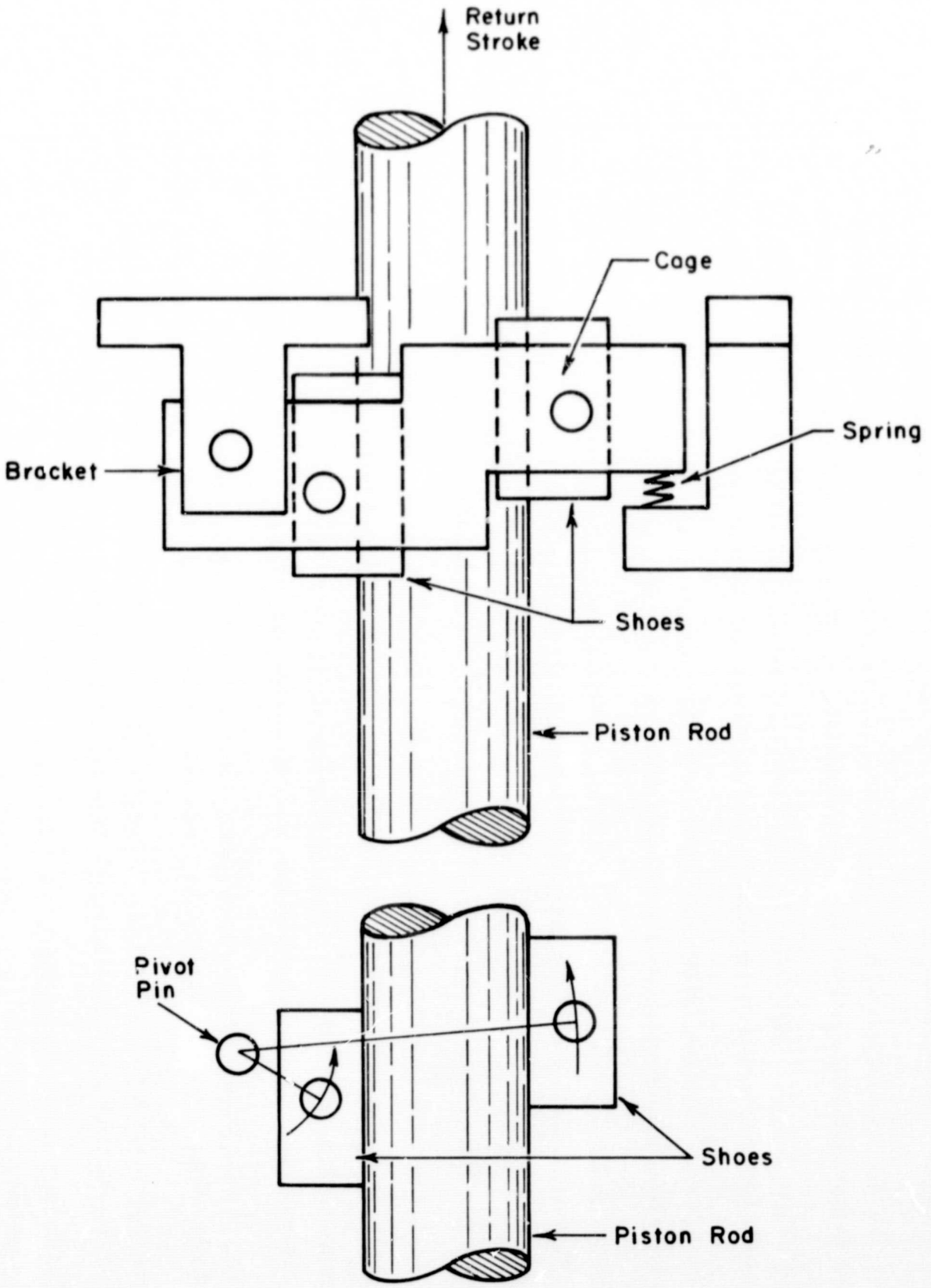

Figure 8.9. Rebound Brake

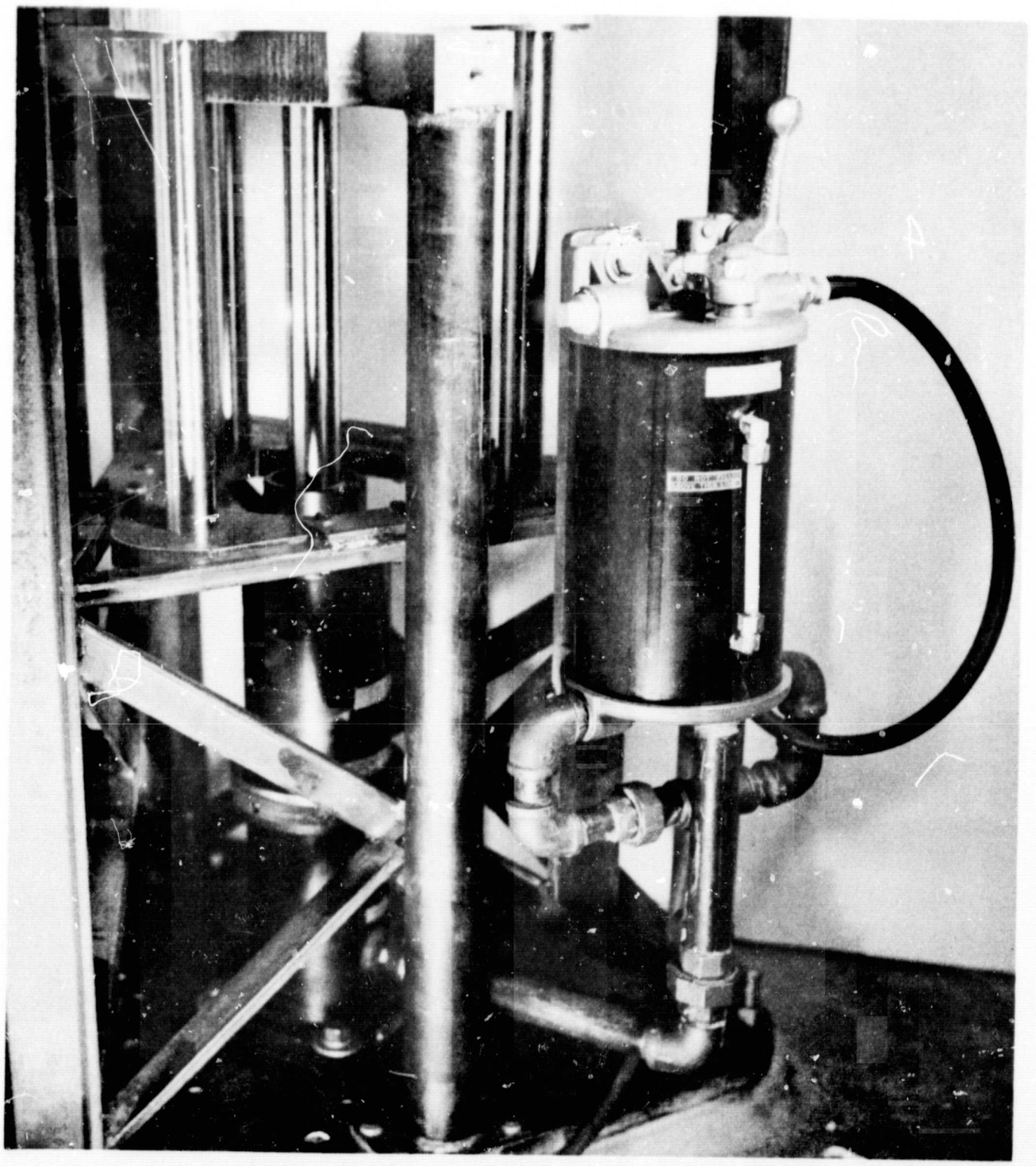

Figure 8.10. Specimen Support Table and Hydraulic Shock Absorber

The shock absorber is an Ace Controlls Model AHA 3X12-SX designed specially for this application.

h. Experimental Results

The results of the tests conducted on the energy absorbing devices using the static and dynamic testing machines are included in another section of this report.

IX. MARKET ANALYSIS

A market analysis for energy absorbing devices was initiated with the help of Professor Sciullo of the School of Business Administration. A wide range of possible applications was uncovered in this study. They are listed below.

1. Protection of highway fixed obstacles and guard rails
2. Automobile protection
3. Seat belt restraints
4. Use on trains, elevators, and subways
5. Cargo adaptations - protection in packaging
6. Dump trucks and bulldozers
7. Stopping planes on aircraft carriers
8. Helicopters - under seats and on undercarriages to absorb vertical crash impact
9. Platform airdrops
10. Front end of locomotives
11. Camper trailers
12. Trailer trucks
13. Parking garages - guard rails and elevators
14. Energy absorbing helmet liners
15. Absorption pack on the back part of seats in buses to protect passengers when thrown forward (to avoid being a hindrance like a seat belt)

However, since almost all of the NASA patents on energy absorbing devices are high performance, nonreusable devices, this narrowed down the market for applications accordingly. Only those applications seemed suitable which called for very large amounts of energy absorption on infrequent occasions, where the necessity of replacing the energy absorber would be a minor consideration.

Applications to highway safety (items 1, 2, and 3 above) therefore stood out as the most promising. There is a widespread need for protection around fixed highway obstacles such as bridge abutments and

highway bifurcations which claim a large number of lives each year. Guard rails on highways at dangerous locations are widely used in an energy absorbing capacity. Protection for automobiles in collisions and energy absorbing seat belt restraints for passengers are related applications for highway safety.

To sum up, it seems that application of energy absorbing devices to protection of fixed highway obstacles, automobile protection and seat belt restraints are the best market for high-performance nonreusable energy absorbing devices. The market for these applications is big enough so that concentration on them to the exclusion of other applications at the present time appeared to be well justified. Impact protection for the front end of locomotives to reduce grade crossing accidents looks promising, also, but consideration of this application has been postponed.

X. APPLICATIONS AND DESIGN

A. Introduction

Applications and design go hand-in-hand. Design engineering studies cannot be done without a specific application in mind, and energy absorbing devices cannot be used without being designed into a system that will give the required performance for the intended application. At the present time, applications have been narrowed down to the protection of fixed highway obstacles, automobiles and seat belt restraints. This has provided the design effort with well defined goals.

Early in the program, three background questions were investigated, and reports were written on the findings. The questions are:

1. What happens in an automobile collision?

2. What is human tolerance to deceleration?

3. What do automobile accidents show that is pertinent to the application of energy absorbing devices?

The information providing answers to these questions is presented in the following appendices - 3, 4 and 5 of this report.

Appendix 3. G-Loadings on Automobile Passengers During Collision

Appendix 4. Investigation of Human Tolerances to Decelerations

Appendix 5. Survey of Automobile Accident Statistics

B. Some Design Considerations Regarding Energy Absorbing Devices in Vehicle Crash Protection

The primary purpose of energy absorbing devices must be to prevent or minimize injury during collisions by limiting the g load on the occupants of the vehicle. It appears to be widely accepted that the extent of human injury depends in some manner on the time history of g loading. Therefore, the allowable or design g loading, denoted by $\bar{g}$, is in general, a function of time. We do not yet have reliable information concerning this, and for purposes of simplicity we shall assume that $\bar{g}$ is a constant in the remainder of this discussion.

In order for energy absorbers to be effective, secondary collisions, i.e., collisions between occupants and the interior of the car must be prevented. The simplest means of accomplishing this is through the use of seat harnesses. In our discussion of energy absorbing devices, it will be assumed that seat harnesses have been provided and are in use at the time of impact.

The two obvious locations where energy absorbing devices can be placed on existing cars are (a) between the bumpers and the car body and (b) between the harnesses and the car frame. These placements are shown schematically in Figure 10.1, the former denoted by D_b and the latter by D_d.

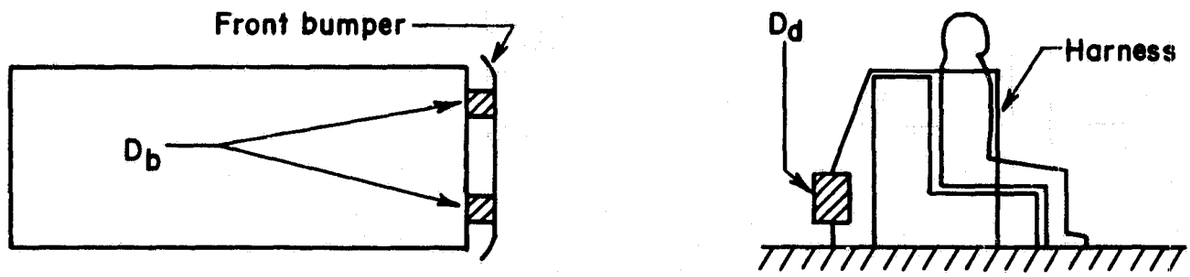

Figure 10.1. Location of Energy Absorbing Devices in Passenger Vehicles

In order to discuss the D_b and D_d devices, we shall examine an often fatal accident situation, namely that of a head-on collision between a car and a large stationary object, e.g., tree, telephone pole, or brick wall. Assume that a car of mass m_c has a single occupant of mass m_d and is travelling with velocity v when it strikes a fixed object. With no energy absorbing device, the car body itself acts as an energy absorber and the initial kinetic energy of the car and driver is approximately equal to the work done in deforming and tearing the body of the car. The driver, being rigidly harnessed to the seat, experiences the same deceleration a as the car frame, namely

$$a = \frac{F_c}{m_c + m_d} \tag{10.1}$$

The force F_c depends on the force-displacement relation for the car, information which we do not presently have available, but which we are

attempting to obtain for at least a typical American-make car. For a front-engine car, however, we can speculate that the major characteristics of the force-displacement relation are as shown in Figure 10.2.

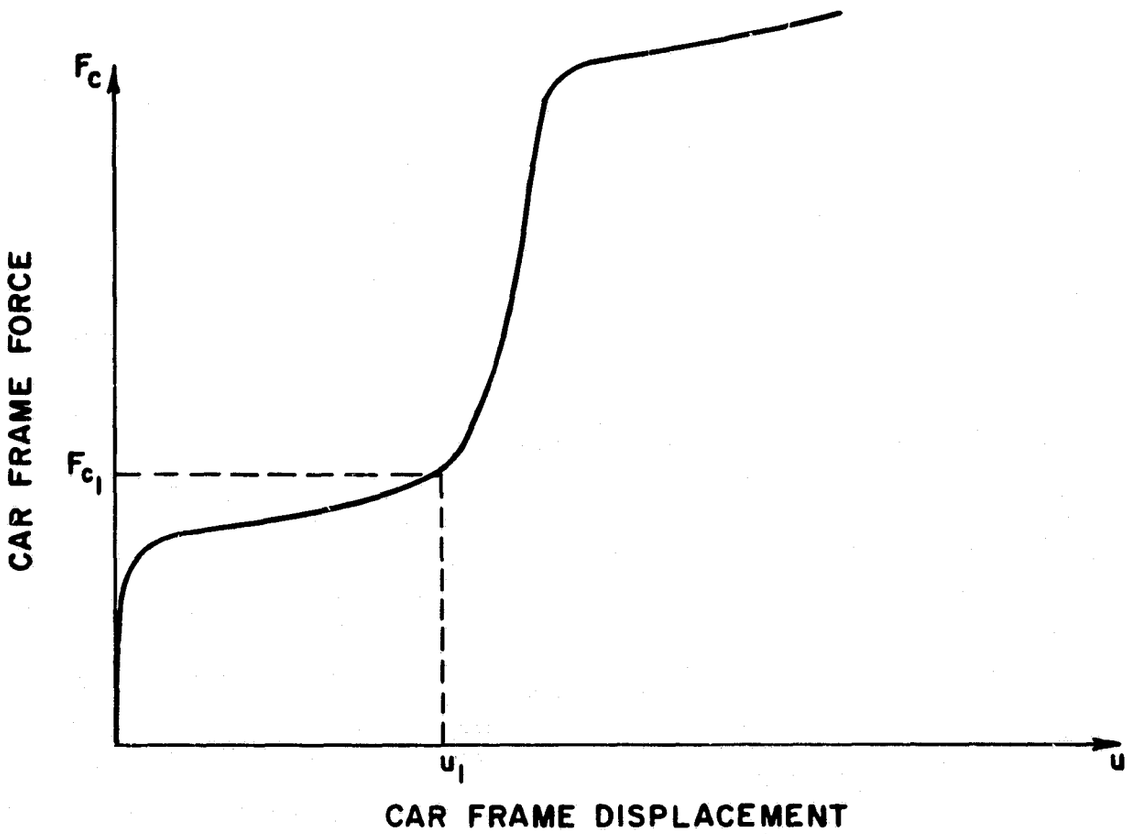

Figure 10.2. Car Frame Displacement

The initial rise in F_c occurs as a result of elastic and plastic flow. Then buckling and/or fracture occurs producing large displacements. After the displacement, u_1, is attained, the front end of the car strikes the engine block and much larger forces are needed to produce further displacement. Since severe injury does not always result from low velocity collisions, the g loads produced by F_{c_1} are apparently less than $\bar{g}$ for most cars. The work done on the car is

$$W_c = \int_0^u F_c \, du \tag{10.2}$$

or simply the area under the force-displacement curve up to the displacement u where the car has come to a complete stop. Ignoring such effects as energy conversion to heat, the work W_c must equal the initial kinetic energy K of the car, i.e.,

$$W_c = K = \frac{1}{2}(m_c + m_d)v^2 \qquad (10.3)$$

where m_c and m_d are the masses of the car and driver respectively. The safety of the driver from (10.1), depends on F_c, which, from (10.2) and (10.3) depends on K. When K is sufficiently large it must be absorbed by displacements $u > u_1$, in which case the force F_c becomes high enough to produce severe decelerations.

Let us now examine how the chances of injury can be reduced through the use of an energy absorber. For simplicity we shall assume that the force-displacement relations for the car, for D_b, and for D_d are as shown in Figures 10.3, 10.4, and 10.5. The "stroke" or maximum displacement of D_b and D_d are u_b and u_d respectively. At these displacements the devices have "bottomed out" and are no longer of any value.

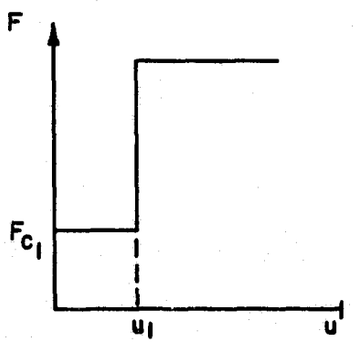

Figure 10.3. Force-Displacement Relationship for Car

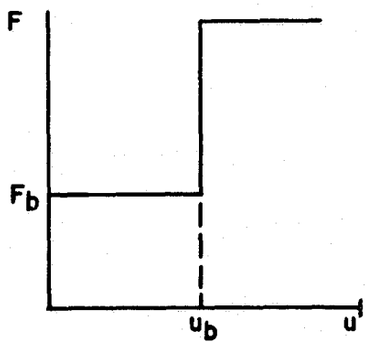

Figure 10.4. Force-Displacement Relationship for D_b

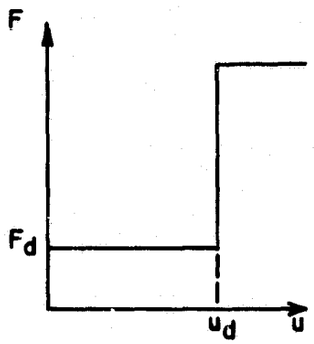

Figure 10.5. Force-Displacement Relationship for D_d

a. Use of a Bumper Energy Absorber

If a bumper device D_b is used, the force F_b it transmits must be such that

$$F_b \leq (m_c + m_d)\,\bar{g} \tag{10.4}$$

if injury is to be avoided. However, F_b and u_b should be as large as possible in order to absorb large amounts of energy, for if

$$K > F_b\,u_b \tag{10.5}$$

the energy absorber will bottom out and the remaining energy, i.e., $K - K_b\,u_b$, will be absorbed by deformation of the car. Since F_b is constrained by (10.4) an increase in safety can only be obtained by increasing the stroke of the device. For bumper devices the maximum stroke is probably anywhere from 6 inches to 12 inches depending on the device and the car in which it is installed. If $\bar{g}$ is 20g (g = acceleration due to gravity) and the combined weight of car and passenger is 4000 lbs., then F_b is 80,000 lbs at most, and D_b will be able to absorb no more than 80,000 ft-lbs, which is approximately the kinetic energy of a car traveling at 25 mph. We have assumed that for most cars $F_{c_1} < (m_c + m_d)\,\bar{g}$. Thus, if $F_b = (m_c + m_d)\,\bar{g}$ we shall have the car body crumpling before the energy absorbing device D_b is activated. There is nothing wrong with this from the standpoint of safety since the crumpling of the car body provides additional energy absorption at safe g loads. However, it might be difficult to sell a product which, for low velocity impacts, remained intact while the fenders needed replacement. It therefore seems reasonable to design D_b such that $F_b < F_{c_1}$ whenever the energy absorbing capabilities of D_b are not severely reduced in the process.

b. Use of a Harness Energy Absorber

Design considerations for a harness energy absorber D_d are much the same as for a bumper device. Force F_d and stroke u_d should be as large as possible in order to provide the maximum amount of energy absorption. However, F_d is constrained by the safety requirement

$$F_d \leq m_d\,\bar{g} \tag{10.6}$$

while u_d should not be sufficiently large to allow secondary collisions to occur. The stroke of D_d will be limited by the distance between the driver and the steering column, approximately one foot. On harnesses for the passengers or on cars with collapsible steering columns, u_d can be larger than a foot. A harness device only absorbs the kinetic energy of the harness wearer. Thus, for $\bar{g}$ = 20g, w_d = 150 lb, and u_d = 1 ft, the maximum work done on D_d is 3000 ft-lb, which is about equal to the kinetic energy of a 150-lb man traveling at 24 mph. The device D_d will, of course, not be activated until the force applied through the harness reaches F_d. Until this time the harness acts as a rigid constraint and the force is equal to the product of the wearer's mass and the acceleration of the car body. Thus, when $F_d > F_{c_1}$, the device will not be activated until the car body has been compressed a distance equal to u_1. During this time the car and driver have been decelerating from the velocity at impact so that when D_d is activated, the kinetic energy of the driver will have decreased by an amount approximately equal to $F_{c_1} u_c$. Thus, in the example given, safety is afforded when the velocity of the driver at the time when D_d is activated is less than 25 mph. The crumpling of the car body at fairly low loads therefore provides additional safety just as in the case of the bumper energy absorber.

c. Comparison of D_b and D_d

For most cars D_d will be able to have a stroke comparable to D_b and will therefore be able to give protection at higher impact velocities. Further, a harness device, having only to absorb the kinetic energy of a single person rather than that of an entire car, will probably cost a good deal less to manufacture than a bumper device and should also be simpler to install. However, the effectiveness of a bumper energy absorber depends little on the weight of the occupants of the car, for in general, this weight is at most 20% of the weight of the car. Thus, if F_b is designed such that it is equal to $m_c \bar{g}$, then a fully loaded car lowers the deceleration during impact to a value only slightly lower than $\bar{g}$, and the efficiency of the device is not greatly impaired. On the other hand, consider a harness device which is designed for a 200-lb man. If his 100-lb wife drives the car, the g load she sustains during impact will be $2\bar{g}$, so that the energy absorber offers her no protection at all. On the other hand, if the device is designed for the 100-lb wife, it will substantially decrease the protection afforded the husband. The effect of the harness wearer's weight becomes even more severe when small children are considered. This difficulty is caused by the fact that the devices under consideration are "force limiting" rather than "acceleration limiting."

d. Use of D_b Together with D_d

The use of a bumper device together with a harness energy absorber can increase safety, for a properly designed bumper device will lower the kinetic energy of the occupants at the time the harness devices become operative. Thus, if F_b produces car decelerations $g_c < \bar{g}$ while F_d produces driver deceleration $g_d \leq \bar{g}$ with $g_c < g_d$, then D_d will not be activated until D_b bottoms out.

However, if the car deceleration is greater than g_d then D_d is activated immediately and must absorb the entire initial kinetic energy of the driver. If it does not, the driver will displace u_d and then quickly decelerate to the velocity of the car (the velocity of the car will be less than that of the driver since it has higher rate of deceleration). The magnitude of the secondary deceleration is likely to be greater than $\bar{g}$ because of the rigidity of the seat harness. Even if this is survived, the occupant now becomes subject to the high g loads which are likely when D_b bottoms out. We conclude that the bumper device, when used with a harness device, is of little help unless $g_c < g_d \leq \bar{g}$.

Let us now consider a combination of the examples previously given for D_b and D_{d_1} where F_b is now slightly less than $(m_c + m_d)\,\bar{g}$ and F_c is equal to $m_d\,\bar{g}$. D_d offers protection if it becomes operative when the velocity of the driver is $\leq$ 25 mph. The bumper device can safely absorb about 80,000 ft-lb, which is what is necessary to reduce the speed of the car from 36 to 25 mph. Thus, by properly using the two devices in tandem the allowable speed at impact is increased from 25 to 36 mph. The above discussion ignored the effect of the crumpling of the car body. As before, this will increase the allowable speed of impact.

e. Comments

We have seen that the installation of energy absorbing devices can significantly improve the chances of sustaining a head-on collision without injury. They cannot, however, provide protection in high-speed, head-on collisions under present car designs. In order to obtain a rough idea of what can be done by car redesign we shall introduce a new parameter - the stopping distance s, i.e., the distance traveled by the driver between the moment of impact and the time he comes to a complete stop. Under the condition of constant deceleration the g load

sustained by the driver for a given initial velocity is inversely proportional to the stopping distance for

$$a = \frac{dv}{dt} = \frac{v}{\bar{v}/s} = \frac{1}{2}\frac{v^2}{s} \tag{10.7}$$

where $\bar{v} = v/2$ is the average velocity during impact. Again, assuming $\bar{g} = 20g$, the safe stopping distance is

$$s = \frac{v^2}{1240} \tag{10.8}$$

For example, if v = 36 mph = 51 fps then the stopping distance is two feet, which is equal to the stopping distance provided by $D_b + D_d$ in the examples. If we wish to provide safety for 60 mph head-on collisions, then the stopping distance must be about 5-1/2 ft. This is clearly impossible unless the entire front end of the car is designed to act as one long energy absorbing device. In order to do this without lengthening the car, the engine must be either moved or redesigned.

We have limited ourselves to a discussion of head-on collisions, but the concepts involved can readily be applied to other impact situations. Thus, safety in general, depends on controlled deceleration over a distance which is sufficiently long so that absorption of the changes in kinetic energy which occur during impact can be effected. It follows that the distance between an occupant and the interior of the car should be as large as possible and therefore complete safety can only be approached by increasing the dimensions of a car. For crashes with fixed highway obstacles, the provision of energy absorbing systems around the obstacle can provide a great deal of protection since much more additional stopping distance is available.

The analysis contained herein is rather elementary and is intended only as a first estimate of the actual accelerations, forces, etc., which occur during impact. A more complete description of impact mechanics, depending on the solution of a rather difficult stress wave propagation problem, may prove to be of value when more information concerning basic parameters is known, e.g., the relationship of $\bar{g}$ with time and the dynamic operating characteristics of the energy absorbers.

Even these approximate considerations are quite valuable in providing guidance for the design of protection systems for fixed

highway obstacles, cars and seat belt restraints. Design efforts are therefore proceeding concurrently with more sophisticated analyses of energy absorbing devices.

C. Current Activities

Currently five questions are under investigation. These are:

1. Study of a specific highway bifurcation or gore area. This study is now focused upon determining the possible directions and speeds of impact of vehicles against the gore area. This specific information will be needed for the design of an energy absorbing device for buffering this bifurcation. This question is being studied in cooperation with the Colorado Division of Highways.

2. Consideration of automobile configurations to promote redirection upon collision. Could automobiles be designed to glance off each other or off obstacles at the time of collision rather than coming to a crunching halt?

3. Consideration of passenger compartment location and possible energy absorption and redirect detachment of the passenger compartment at the time of collision.

4. Analysis of the dynamics of the passenger-seat belt system when the seat belt contains an energy absorbing device.

5. Application of energy absorption to make the windshield and dash board area more survivable for the unrestrained passenger.

XI. EXPLOITATION OF RESULTS

Pending the identification of the best patented energy absorbing device, we have conducted exploratory discussions with a number of organizations.

We have corresponded with Lowell G. Turner, Division Patent Counsel of the Lockheed Corporation, which owns Patent No. 3,236,333 (which is an improvement of the NASA Patent No. 3,143,321) with regard to the possibility of our undertaking the exploitation of this patent. Mr. Turner has expressed a willingness to discuss terms and conditions of such an agreement with us. We have delayed any further discussions with Lockheed until we have conclusively established the relative merits of their patent.

We have applied to Mr. Gayle Parker, in the Office of the General Counsel of NASA for an exclusive license for Patent No. 3,143,321, in order to establish a precedent for acquiring rights and exploiting a NASA patent. This application was turned down on the grounds that the Department of Transportation had funded a research program with Southwest Research Institute for applying this specific patent to guard rail use (although it is by no means clear as that this is the best patent).

We have discussed our exploitation plans with Dr. Armand Fredericksen of King Resources, Denver, and Mr. Lee Inscho of the Gates Rubber Company, Denver. Both people have expressed an interest in exploiting our end results when they become available, provided, of course, that the economic forecasts for these energy absorbing patents are favorable.

The essentials of the exploitation problem with private companies are turning out to be the question of patent ownership and the availability of an exclusive license from NASA, if the best patent is NASA owned. It is the opinion of members of the National Inventors Council that no one will be willing to take on the costs of exploiting a new device without either patent protection or an exclusive license from NASA.

We have made contacts with the Colorado Highway Department, which has proved very receptive to the idea of using the results of our program to design protection systems for fixed highway obstacles. We are presently working with them to define their requirements and arrive at an acceptable design incorporating either the tube and mandrel or collapsing tube.

We have also made contact with a small company in Los Angeles called Mechanics Research Incorporated, which owns some of the patents on energy absorbing devices. Conversations with Mr. Platus, an inventor/stockholder in this company indicated they would be interested in using the end results of this program. In fact, they have referred to this program in a recent proposal they made to the Department of Transportation, stating they would use our results.

To sum up our findings on the exploitation of unused patents for energy absorbing devices,

1. If the best patent turns out to be one held by NASA, an exclusive license will be necessary for a private company to undertake the manufacturing and marketing.

2. If the University can acquire an exclusive license to this patent from NASA, it can benefit directly from the exploitation process by sub-licensing it to a manufacturer.

3. If the best patent turns out to be privately owned, the results of this program may well provide enough of a stimulus to get it into production and use. The University will not benefit directly from the exploitation of such a patent.

As part of the program on the exploitation of unused NASA patents, a 15-20 minute documentary film is being prepared with the help of the Department of Mass Communications. The purpose of this film is to document our efforts on this program and to explain the multidisciplinary effort required to reduce a patent or a new scientific discovery to a new product or a new technology. It explains the multidisciplinary nature of engineering, and shows how this particular project educates the engineering students in the nontechnical aspects as well as the technical aspects of their profession.

The basic purpose of this film is to show what an engineer can best contribute to society, and how this particular program educates him for that purpose.

XII. BY-PRODUCTS OF THIS PROGRAM

There have been a number of interesting by-products in this program.

A. Department of Transportation

After seeing our scale model impact tester and discussing the scale model testing capability we have developed on this program, Mr. Tamanini of the Department of Transportation recommended that we make our capabilities available to State Highway Departments to conduct quick and inexpensive evaluation of new protective devices that are proposed to them by different manufacturers.

As a result of his visit, Colorado State Highway Department representatives have expressed an interest in using the results from this research program for designing the protection for a fixed highway obstacle which has claimed several lives to date. We are therefore engaging in a cooperative effort with them to apply our results to their needs.

B. American Society Engineering Education

The Design Engineering Committee of the American Society of Engineering Education expressed an interest in hearing about this program. Professor Ezra briefed them on it in March of this year and Professor Parks will be presenting an invited paper on this program at the National Meeting of the American Society of Engineering Education. in June 1969.

C. Small Business Administration

The Small Business Administration has been charged with the responsibility of finding ways and means of making new technology available to small business concerns which need new products and which wish to expand. Professor Ezra gave a talk on this program in Denver to a meeting of technology utilization officers of the Small Business Administration. They were:

1. Levin W. Foster, S.B.A. Office, John F. Kennedy Bldg., Boston, Mass.

2. Bruce D. Gipsen, S.B.A. Office, Dallas, Texas

3. Arthur T. Gilmore, S.B.A. Office, New York, New York

4. Nicholas Kondur, S.B.A. Office, San Francisco, California

5. Jack Lang, S.B.A. Office, Los Angeles, California

6. T. F. Lawrence, Jr., S.B.A. Office, Atlanta, Georgia

7. Leonard Palmer, S.B.A. Office, Denver, Colorado

This meeting resulted from a contract which the Technology Utilization Division of NASA has with our Industrial Economics Division. The above S.B.A. representatives expressed an interest in our program and a number of them have been actively making our efforts known to appropriate small businesses. In particular, Mr. Leonard Palmer of the S.B.A. Office in Denver has been actively steering heads of small companies in the Denver area to us. It is possible that S.B.A. will be very helpful in the exploitation of the end results of our program.

D. NASA Pasadena Office

Mr. Paul McCaul, of the NASA Pasadena Office, called and asked our advice on the merits of a particular energy absorbing patent owned by Aerospace Research Associates, whose ownership was being disputed by NASA. Our advice was that this particular device, consisting of rolling toroids between two concentric cylinders (see Figure 5.2) had been evaluated by us, and found to be less cost-effective than several other patents. (It is interesting to note that the Department of Transportation, which did not use a systematic screening approach to find the best energy absorbing device, has funded full scale evaluation on this device, and that the New Mexico Highway Department has purchased and installed three of these.)

E. Educational

As a result of this multidisciplinary research program a number of engineering students are being exposed to and trained in the solution of the nontechnical problems of exploiting a new technical idea. They are being made aware of the large gap between a new patent and the resulting product, and are learning how to bridge this gap.

The engineering faculty are getting a firsthand opportunity to practice their profession. This is important because the applied nature of the engineering profession presents few opportunities for an engineering professor to practice his profession on a university campus, in contrast with a professor of physics or mathematics or chemistry who gets every opportunity to do physics or math or chemistry in a university environment.

The faculty of the Law School and School of Business Administration seem to have the same difficulty as the engineering faculty in practicing their profession in a university. It was interesting to note that the graduate business administration students on this program were well trained in the details of running an existing company, but knew little about what it took to start a new enterprise or to exploit a new product.

A number of promising graduate engineering thesis problems on the theoretical aspects of energy absorption have been identified. They are the following:

1. Folding Tube:

Determination of the Folding Mode:

Under direct axial load the tube forms folds where cross sections are either circles or regular polygons. It will be necessary to develop a theory to predict the folding mode as a function of tube diameter, wall thickness, and material strength properties. The study of the effect of initial imperfections and lateral components of load on the buckling mode is also appropriate.

Prediction of Force-Displacement Characteristics:

The axial force necessary to statically fold a cylindrical tube oscillates about an average value. The magnitude of the oscillation apparently depends on the buckling mode and the work hardening characteristics of the material. A study of the relationships between these parameters is suitable for graduate work.

2. Extrusion Device:

This device involves forcing a soft plastic through a nozzle. An analysis of a viscoelastic material forced through an opening is a far from trivial problem since the material would be well into the nonlinear range.

3. Cyclic Plastic Deformation:

A typical problem suggested by this type of device would be the large deformation cycling of an elastic-plastic beam. Such a problem involves geometric as well as material nonlinearities.

F. Interaction with Other Universities

The University of Utah and Brigham Young University have been briefed on our program and have expressed a desire to use our results and assistance on a D.O.T. project they are bidding on. In response to D.O.T. request for proposal entitled "Study of Design of Passenger Vehicle Bumper and Underride Guards for Heavy Vehicles," a joint team of the University of Utah and Brigham Young University has submitted a proposal in which they state they will use the results of our research program and our consulting services in the execution of this contract if it is awarded to them.

XIII. LIST OF INTERNAL PROJECT REPORTS AND PUBLICATIONS

Several internal papers and reports on different aspects of this project have been prepared by students, faculty and research staff. One paper entitled "Dangerous at any Velocity" was presented by a Mechanical Engineering senior at a regional student chapter meeting of the American Society of Mechanical Engineers at Laramie, Wyoming on April 18, 1969. Another paper entitled "Planning and Control of Multi-Disciplinary Research and Development Projects" was presented by a Civil Engineering senior at a regional student chapter conference of the American Society of Civil Engineers at Rapid City, South Dakota on May 2, 1969.

The following papers were prepared by the non-engineering students participating in this project:

	Title	Student	Affiliation
1.	Five Patents Covering Energy Absorption Devices: Do They Overlap?	J. P. Gatlin	Law School
2.	Classification of Information in a Research Project	Carol Coltrane	Grad. School of Librarianship
3.	Organization Manual for NASA Patent Exploitation	R. L. Booton	School of Business Administration
4.	An Investigation of Selective Dissemination of Information as a Service for Librarians for an Academic Research Program Sponsored by NASA	L. J. Cangemi	Grad. School of Librarianship
5.	Management Control of the NASA Patent Project, University of Denver	T. Hopper	School of Business Administration

The following papers on different technical aspects of the project have been prepared by engineering students and faculty in the course of the past year's work:

1.	Some Design Considerations Regarding Energy Absorbing Devices on Automobiles	Prof. M. Kaplan
2.	An Analysis and Mathematical Model of a Frangible Tube Energy Dissipater (Patent No. 3, 143, 321)	J. Pereira and D. Freiburger
3.	Current Research in Automobile Safety	P. Rexroth
4.	Analysis of Circumferential Stresses Developed in Cyclic Deformation of Toroids	Prof. R. Green, J. Freeman, J. Peckis, G. Harvey
5.	Analysis of Energy Absorption by the Shearing of Sheet Metal (Patent No. 3, 232, 383)	Prof. M. Kaplan
6.	Dangerous at any Velocity	D. Freiburger
7.	G-Loadings on Automobile Passengers During Collision	Prof. W. Parks
8.	Applications for Energy Absorption Devices	L. Gallegos
9.	Investigation of Human Tolerances to Decelerations	L. Buyck
10.	Guardrails and Median Barriers	C. Lee
11.	Cyclic Energy Absorber	Prof. R. Green, J. Lemaire, J. Reyes J. Pereira

An invited paper on this project will be presented by Professor W. Parks at the Annual Meeting of the American Society for Engineering Education, June 23-27, 1969.

Analytical investigations will be published when the required test results are available.

XIV. PROPOSED PROGRAM ACTIVITIES FOR SECOND YEAR

In the original proposal for this program, it was stated that those patents which showed no promise would be dropped, and those that did would continue to be worked on during the second year. This proposed plan will be adhered to.

Out of an initial set of 46 patents, 39 have been dropped from consideration. The remaining seven will be worked on extensively.

Derivation and solution of mathematical models for each of these remaining patents will be completed, and performance predictions will be made. A number of one-fifth scale models will be fabricated for each of these patents and tested, first statically with a regular testing machine, and then dynamically with the impact tester. The preliminary static testing will provide results which will ensure that the impact tester does not get overloaded, and will permit reliable comparative evaluations to be made.

Emphasis during the second year will move to design, applications, economic analysis, and marketing, and the major part of the research effort during the second year will be in these areas.

We will concentrate on applications to highway safety, since these applications are best suited to the high performance, nonreusable type of energy absorbing patents which form the bulk of NASA owned patents in this area, and since the remaining seven patents under consideration are of this nature.

There will be three teams of faculty, students and full time research staff. Using the results of this program to date one team has already begun working with the Colorado State Highway Department to design a protection system for a fixed highway obstacle at a definite location (Interstate Highway 25 and a Broadway off ramp in Denver). This team will extend its efforts during the second year to protection systems for other types of highway obstacles, other State Highway Department needs and Department of Transportation needs. Using the services of our full time research staff (who are engaged in this program on a part time basis) we will bid on related Department of Transportation requests for proposal so that the knowledge gained in this NASA sponsored program is put to use by the Department of Transportation. For example, we have submitted a proposal to D.O.T. in response to an RFP on the Dynamics of Motorcycle Impact. In general, every effort

will be made during the second year to inject the results of this research program into the national highway safety research program.

A second team of faculty, students and research staff will devote its attention to the application of energy absorbing patents to automobiles. We will try to find an automobile manufacturer to interact with in a manner similar to our present efforts with the Colorado State Highway Department. The record of automobile manufacturers on accepting outside ideas, however, is less promising, as shown by their collective action on an exhaust pollution control device developed by Universal Oil Products. Nevertheless, our intended interaction with the Department of Transportation, by means of both solicited and unsolicited proposals, may eventually help to achieve application of energy absorbing patents to automobiles.

A third team will concentrate on applying energy absorbing devices to seat belt restraints. Here again we will attempt to get potential manufacturers to interact with us at an early stage to ensure that the end result will have a high probability of being manufactured and sold.

It may well be that these design and application efforts will provide the knowledge required for the final selection to be made from among the seven remaining patents on energy absorbing devices. It may also turn out that the additional insight and experience we gain in this design and application effort will lead us to reconsider some of the patents we had rejected earlier. We will therefore conduct a second review of all the patents on energy absorbing devices during the second year, now bringing our added experience to bear on the screening process.

The School of Business Administration faculty and students will continue to assist us in managing this program and in conducting the financial analyses necessary to ensure the economic feasibility of exploiting selected energy absorbing patents.

The selection process for the next set of NASA patents for the third year's effort will be modified. First we will start with the recommendations of the patent attorneys from the different NASA centers, then consult with the members of the National Inventors Council.

To sum up, we expect to complete the bulk of our efforts on the exploitation of energy absorbing patents during the second year and to do the preliminary investigation toward selecting a new set of NASA patents for the third year's effort.

The documentary film explaining the basis of this program and what we are doing will be completed during the second year.

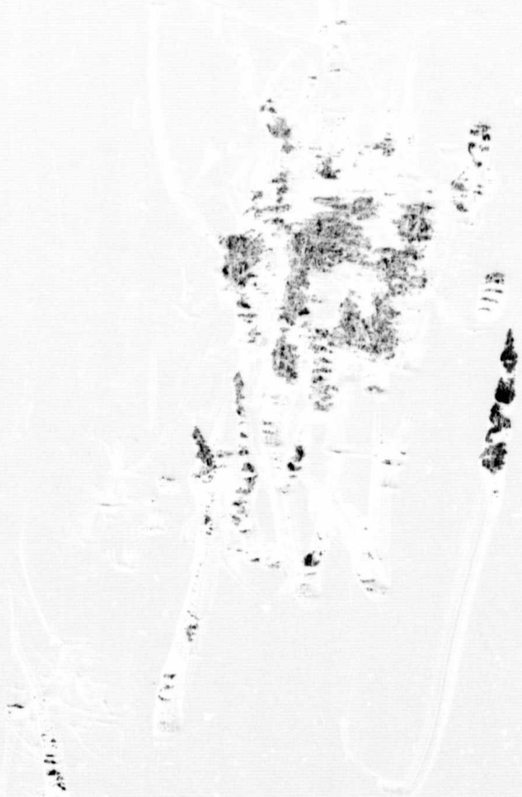

BIBLIOGRAPHY

1. McGehee, J. R., "A Preliminary Experimental Investigation of an Energy-Absorption Process Employing Frangible Metal Tubing." NASA TN D-1477.

2. Brooks, G. W. and Huey D. Carden, "A Versatile Drop Test Procedure for the Simulation of Impact Environments." Noise Control, Shock and Vibration, Vol. 7, No. 5, Sept-Oct 1961, pp. 4-8.

3. Pugsley, A. and M. Macaulay, "The Large Scale Crumpling of Thin Cylindrical Columns." Quarterly Journal of Mech. and Appl. Math, 13, 1-9, 1960.

4. Alexander, J., "An Approximate Analysis of the Collapse of Thin Cylindrical Shells under Axial Loading." Quarterly Journal of Mech. and Appl. Math, 13, 10-15, 1960.

5. Florence, A. and J. Goodier, "Dynamic Plastic Buckling of Cylindrical Shells in Sustained Axial Compressive Flow." Journal of Applied Mechanics, 35, 1, pp. 80-86, March 1968.

6. Lindberg, H. and R. Herbert, "Dynamic Buckling of a Thin Cylindrical Shell under Axial Impact." Journal of Applied Mechanics, 105-112, March 1966.

7. Kempner, J., "Post-Buckling Behavior of Axially Compressed Circular Cylindrical Shells." Journal of the Aerospace Sciences, May 1954.

8. Ernst, H. and M. E. Merchant, Trans. Am. Soc. Metals (1941), p. 299.

9. Merchant, M. E., Journal Appl. Mechanics 11 (1944), A-168.

10. Merchant, M. E., Journal Appl. Phys. 16 (1945), pp. 267 and 318. A similar analysis has been given by V. Piispanen, ibid. 19 (1948), 876.

11. Shield, R. T., "Plastic Flow in a Converging Conical Channel." J. Mech. Phys. Solids, 3, 246.

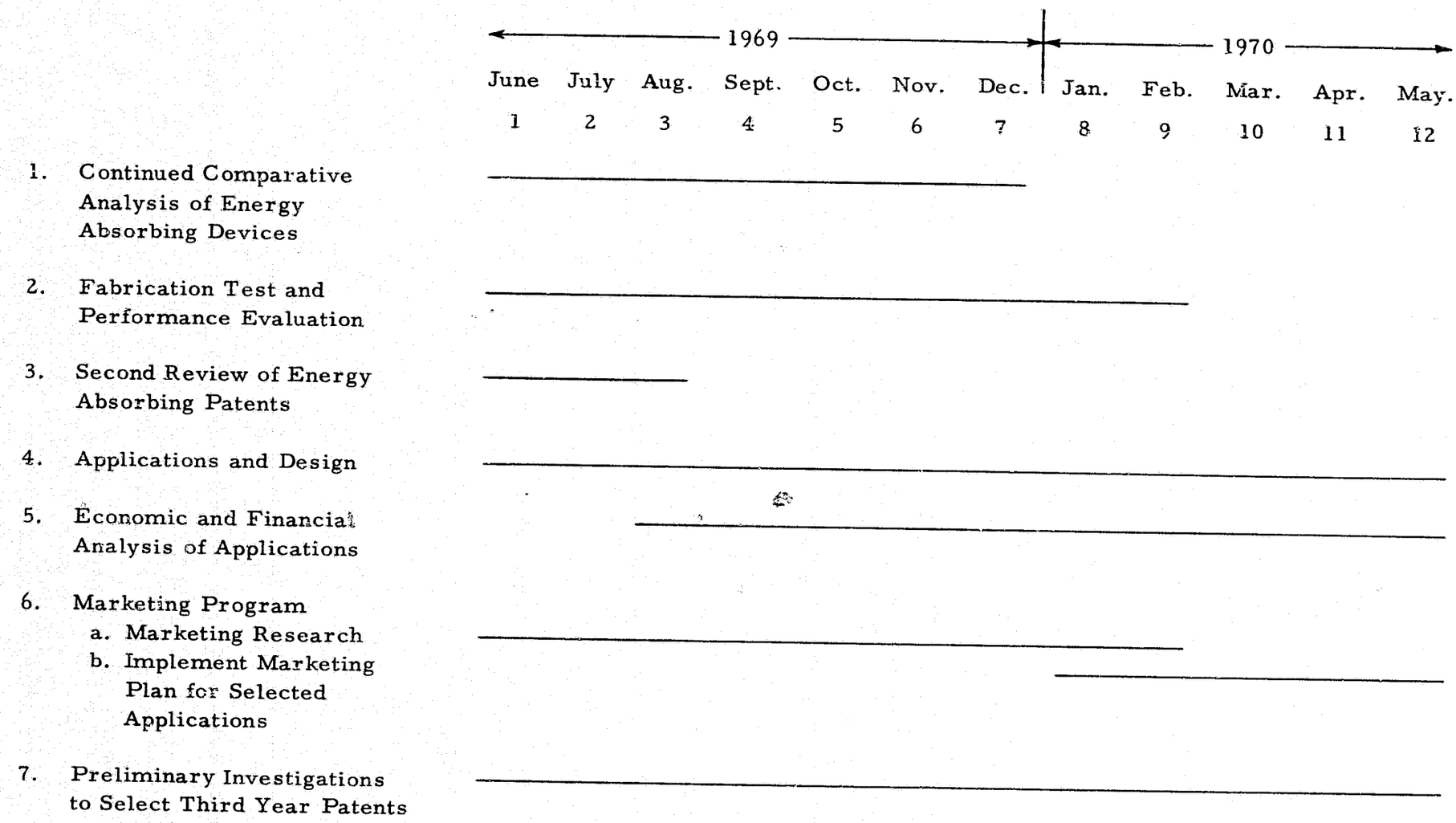

Figure 14.1. Program Plan for Second Year

APPENDICES

APPENDIX 1A PATENT AGREEMENT WITH STUDENTS

Since a number of senior students from Mechanical and Civil Engineering were participating in the program, and since they were not paid University employees, some question arose as to their rights should they be responsible for inventions resulting from their activities. After much discussion the following statement was read and signed by those engineering students who were not being financially supported by this program.

> The Denver Research Institute Project 4114, "Program for Exploitation of Unused NASA Patents", is sponsored by the National Aeronautics and Space Administration. Students enrolled in 83-293, Mechanical Engineering Project, as well as some students enrolled in 83-260, Projects Laboratory, and also, students from other academic departments of the University, will participate in the execution of this project as an opportunity, while learning, to experience an actual engineering activity and have realistic contact with the process of invention and innovation.
>
> The NASA grant to the University funding this project (Research Grant NGL-06-004-078) is made under Section 305 of the National Aeronautics and Space Act of 1958. It is therefore a condition of this grant that the grantee (the University) shall furnish a written report containing full and complete technical information concerning any invention made in the performance of any work under this grant to NASA promptly upon the making of such invention. The term "invention" includes any invention, discovery, improvement, or innovation (whether or not patentable). The Administrator, NASA, shall have the sole power to determine the disposition of the title to and rights under any such "invention". The University is therefore obligated to disclose to NASA any "invention" made by students working under this grant.
>
> I understand and will cooperate with the University to assist it in satisfying its obligations to NASA as set forth in Research Grant NGL-06-004-078, as a condition to my being permitted to participate in Project 4114.

APPENDIX 1B FIVE TUBE AND MANDREL ENERGY ABSORBING DEVICES - DO THEY OVERLAP?

by

James P. Gatlin, Law Student
College of Law

No. 3,143,321 - McGehee - August 4, 1964.

This Patent is not as comprehensive as it first appears. The basic energy absorbing idea is embodied in Claims 1 and 2, with alternatives set forth in Claims 15 and 16, concerning configuration of the end of the tube which receives the shank of the die member. It is noted that in the report by Mr. Freidburger and Mr. Pereira, the conclusion was that approximately 50% of the energy absorption was the result of the bending of the tube fragments. By examining the claims in the patent, the writer feels that this aspect of energy absorption is not covered by the patent. Claims 1 and 2 refer only to an energy absorption process whereby the ultimate tensile strength of the tube material is exceeded by circumferential stress, thereby causing the tube to fragment, and thus energy is absorbed. There is no mention of energy absorption by plastic deformation of the material prior to fragmentation, or for that matter, by friction between the tube and the die. Therefore, the writer feels this patent is limited to a device involving frangible tubes only, whereby energy is absorbed mainly through progressive fragmentation of those tubes when ultimate tensile strength is exceeded. There is a possibility that the bending process was set forth in other claims, but rejected by the Patent Office. This could be ascertained by an inspection of the file wrapper of this particular patent.

The rest of the claims pertain mainly to various applications of the device claimed in Claims 1 and 2.

No. 3,181,821 - Eddins - May 4, 1965.

This appears to be the most unique of the five patents being evaluated. The claims cover two methods of energy absorption. The first, covered by Claims 3, 5 & 9, consist of the extrusion of a tube by mandrels through longitudinal tension, creating forces normal to the internal surface of the tube which in turn develop circumferential stresses greater than yield but below the ultimate tensile strength of the material. The tube is deformed, absorbing energy, but does not fail as was the case in the McGehee patent.

The second method, but still based on the same principle as the first, restricts the buildup of circumferential stresses to below the elastic limit of the material, and then employs a number of mandrels in tandem, each absorbing energy as it deforms the tube through which it is passing. This method is covered by Claims 7 and 8.

The remaining claims concern various applications and variations of the device.

No. 3,236,333 - Mitchell - February 22, 1966.

The device covered by this patent is similar to that covered by the McGehee patent. However, there are two basic differences. First, the tube utilized in this device is a ductile tube rather than a frangible one, and second, a control ring has been added to control the rate of deformation. The primary mode of energy absorption stressed by the claims is plastic deformation of the material, even though the tube must first be split into ribbons in conjunction with the bending. This splitting is accomplished in the same manner as in the McGehee patent, i.e., by creating circumferential stresses exceeding the ultimate tensile strength of the tube material. The writer feels there is no infringement here with the McGehee patent, since the material used is different, and the reasons for exceeding the ultimate tensile strength are different. It is to be noted that the splitting process is further deemphasized by Claims 3 and 4 which provide for notches in the tube to induce splitting and to control it, and Claim 9 which provides for grooves in the tube for further control. It is obvious that these grooves would weaken the tube at that point and reduce the amount of energy absorption achieved by the splitting mode. This seems to be immaterial to the inventor.

The basic device is covered by Claims 1 through 4, and it is to be noted that each claim refers to plastic deformation and provides for a control ring. The remaining claims cover the splitting wedge configuration, and various applications and variations of the device.

No. 3,339,674 - Kroell - September 5, 1967.

This is a very limited patent which appears to be only a variation of the McGehee and Mitchell patents. The only difference is that in the expansion process creating circumferential tension in a tube, the ultimate tensile strength of the tube material is not exceeded, therefore the tube is actually turned inside out, absorbing energy in the

process of first bending the tube wall and then straightening it. The basic process is covered by Claim 1. The file wrapper on this patent may be interesting, since the Patent Examiner referenced both the McGehee and Mitchell patents, and since so few claims were allowed

No. 3,381,778 - von Tiesenhausen - May 7, 1968.

This also is a limited patent, and more than likely an improvement on the Mitchell patent. Basically, the only aspect covered in the claim which concerns energy absorption are the cutters which are employed to cut the tubes. The question which arises in the writer's mind is whether these cutters might have been obvious to a person skilled in the art, after reading the Mitchell patent. If so, the patent would be invalid. However, since the Examiner referenced both Mitchell and McGehee, and a patent was issued, the patent must be presumed valid until proven otherwise in litigation.

Conclusions:

1. It would be safe to say that the Eddins patent does not infringe on any of the other patents in this group, since it utilizes a method for energy absorption unlike that used by any of the other patents.

2. One operating under the McGehee patent, and adhering closely to the frangible tube method of absorption of energy as claimed in that patent, would encounter no infringement problems with any of the other four patents, since any cross-reading of claims would be resolved in favor of the McGehee patent, since it has the earlier date. Any deviation from the claims, however, which infringe, say, on the Mitchell patent, would be resolved in favor of Mitchell.

3. One adhering strictly to that taught by the Mitchell patent likewise should experience no infringement difficulties, since the principle of energy absorption claimed is completely different from that claimed in McGehee, i.e., plastic deformation vs. fragmentation. However, there is the remote possibility that, since McGehee is the earlier patent, litigation might establish that the method taught in Mitchell is nothing more than an extension of that taught in McGehee, which would have been obvious to one skilled in the art of energy absorption, and therefore not patentable. Again, though, the

presumption of validity prevails, especially in light of the fact that the Patent Examiner referenced McGehee when granting the Mitchell patent.

4. The method of energy absorption employed by the Kroell patent is probably safe from infringement actions if strictly adhered to. What probably saves this patent from infringing either McGehee or Mitchell is the fact that the stresses created are maintained below the ultimate tensile strength of the material, whereas in those patents, it must be exceeded. The same doubts arise, however, for the same reasons as set forth above in Conclusion No. 3. It should also be noted that the Examiner has referenced both McGehee and Mitchell while allowing the three claims.

5. It is doubtful whether one could proceed under the von Tiesenhausen patent without infringing at least the Mitchell patent. Whereas the absorption of energy by the shearing action of the cutters is novel and not covered by the prior patents, the plastic deformation is definitely covered by Mitchell and probably explains why only one claim was allowed under this patent. Therefore, one would also have to acquire rights under the Mitchell patent in order to safely exploit the device covered in this patent.

6. In order to make a better evaluation of these patents, it is necessary that those patents referenced by the Patent Examiner in each case he checked. Also, it is probably desirable that the file wrappers of each of the five patents be examined to determine what claims were asked for and denied. And finally, if possible, a local patent attorney who would be willing to assist us in this program should be consulted for his opinion. This consultation should be with the writer, or his winter quarter replacement.

APPENDIX 2 SCALING LAW AND SIMILITUDE REQUIREMENTS FOR DYNAMIC TESTING OF ENERGY ABSORBING DEVICES

by

A. A. Ezra

1. Introduction

A physical phenomenon y may depend on several independent variables $x_1, x_2, \ldots, x_n$ in some unknown manner. The functional relationship between y and all the variables on which it depends can be expressed in general as

$$y = f(x_1, x_2, \ldots, x_n). \tag{1}$$

If the exact nature of the function f were known, then this would be the mathematical expression of the physical law expressed by the dependence of y on $x_1, x_2, \ldots, x_n$. This physical law is independent of the units of measurement and applies just as well to the model as it does to the prototype. Since the variables in a physical problem (excluding electromagnetic phenomena) can be expressed in terms of the four basic dimensions of mass, length, time and temperature, then the n + 1 variables ($y, x_1, x_2, \ldots, x_n$) can be combined into $(n + 1) - 4 = n - 3$ dimensionless groups. Equation (1) can therefore be put into the following dimensionless form, representing the physical law:

$$\pi_1 = F(\pi_2, \pi_3, \ldots, \pi_{(n-3)}). \tag{2}$$

The physical law is the same for model and prototype, and if each of the π terms on the right hand side is made to have the same value for both model and prototype, this will ensure that π_1 has the same value for both. The resulting equality of π_1 for both model and prototype yields the scaling law for the dependent variable. The need to make each of the remaining π terms have the same value for both model and prototype determines the similitude requirements for the independent variables. These similitude requirements apply to the independent variables and yield the corresponding scale factors for them.

Using the subscripts m and p to refer to model and prototype, respectively, we therefore have the following:

Scaling Law: $$\pi_{1p} = \pi_{1m} \tag{3}$$

Similitude requirements:

$$\pi_{2m} = \pi_{2p}$$

$$\pi_{3m} = \pi_{3p} \qquad (4)$$

.

.

.

$$\pi_{(n-3)m} = \pi_{(n-3)p}.$$

The number of scale factors that may be chosen arbitrarily is equal to the number of basic dimensions in the problem. For example, if all the variables in the physical law are expressible in terms of three basic dimensions, i.e., mass, length and time, three scale factors may be chosen arbitrarily, corresponding directly or indirectly to each of them. The remaining scale factors can then be derived in terms of one or more of these three from equation (3).

2. Derivation of Scaling Law and Similitude Requirements

Dependent Variable		Dimensions
a	deceleration	L/T^2
Independent Variables		
V	velocity of impact	L/T
M	impacting mass	M
K	strain hardening coefficient of deforming material	M/LT^2
n	strain hardening exponent of deforming material	-
ρ	density of material	M/L^3
E	modulus of elasticity	M/LT^2
ϵ	ductility of material, i.e. strain at fracture	-
σ_u	ultimate strength of material	M/LT^2

Independent Variables		Dimensions
L	stroke of device	L
λ_i	any typical length measurement associated with the device (i.e. thickness, diameter, etc.)	L
μ	coefficient of friction between energy absorbing surfaces	-

Since there are twelve variables and three basic dimensions, i.e. mass, length and time, from Buckingham's Pi Theorem the problem can be formulated in terms of nine dimensionless variables:

$$\pi_1 = \frac{aL}{V^2} \qquad \pi_6 = V\sqrt{\rho/E}$$

$$\pi_2 = \frac{MV^2}{KL^3} \qquad \pi_7 = \lambda_i/L$$

$$\pi_3 = \epsilon \qquad \pi_8 = n$$

$$\pi_4 = K/E \qquad \pi_9 = \mu .$$

$$\pi_5 = \sigma_u/E$$

Since there are three basic dimensions in the problem, three arbitrary scale factors can be chosen. They are the following:

$$n_1 = L_p/L_m$$

$$n_2 = \rho_p/\rho_m$$

$$n_3 = K_p/K_m .$$

Choosing a 1/5 scale model, and using the same material for both model and full scale energy absorbing devices,

$$n_1 = 5$$

$$n_2 = 1$$

$$n_3 = 1.$$

The scale factors for the remaining variables are derived by equating the small scale values of the dimensionless parameters to the full scale values.

Using the subscripts p and m to denote full scale prototype and subscale model respectively we get the following scale factors:

$a_p = 1/5\ a_m$ $\qquad$ $\sigma_{um} = \sigma_{up}$

$V_m = V_p$ $\qquad$ $n_m = n_p$

$\epsilon_m = \epsilon_p$ $\qquad$ $\mu_m = \mu_p$

$M_m = 1/125\ M_p$ $\qquad$ $M_p V_p^2 = 125\ M_m V_m^2$.

From these results we can see that the measured decelerations on the one-fifth scale model will be five times the full scale value. The scale model tester must deliver a velocity of impact equal to the full scale crash situation, and using a scale model mass of 1/125 full scale, the scale model energy delivered should be 1/125 the full scale value.

It is interesting to note that the kinetic energy absorbed per unit mass is the same for both model and full scale.

The kinetic energy per unit mass is $\frac{1}{2}\frac{M_p V_p^2}{M_p} = \frac{V_p^2}{2}$.

The kinetic energy per unit mass is $\frac{1}{2}\frac{M_m V_m^2}{M_m} = \frac{V_m^2}{2}$.

The ratio of the two is given by $\frac{V_p^2}{V_m^2} = 1$.

Hence, the mechanical efficiency of a scale model will be exactly the same for the scaled up version.

APPENDIX 3. G-LOADINGS ON AUTOMOBILE PASSENGERS DURING COLLISION

by

W. H. Parks

Available literature gives data on instrumented automobile collisions for moderate crash speeds, usually under 40 miles per hour. The highest speed reported for a staged collision was 52 mph for a head-on crash.[1]

Few motorists are aware of the violence they will encounter during a collision. Most of us have experienced a panic-braking episode where as passengers we were shaken up and even thrown against the dash. In panic braking, passenger compartment decelerations of 0.6 to 0.9 g's may be encountered.[2] In a 30 mph head-on collision the passenger compartment decelerations will be about 35 g[1] or about 50 times as violent as the panic-breaking episode.

Automobile Decelerations During Collision

The automobile crash is an inelastic impact with the coefficient of restitution almost always under 0.10.[1] The kinetic energy of the vehicles is absorbed in the inelastic crushing of car structure. Decelerations are highest at the point where the bumper contacts the obstacle and decline as consideration moves back through the crush region. An important point is the fact that for the moderate-velocity crashes described in the literature, the passenger compartment remains essentially intact and undistorted and decelerates as a unit. An exception to the integrity of the passenger compartment is the side-impact collision where the striking car bumper goes over the rocker panel of the struck car and invades the passenger compartment. Front-end crush in head-on collisions ranged from 1.2 feet at 21 mph to 3.5 feet at 52 mph.[1] Peak decelerations of the passenger compartment are about two or three times what they would be if a constant crushing resistance were provided to achieve a uniform deceleration.[1] Collisions happen in a split second. The car, including the passenger compartment, is stopped in 100 milliseconds (1/10 second) after contact is made.

Passenger Decelerations During Collision

During a collision the passenger compartment is brought to rest in about 1/10 second. During this time the unrestrained passenger moves forward at original velocity closing the gap between himself and the dash or the windshield. About the time the windshield stops, the passenger crashes into it full-tilt at original velocity. It is the secondary collision of the passenger with a now-stationary object which causes the injuries and fatalities in auto collisions.

During the secondary collision the g-forces exerted on the human body are highly localized such as the head against the dash or the chest against the steering column. Normally the localized deceleration resulting is several times as great as the peak deceleration of the passenger compartment itself. In a 30 mph head-on crash a human head would experience a peak deceleration of 80 g's in striking a specially-designed energy-absorbing instrument panel. This panel was designed to collapse 9 inches under the blow exerted by the head.[3] Think of what it is like to strike a rigid dash.

The secondary collision would be avoided if the passenger were caused to decelerate at the same time as the car is decelerated. This would be accomplished if the passenger were leaning against the dash at the instant of collision. It would also be accomplished if the passenger were firmly attached to the structure of the passenger compartment. The passenger is not yet convinced that he should be completely strapped in. Nor is he convinced that he should be encapsulated so that a motion of only an inch or two from his normal seated position will bring him in contact with a formed and padded life-saving structure.

Because of slack in restraint devices and flexibility of seat structures, onset of deceleration of the restrained passenger lags behind the deceleration of the passenger compartment. Unfortunately, this results in an increase of the peak deceleration so that the peak deceleration of the restrained passenger is likely to be 50% higher than the peak deceleration of the passenger compartment. These decelerations, however, are tolerable at moderate crash speeds.

Progress Toward Increased Survivability in Passenger Compartments

Passive safety devices are those which do not require passenger cooperation to function. In this field substantial progress is being made

toward making the secondary collision more survivable, at least for moderate crash speeds. The unrestrained motorist will have a secondary collision. The name of the game is to provide a collision surface which will not kill him. Improved door latches will keep him within the passenger compartment. It has long been known that the steering column is a very mean thing with which to collide. The introduction of energy absorption structure into the steering column has apparently brought this menace under control.[4] The introduction of head rests virtually eliminates whip lash (except for those motorists who wear their head rests in the trunk). Energy absorbing dash boards are coming.[3] Some cars now have increased structure in the doors to promote a glancing impact and prevent intrusion of the striking car into the passenger compartment of the struck car for a side impact.[5] Glass and the frame structures for retaining the glass remain a problem. Progress is being made in developing a glass sandwich which in large expanses will absorb large amounts of energy while minimizing laceration. The sheet metal retaining the glass is being redesigned. However, the frames, and the glass itself near the frames, remain things to avoid during the secondary collision.

The Place of Lap and Shoulder Belts

The lap belt avoids ejection from the car during collision. This includes prevention of an excursion through the windshield. Instead of going through the windshield the passenger will jack knife and hit the dash. This is rough, but energy absorbing dash boards are coming. The addition of the shoulder belt promises to minimize secondary collision. At present, only about 30% of the installed lap belts are used regularly.[6] No doubt the usage of shoulder belts is even substantially lower than this.

Deceleration Data

Head-on Collisions

25 mph	25 g's Passenger Compartment Deceleration	1
52 mph	70 g's Passenger Compartment Deceleration	1
35 mph	16 g's Passenger Compartment Deceleration	7

Barrier Collisions

30 mph	15 to 25 g's Passenger Compartment Deceleration	3
35 mph	35 g's Passenger Compartment Deceleration	8
25 mph	20 g's Passenger Compartment Deceleration	9

Rear-End Collisions

Struck car stationary as at a stop light
Striking car velocity 23 mph.
Passenger car acceleration 7.5 g
Maximum head accelerations 22g 10
(No head rests)

Side-Impact Collisions

a. Struck car stationary 11
Striking car at 40 mph striking either front wheel or rear wheel. Included angle between car centerlines 105°.
Passengers (dummies) experienced head g's of 20 to 108 depending upon whether they struck glass only or first struck sheet metal frame around glass. Where they struck glass only, g's ranged from 20 to 56 depending upon position of passenger, what kind of glass and whether passenger struck near center or edge of glass. The low value of 20 g's occurred where the shoulder of the dummy had prefractured the glass. The high value of 100 g occurred where the head struck a sheet metal panel.

b. Both cars moving at same speed 12
Ninty degrees intersection of paths
Passenger Compartment decelerations

Struck Car	5 g	at 10 mph
	27 g	at 40 mph
Striking Car	4 g	at 10 mph
	17 g	at 40 mph

BIBLIOGRAPHY FOR APPENDIX 3

1. Severy, D. M., J. H. Mathewson, and A. W. Siegal, "Automobile Head-on Collisions Series II," SAE Transactions Vol. 67, 1959, pp 238-262.

2. Mathewson, J. H. and D. M. Severy, "Rapid-Deceleration Tests of Chest-Level Safety Belt," Bulletin No. 73 Highway Research Board 1953, pp 42-52.

3. Halliday, V. D. etal, "Providing Increased Survivability in Passenger Car Instrument Panels," Proceedings General Motors Corporation Automotive Safety Seminar, July 11-12, 1968.

4. Marquis, D. P. and T. Rasmussen, "Status of Energy Absorption in Steering Columns," Proceedings General Motors Corp. Automotive Safety Seminar, July 11-12, 1968.

5. Hedeen, C. E. and D. D. Campbell, "Side Impact Structures," Proceedings General Motors Corporation Automotive Safety Seminar, July 11-12, 1968.

6. Louton, J. C. and T. W. Ruster, "Restraint Systems, Design and Performance Parameters," Proceedings General Motors Corporation Automotive Safety Seminar, July 11-12, 1968.

7. Roth, H. P., "Physical Factors Involved in Head-on Collisions of Automobiles," Proceedings Highway Research Board Vol. 31, 1952, pp. 349-356.

8. Severy, D. M. and J. H. Mathewson, and A. W. Siegel, "Barrier Collisions, Series IV; An Evaluation of Motorist's Force and Injury Control Systems," Highway Research Board Proceedings, Vol. 40, 1961, pp 541-556.

9. Severy, D. M. and J. H. Mathewson, "Automobile-Barrier Impacts," Bulletin No. 91 Highway Research Board, Jan. 1954, pp 39-54.

10. Severy, D., "Engineering Studies of Motorist Injury Exposures from Rear-End Collisions," Traffic Safety a National Problem, National Academy of Engineering 1967.

11. Severy, D. M. and H. M. Brink, "Safety Glass Breakage by Motorist During Collisions," Ninth Stapp Conference 1966, pp 205-236.

12. Severy, D. M., J. H. Mathewson and A. W. Siegel, "Automobile Side-Impact Collisions, Series II," Traffic Safety, Dec. 1964, pp 99-107.

APPENDIX 4. INVESTIGATION OF HUMAN TOLERANCES TO DECELERATIONS

by

Larry Buyck

It has become increasingly apparent that vehicles can be accelerated or decelerated by various means yielding a great range of effects on the passengers aboard. These effects may be detrimental to the life functions of any human passengers.

In the attempt being made to apply energy absorbing devices to reduce or to spread over a greater length of time the loads on passengers during quick stops, the human limitations must be considered, these limitations being the endurance limits of the human body. An energy absorbing device that could not sufficiently reduce the loads on passengers during impact would be of no use.

The purpose of this report, then, is to examine the current knowledge of these human tolerances.

When considering these humar tolerances several things must be considered. First the maximum accelerations which various parts of the body can withstand from various directions together with the time duration these accelerations can be withstood. Secondly the extent of injuries sustained by non-fatal accelerations. Also the strengths of various bone structures are considered.

Immediately a problem is foreseen in gathering such data. People cannot be accelerated in the laboratory to their death to obtain their tolerance limits nor are the people that die in accidents instrumented so that the scientist may read the tolerance limits directly. Thus all such tolerance limits are obtained by three methods singularly or in combination.[1, 3, 4, 6, 7, 10]

1. By testing lower primates to their limits and relating the data to humans.

2. By testing humans at low acceleration and extrapolating the data.

3. By testing cadavers.

All methods require some expert opinion as to what the conversion factors may be.

Despite the many variables involved much of the present data available is in close agreement.

Table 1 is a condensation of several like tables indicating the human tolerance limits to acceleration in g's. It should be noted that this table is for accelerations obtained from a front end collision only.

Table 1[3, 6, 7, 8, 9, 10]

Body Area	Tolerance Limit (g's)
Skull:	
Forehead Fracture	245
Base Fracture	515
Brain Concussion	300-600
Brain Contusion	350-500
Chest: Heart-lung Area	77
Vertebral Column	18 (Compression), 12 (Tension)
Whole Body	40-60 (For forward deceleration, lap belt plus shoulder harness)

It is interesting to note that at these tolerance levels most deaths occur from hemoraging either of the brain or heart-lung area.[8, 10]

The g loadings in Table 1 are given for the average duration of acceleration, for the respective body parts, sustained during front end collision. However, the tolerance limit changes with the duration. Figure 1 illustrates this point.

Table 2 is a comparison table for non-fatal injuries.

Table 2[10]

Body Area	(G's)	Duration (msec)	Injury Expected at Tolerance Limit
Face	40	30	Soft tissue damage with possibility of some facial bone fracture
Head (skull)	100	4	Minimum to moderate concussion
	75	8	
	50	30	
Chest	60	100	Reversible injury to organs of the thorax

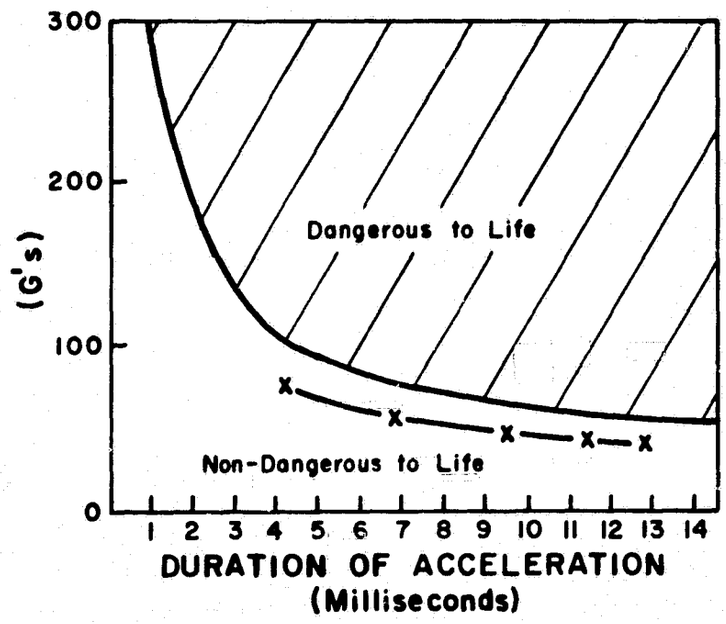

Figure 1. Acceleration vs Time

——— Tolerance for the human brain in forehead impact with plane, unyielding surfaces

X———X Tolerance for the whole human body restrained by lap belt only[4] (does not hit anything)

Table 3 considers accelerations obtained fr m various impacts from various directions together with durations. These accelerations are for the passenger compartment and may be considered to be on the passenger if he is sufficiently restrained from movements different from the passenger compartment by lap belts and shoulder harnesses. An indication of the human tolerances to G's is indicated by the stepped line. Columns 1, 2, 3 and 5 have already been considered being forward collisions. Column 4 is in close agreement with other reports that place the tolerable G loading for side impacts at about 30 G's.[3] Column 6 considers the rear end collision. The rear end collision tolerance limit is in dispute. Table 3 places the limit at something slightly greater than 20 G's for 0.16 second.[3]

Another report states a figure nearly twice that value at that duration. Still another report states 5.2 G's will yield severe injury.[11] It is evident that more research must be done concerning rear end collisions.

Last to be considered is structural strength of the human body. Although broken bones are seldom fatal their strength should be a secondary consideration for the protection of vital organs and absorption of energy during collision (see Table 4 and Figure 2).

It has been stated that the data presented herein is largely extrapolation from test data. The methods of extrapolation are from expert opinion and may not be correct. However, in most cases three different methods yield the same result. This is a good indication of good results. Where there is disagreement more research must be carried out.

Table 3[3]

Column	1	2	3	4	5	6
			Front Car Stationary Left Side Collision		Front Car Stationary Rear Collision	
	Barrier	Head On Both Moving	Rear Car $\Delta v = 0.9v$	Front Car $\Delta v = 0.7v$	Rear Car $\Delta v = 0.7v$	Front Car $\Delta v = 0.6v$
Car speed 15 miles/hour (v)						
Accel.	-15G	-14G	-11G	+9G	-6G	+5G
Period	0.091 sec	0.098 sec	0.11 sec	0.11 sec	0.16 sec	0.16 sec
Distance	1.0 ft	1.0 ft	1.1 ft	0.8 ft	1.2 ft	1.1 ft
Car speed 30 miles/hour Marginal or unsurvivable with present structures and lap belt only						
Accel.	-30G	-28G	-22G	+18G	-12G	+10G
Period	0.091 sec	0.098 sec	0.11 sec	0.11 sec	0.16 sec	0.16 sec
Distance	2.0 ft	2.1 ft	2.2 ft	1.6 ft	2.4 ft	2.2 ft
Car speed 45 miles/hour						
Accel.	-45G	-42G	-33G	+27G	-18G	+15G
Period	0.091 sec	0.098 sec	0.11 sec	0.11 sec	0.16 sec	0.16 sec
Distance	3.0 ft	3.1 ft	3.3 ft	2.4 ft	3.6 ft	3.3 ft
Car speed 60 miles/hour						
Accel.	-60G	-56G	-44G	+36G	-24G	+20G
Period	0.091 sec	0.098 sec	0.11 sec	0.11 sec	0.16 sec	0.16 sec
Distance	4.0 ft	4.2 ft	4.4 ft	3.2 ft	4.8 ft	4.4 ft

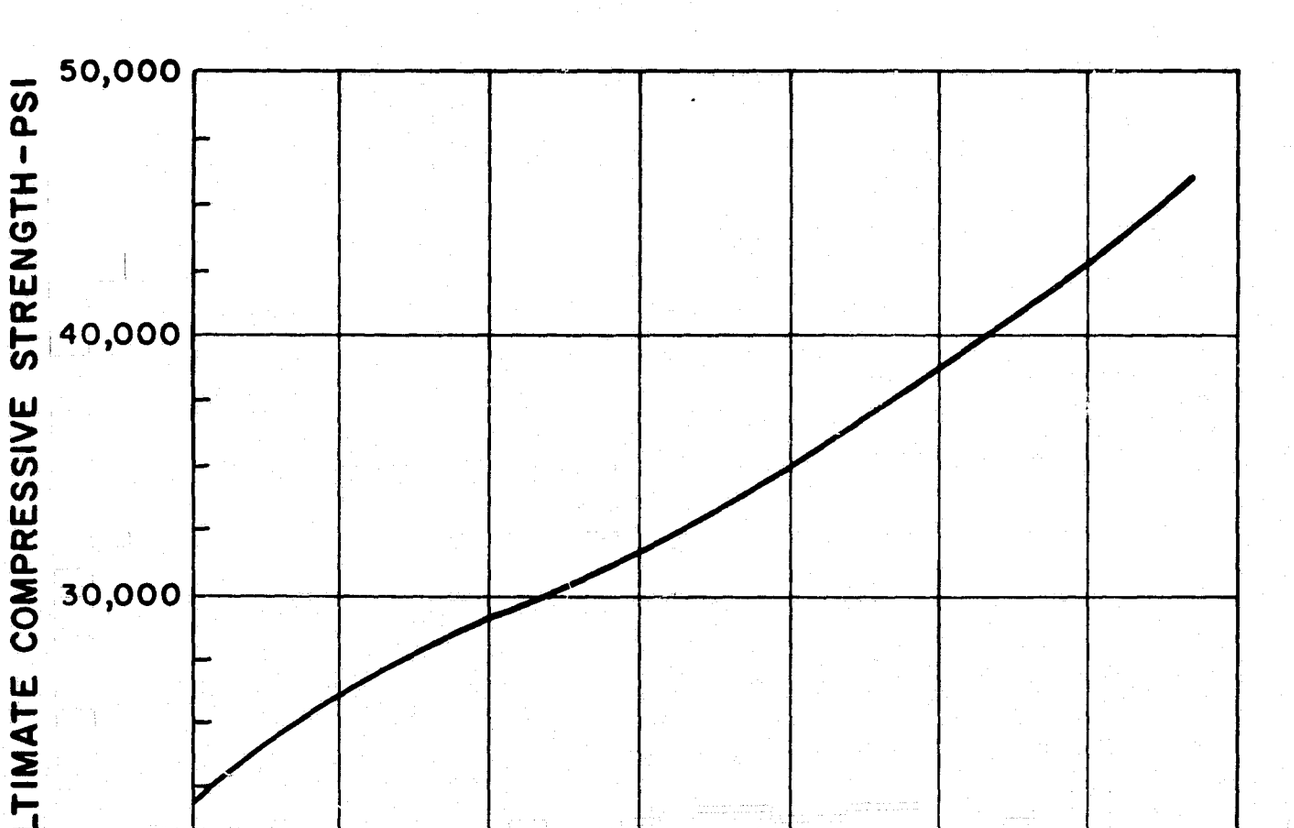

Figure 2. Human Femur Bone Strength

Table 4[2]

BONE	
Modulus of Elasticity	3.56×10^6 psi
Tensile Strength	8,320 psi
Compressive Strength	32,570 psi

Skeletal Structure Strength

	Compressive Breaking lbs.	Bending Breaking lbs.	Source
Clavicle	425	230	(a), (b)
Humerus	1,115	335	(a), (c)
Radius	735	135	(a), (c)
Ulna	500	100	(a), (c)
Femur	1,850	500	(a), (c), (d)
Tibia	2,340	655	(a), (c)
Fibula	135	100	(a), (c)
Patella	1,500	-	(a), (d)

(a) "Elasticity and Strength of Bones" by Otto Messerer, Stuttgart, Germany, 1880.

(b) "The Human Body in Equipment Design" by Damon, Stoudt and McFarland, 1966.

(c) "Biomechanics: Strength of Biological Materials" by Dr. Hiroshi Yamado of the Kyoto Prefectural University of Medicine

(d) Ninth Stapp Conference, Pages 237-248, and GMR-506, Page 10, by Patrick, Kroell and Mertz, Jr.

REFERENCES FOR APPENDIX 4

1. Advani, S. H. and Lombard, C. F. "Impact Protection by Isovolumetric Constraint of the Torso" 10th Stapp Car Crash Conference, p. 196-206. 1966.

2. Cichouski, W. G. "A Third Generation Test Dummy - 'Sophisticated Sam'" GMC Automotive Safety Seminar, Chap. 15 1968.

3. Clark, C. and Blechschmidt, C. "Human Transportation Fatalities and Protection Against Rear and Side Crash Loads by Airstop Restraint" 9th Stapp Car Crash Conference, p. 19-64, 1965.

4. Gadd, C. W. "Use of Weighted-Impulse Criterion for Estimating Hazard" 10th Stapp Car Crash Conference, p. 164-174, 1966.

5. Halliday, Holcombe, Hoover and Parr. "Providing Increased Survivability in Passenger Car Instrument Panels" GMC Automotive Safety Seminar, Chap. 15, 1968.

6. Harris, Hirsh, Ommaya and Yarnell. "Scaling of Experimental Data on Cerebral Concussion in Sub-Human Primates to Concussion Threshold for Man" 11th Stapp Car Crash Conference, p. 47-52, 1967.

7. Mertz, H. J. Jr. and Patrick, L. M. "Investigation of Kinematics and Kinetics of Whiplash" 11th Stapp Car Crash Conference, p. 175-200, 1967.

8. Roberts, V. L. "Heart Motion Due to Blunt Trauma to the Torso" 10th Stapp Car Crash Conference, p. 242-248, 1966.

9. Stapp, Col. John P. "Review of Air Force Research on Biodynamics of Collision Injury" 10th Stapp Car Crash Conference, p. 325-342, 1966.

10. Wilfert, Karl. "Comprehensive Vehicle Safety Development" 10th Stapp Car Crash Conference, p. 94-115, 1966.

11. Zaborowski, A. V. "Lateral Impact Studies, Lap Belt - Shoulder Harness Investigation" 9th Stapp Car Crash Conference, p. 93-127, 1965.

APPENDIX 5. SURVEY OF AUTOMOBILE ACCIDENT STATISTICS

by

Douglas Edward Freiburger

March 7, 1969

Preface

The purpose of this paper is to present a summary of statistical information relating to automobile accidents. The specific reason for making this summary is to obtain information that can be used in the Senior Lab Project Class of the Engineering College at the University of Denver, where designs for energy-absorbing, and posssibly life-saving devices for automobiles are under consideration.

The intent of this paper is to present useful information regarding the relationships between accidents, speed, and driver and vehicle characteristics, in addition to information about the actual magnitude of the problem.

Part I- The History of Automobile Accidents

The first reported vehicle to move under its own power was a steam tractor built by Augnot in France in 1769. In 1870, a century later, Siegfreid Markus built the first car powered by an internal combustion engine, although it was not until approximately 1885, by a man named Benz, that motorcars were produced in any appreciable number.[18]

In 1893, the first recorded collision between two motor vehicles occured at Auterix France when Baron DeZuylen drove his horseless carriage into Count DeDions motor brake, causing apparently only minor injuries to each.[18] The first fatal motorcar accident in the United States occured in New York City on September 13, 1895, when W. H. Bliss was knocked down and killed by a horseless carriage while graciously assisting a lady passenger to alight from a trolley car.[15] In February of 1895, in England, the wheel of a Daimler motorcar collapsed, and the two occupants were thrown out and killed.[18] These, and other, less severe injuries that must have occured, were the beginning of an epidemic whose end is not in sight yet.

Dr. F. D. Woodwad, in the May 1966 issue of the Southern Medical Journal, states that "The leading cause of death in this country today is cardiovascular disease; the second is cancer; but close behind are deaths due to automobile accidents if figured on the man-years of life lost; for the first two are primarily diseases of the older age groups, wheras the death rate from automobile accidents is highest in youths."[23] The following

Table 1-Births and Deaths U.S.

		Rate
Population (1963)	189,000,000	
Population (1964)	191,000,000	
Births/year (1964)	4,054,000	2120/10⁵ people
Deaths/year (1964)	1,801,000	941/10⁵ people
Deaths/year (1963) About	1,800,000	
Heart (1963)	707,830[a]	380/10⁵ people
Cancer (1963)	285,362[a]	150/10⁵ people
Stroke (1963)	201,166[a]	110/10⁵ people
Accident Deaths (1963)	104,300[b]	56/10⁵ people
Auto (1963)	43,600[b]	23/10⁵ people
Auto (1964)	47,700	25/10⁵ people
Home (1963)	29,000[b]	
Work (1963)	14,000[b]	
Train (1964)	13[c]	
Inter-city Bus (1964)	130[c]	
Scheduled U.S. Airplanes (1964)	200[c]	
General Aviation (1961)	794[d]	
USAF Military Aviation (1961)	297[e]	
Other Accidents (1963) About	16,000[b]	
Other causes of death: About	500,000	

Ref. (2) pg. 24

Figure 2- Involvement rate by sex and age of passenger-car driver, day and night. Rural Accidents

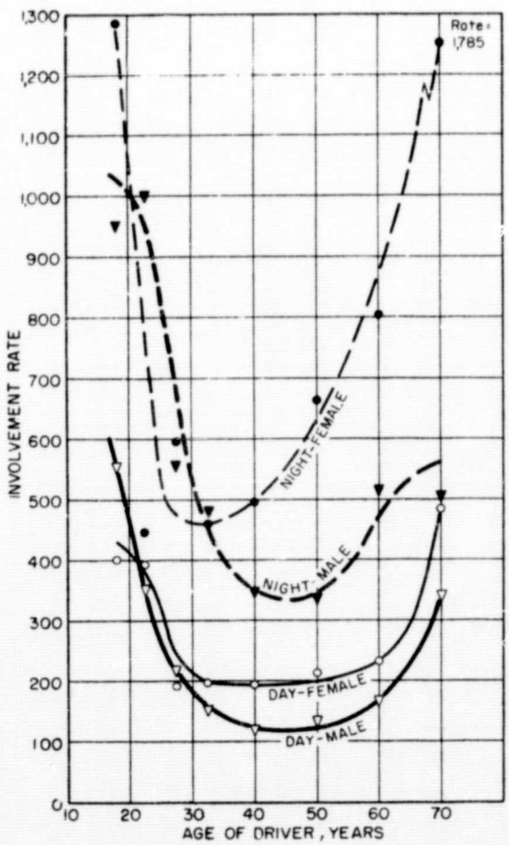

Ref. (22) pg. 19

Table (1) and Figure (2) give an idea of this problem.

Part II - The Magnitude and Characteristics of the Automobile Epidemic

The idea that the automobile accident problem is reaching epidemic proportions is becoming more apparent every day. In 1967, there were a total of 53,100 motor-vehicle deaths as compared to a total of 36, 369 total motor-vehicle deaths in 1937. Currently there is a motor-vehicle injury every seventeen seconds. In 1965, the accident death rate per 100,000 population, (by place of residence for the United States), was 25.4 for motor vehicle accidents, out of a possible 55.7 for all types of accidents. [4]

One obvious reason for the increasing motor-vehicle death rate is the increasing number of cars on our roadways. In 1966, there were approximately 94,179,00 registered motor-vehicles, 78,315,00 of which were automobiles, driving on approximately 3.7 million miles of roadways in our country. In 1966, there were 8,598,326 cars produced in our country's factories, while approximately only 6,000,000 cars were scraped during the previous year. The average age of passenger cars in the United States in 1966 was 5.7 years, and the U.S. has about 54% of all the World's passenger cars.[1]

The following three tables (3,4, & 5) give one an idea of the most common model car in the country today, the average length of trip that a car is used for, and the most frequent uses and number of people in a car during those uses.

In 1966, it was estimated that Americans traveled 744,844,000,000 miles im passenger cars for an approximate average of 9,500 miles per vehicle.[1]

Table 3-Passenger Car Factory sales by Body Type-1966

	Number
4-Door Sedan	2,333,277
2-Door Sedan	546,167
Convertible Coupe	394,679
2-Door Hardtop	3,359.060
4-Door Hardtop	1,078,669
2-Door Station Wagon	369
4-Door Station Wagon	880,407
Chassis	5,698
Total	8,598,326

Ref. (1)

Table 4-Distribution of Trips and Vehicle-Miles of Travel for Cars

Trip Length	Trips	Vehicle Miles
Under 5	59.6	13.2
5-9	19.9	15.4
10-14	8.1	11.2
15-19	4.2	8.2
20-29	3.7	10.4
30-35	1.6	6.5
40-49	.8	4.3
50-99	1.3	10.8
100 & over	.8	20.0
		100.0

Ref.(1)

Table 5-Distribution of Passenger Car Trips, Travel & Occupancy, by Major Purpose of Travel

Purpose of Travel	% of Trips	Vehicle Miles	Occupants/Car
Earning a Living:			
To & from work	33.6	26.8	1.3
Related Business	12.2	16.8	1.3
	45.8	43.6	
Family Business	29.5	19.0	1.9
Education, Civic & Religon	7.6	3.7	2.4
Social & Recreational	17.1	33.7	2.4
All Purpose	100	100	1.7

Ref.(1)

The automobile accident is a complex thing to study. There are many variables which come into play, although, perhaps the more important ones involve the relationships between accidents, speed, and driver and vehicle characteristics.

There have been a number of pertinent studies done in the past few years which examine the above mentioned relationships and which give other useful information. The rest of this paper will be dedicated to presenting this type of information, since the aim of this paper is to present information that could be useful in indicating a need for a mechanical design which might reduce the number of traffic fatalities. A major factor in presenting this information is that a majority of the studies available today have taken their data from a limited population area, and are not nation wide. Most of the studies available are classified as either rural or urban.

Part III - The Most Common Types of Accidents and Their Frequency

Impacts in auto accidents are usually classified into four categories: front impact; side impact, (right and left in some cases); rear impact; and the roll-over type of impact. Four different studies are presented in Tables and Figure 6-9 to show the relative frequency of each type. Although the studies vary between rural and urban, and even between rural and rural, and urban and urban studies, the general conclusion that is reached is that the front impact type of accident is the most common, with the side impact second, rear third, and roll-over type impact fourth.

Accidents are also classified as to where they occur. Table (10),

Table 6-10,000 Rural Injury Accidents

Front Impact	54%
Roll-over	23%
Side Impact, left side	6%
Side Impact, right side	9%
Rear Impact	5%
Not Reported	3%

Ref.(2)pg.51

Table 7-Auto Impact Type Analysis-National Safety Council-1965

	Fatal Accidents	Urban Injury Accidents
Front Impact		
Fixed Object 6.6 + 5 est. =	11.6 est. %	4.5 est %
Head-on into another car, both moving	16.0	4.6
Into side of another car	7.5	18.6
Into rear of another car	3.6	22.7
More yielding than a car	20.5 est.	3. est.
Pedestrian	17.5	3.2
Side Impact		
Hit by another car	7.5	18.6
Other	5 est.	1 est.
Rear Impact		
Hit by a faster car	3.6	22.7
Into pedestrian	0.3	0.1
Roll-over 1.9 + 5 est. =	6.9 est.	1 est.
	100%	100%

Ref.(2) pg.51

Table 8-Distribution of Impacts

	ACIR	TARU
Front	53%	42.5%
Side	14	46.7
Rear	6	6.8
Rollover	23	3.8

Above table is a comparison of two studies-ACIR= Urban - TARU=Rural

ACIR=Automotive Crash Injury Research of Cornell Laboratories
TARU=Traffic Accident Research unit, University of Adelaide, Australia

Ref. (17) pg.310

Figure 9- Percentage Distribution of Crash Conditions By Impact Area

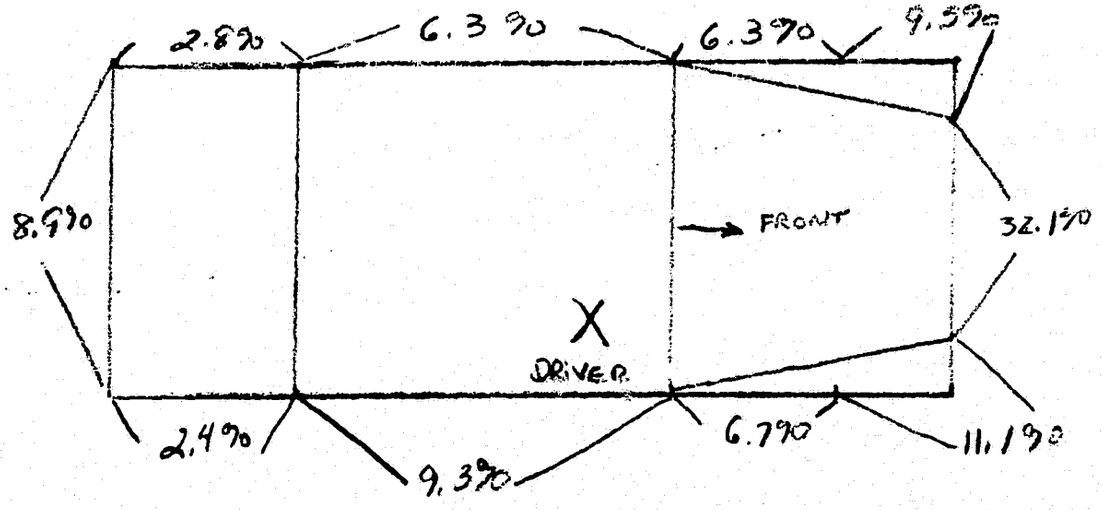

University of Birmingham, England Study Ref.(13) pg.75

Table 10-Comparison of Types of Automobile Accidents Occuring in Rural and Urban Regions

Type of Accident	Urban		Rural	
	Fatal	Non-fatal	Fatal	Non-fatal
	Per cent	*Per cent*	*Per cent*	*Per cent*
Pedestrian accidents at intersections	23.0	19.0	2.0	1.0
Pedestrian accidents between intersections	40.0	22.0	23.0	7.0
Two-car accidents at intersections	9.0	28.0	7.0	17.0
Two-car accidents between intersections	7.5	14.0	25.0	39.0
Non-collision accidents	9.5	5.5	31.4	26.3
Fixed object accidents	2.5	1.4	3.2	3.5
All others	8.5	10.1	8.4	6.2

From National Safety Council Information, 1940 Ref.(3) pg.17

Table 11-1963-64 Study Done by the University of Adelaide, Australia An Analysis of 183 Automobile Accidents.

Type of Accident	No. of Cars	
Collision between two cars		
Initial Collision between two cars		108
and Subsequent Collision With:		32
1 or more motor vehicles	15	
Utility pole	8	
Building	4	
Curb	3	
Tree	1	
Ditch	1	
Single-Car Accident		30
Collision with utility pole	8	
Roll-over only	8	
Roll-over followed by		
collision with utility pole	6	
collision with tree	3	
Collision with assorted fixed objects	2	
Collision With Parked Vehicle		13
		183

Ref. (18)

although rather outdated, gives an idea as to the frequency of where accidents occur most often. From this study, it can be concluded that the majority of accidents occur at intersections. This conclusion is reinforced by a second study done in Australia by certain physicians, engineers, and law enforcement officers, in which it was stated that, "..of collisions between cars, 75% happened at intersections".[18] From this same study the following breakdown of 183 accidents was presented as in Table (11).

Studies also have been done on when traffic accidents occur, not only according to the hour of the day, but also according to the day of the week and month of the year. Table (12) presents the results of a study done in Southern Michigan, which indicated that the most frequent time for accidents is between 8 p.m. and midnight. Figure (13) presents three graphs which indicate when accients occur most frequently, as determined from a study done in Canada. This study indicates that accidents occur most frequently at 5 p.m., on Saturday, and in December, (although this does not mean that the most frequent time for accidents is 5 p.m. on a Saturday in December!). This type of study though, is very dependent on the type of area and geographical location.

Part IV - Circumstances That Contribute to Automobile Accident Rates

Many factors contribute to the injury and death rate in automobile accidents. Speed, poor road conditions, poor vision, mechanical failures, and the drinking driver, are all things that can cause accidents.

Table 12-Time & Day of Week of Fatal Automobile Accidents

Time Period	Day of Week Mon.	Tues.	Wed.	Thur.	Fri.	Sat	Sun.	Fatalities 1	2	3	4	Total
8 am-noon	3	1	4	-	1	5	-	11	2	-	1	19
Noon-4pm	2	4	2	2	2	4	0	20	5	1	1	37
4pm-8pm	3	1	1	4	1	6	4	18	2	-	-	22
8pm-midnight	3	4	2	5	11	7	4	25	6	3	-	40
Midnight-4am	3	1	1	7	3	5	7	24	4	2	-	38
4am-8am	-	1	2	2	4	3	2	13	1	-	-	15

From a study done in the Washtenau County of Southeastern Mich.

Ref. (8)pg.38

Table 13- When Accidents Occur.

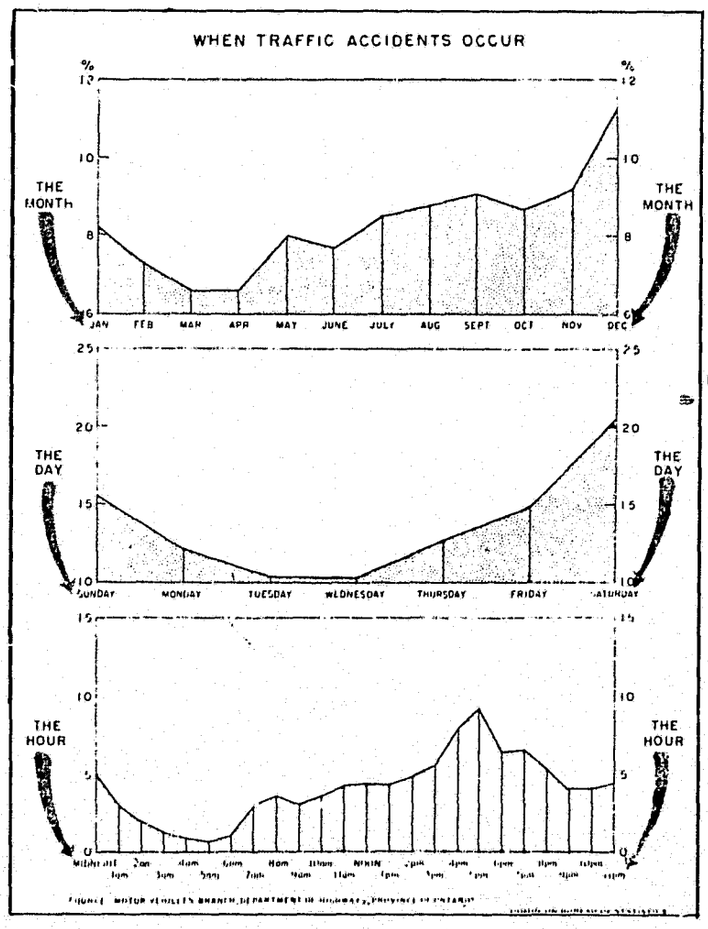

From a Canadian Study Ref. (9) pg. 25

Dr. F. D. Woodwad, as mentioned previously, states the following about circumstances that contribute to the rate of automobile accidents: "... the greatest number of deaths are caused by the driver who has been drinking. He accounts for 33% or more of all the crashes and 50% or more of the deaths. Next in frequency is the speeding and reckless driver who accounts for approxiamately 30% or more of all auto deaths. The remainder are caused by many things, such as mechanical failure, physiological states such as sleep and fatigue, pathological conditions such as epilepsy, ..." [23] His figures are confirmed by a study done by a Dr. D. F. Huelke, as found in the March 1968 issue of the Journal of the AMA. His findings are found in Table (14) below.

Table 14

DRINKING OF DRIVERS AT FAULT BEFORE FATAL ACCIDENTS

Alcohol States of Driver	No. of Cases	%
Had been Drinking	69	50
Had Not Beem Drinking	36	26
Unknown	34	24

Ref. (8) pg. 1101

Speed is not only an important factor by itself in contributing to auto accidents, but also adds to the severity of all accidents no matter what the original circumstance was intially.

A major study of how speed contributes to auto accidents is found in a U.S. Department of Commerce Bulletin, put out by its Bureau of Public Roads in July 1964.

Figure 15-Injury rate by travel speed, day and night

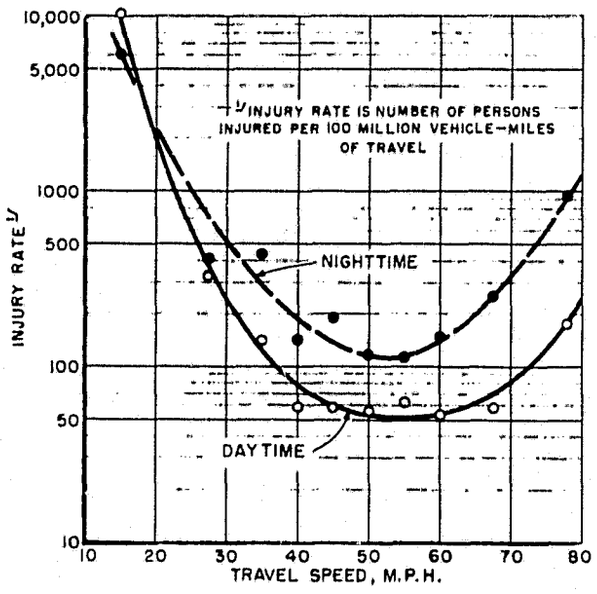

Ref. (22) pg.13

Figure 16-Property damage by travel speed, day and night.

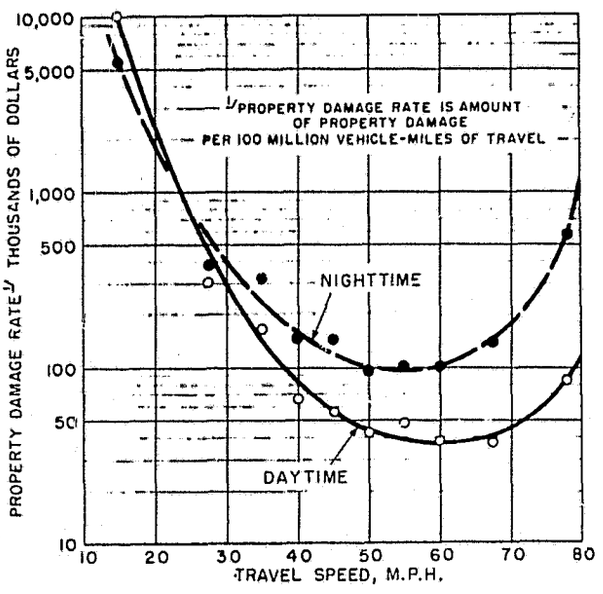

Ref. (22) pg.13

Table 17-Involvement, injury, fatality, and property damage rates by travel speed, day and night.

Travel speed	Vehicle-miles			Vehicle involvements		Persons: Injured			Persons: Killed			Property damage		
DAY														
M.p.h.	*Number*	*Percent*	*Cumulative percent*	*Number*	*Rate* [3]	*Number*	*Rate* [3]	*Per 100 involvements*	*Number*	*Rate* [3]	*Per 100 involvements*	*Amount*	*Rate* [3]	*Per 100 involvements*
Standing				493		90		18	1	(2)	(2)	$119,900		$24,000
22 or less	2,736,000	0.1	0.1	1,183	43,238	278	10,161	23	17	621	[1] 1	275,900	$10,084,000	23,000
23-32	28,850,000	1.0	1.1	331	1,147	95	329	29	2			87,300	303,000	26,000
33-37	64,497,000	2.3	3.4	355	550	90	140	25	1			106,000	164,000	30,000
38-42	250,142,000	9.0	12.4	558	223	147	59	26	6	[1] 2	[1] 1	165,900	66,000	30,000
43-47	395,097,000	14.2	26.6	698	177	233	59	33	3			219,400	56,000	31,000
48-52	714,925,000	25.7	52.3	911	127	404	56	44	24	[1] 3	[1] 3	314,400	44,000	35,000
53-57	513,552,000	18.5	70.8	700	136	323	63	46	17	[1] 3	[1] 2	247,850	48,000	35,000
58-62	462,238,000	16.7	87.5	441	95	243	53	55	17	[1] 4	[1] 4	175,100	38,000	40,000
63-72	307,786,000	11.1	98.6	259	84	180	58	69	15	[1] 5	[1] 6	113,700	37,000	44,000
73 or more	38,841,000	1.4	100.0	54	139	68	175	126	12	[1] 31	[1] 22	32,450	84,000	60,000
TOTAL	2,778,664,000	100.0		5,983	215	2,151	77	36	115	4	2	1,857,900	67,000	31,000
NIGHT														
Standing				255		52		20	6	(2)	(2)	$65,000		$25,000
22 or less	1,990,000	0.2	0.2	473	23,769	120	6,030	25	2			110,950	$5,575,000	23,000
23-32	13,284,000	1.5	1.7	206	1,551	55	414	27	3	[1] 15	[1] 2	51,550	388,000	25,000
33-37	22,701,000	2.5	4.2	254	1,119	100	440	39	9			78,450	346,000	31,000
38-42	99,996,000	11.2	15.4	418	418	142	142	34	7			144,650	145,000	35,000
43-47	136,057,000	15.2	30.6	559	411	259	190	46	13	[1] 10	[1] 2	194,700	143,000	35,000
48-52	274,039,000	30.7	61.3	686	250	321	117	47	29	[1] 11	[1] 4	263,050	96,000	38,000
53-57	164,739,000	18.5	79.8	454	276	186	113	41	18	[1] 9	[1] 3	165,700	101,000	30,000
58-62	105,028,000	11.8	91.6	250	238	157	149	63	5			105,750	101,000	42,000
63-72	66,181,000	7.4	99.0	195	295	168	254	86	21	[1] 32	[1] 11	92,250	139,000	47,000
73 or more	8,492,000	1.0	100.0	83	977	80	942	96	25	[1] 294	[1] 30	47,900	564,000	58,000
TOTAL	892,507,000	100.0		3,833	429	1,640	184	43	138	15	4	1,319,950	148,000	34,000

[1] Rate based on 10-29 accident involvements.
[2] Less than 10 accident involvements; rate not computed.
[3] Rate is the number of involvements, persons injured, persons killed, or amount of property damage per 100 million vehicle miles.

Ref.(22) pg.12

The major conclusion that can be reached from this study refutes the current slogan which says that "Speeed Kills".

Figures (15 & 16) and Table (17) clearly indicate that the greatest number of accidents, the highest injury and death rate, and the greatest amount of property damage per a certain number of vehicle miles occurs at the lower speeds of about 20 miles per hour. The graphs do indicate a trend toward higher rates at excess speeds, but they emphasize that a greater number occur, in the study population involved, at lower speeeds.

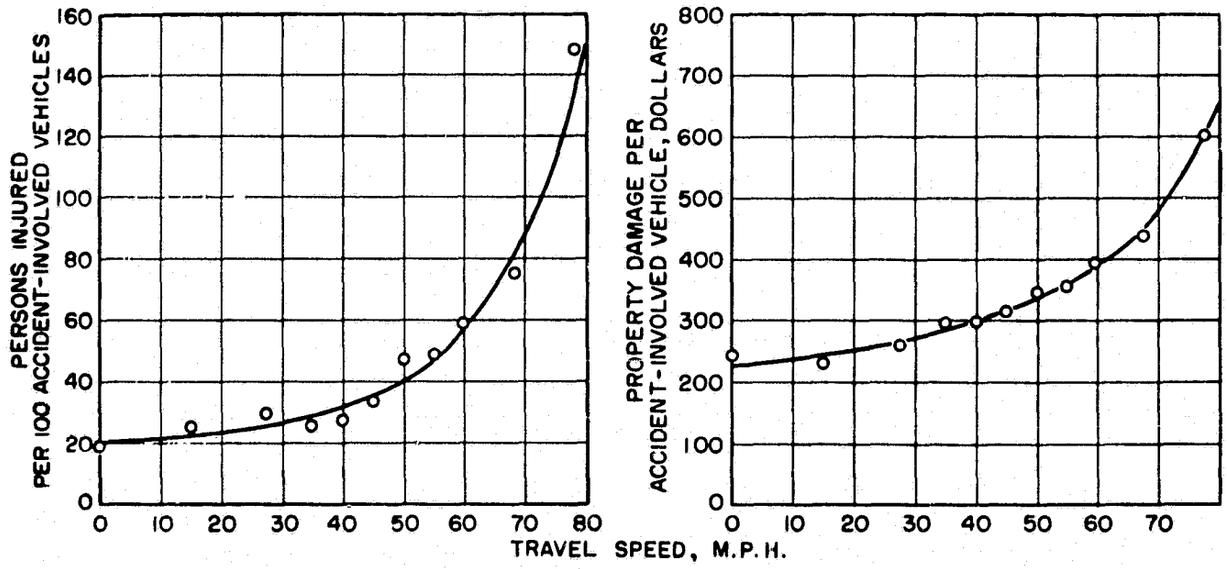

Figure 18. - Persons injured per 100 involvements and property damage per involvement by travel speed, day. Rural Accidents Ref (22) pg.11

Comparing Figures (15 & 16) and Figure (18) above, all from the same study, shows the point just made. Excessive speed does cause more injury amd more severe damages in an accident, but by the number of occurences, lower speeds are actually more dangerous in our society today.

Figure 19-Percentage of accident involvements by travel speed and type of collision for all vehicles, day.

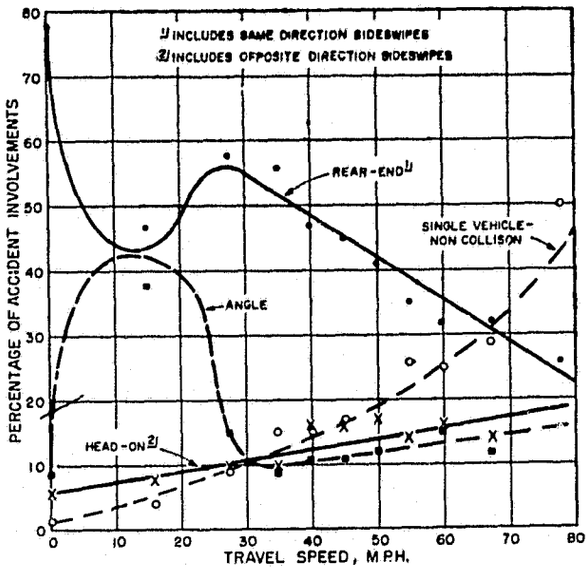

Ref. (22) pg. 36

Table 20-Involvement rate by type of collision, by travel speed, day and night.

Travel speed, m.p.h.	Rate of accident-involvements by type of collision				
	Rear-end	Head-on	Angle	Other	None
DAY					
22 or less	20,066	3,399	16,118	1,462	1,572
23-32	662	118	177	[1] 80	[1] 97
33-37	312	56	50	50	85
38-42	106	37	26	23	33
43-47	81	28	19	19	30
48-52	53	22	16	16	22
53-57	45	19	19	14	36
58-62	31	16	14	11	24
63-72	27	12	10	10	25
73 or more	[1] 36	(2)	(2)	(2)	[1] 70
NIGHT					
22 or less	11,558	2,764	7,688	1,854	[1] 502
23-32	813	233	[1] 218	[1] 166	[1] 113
33-37	564	216	[1] 88	[1] 119	[1] 119
38-42	155	76	37	75	66
43-47	166	74	38	80	46
48-52	72	43	24	55	54
53-57	109	41	19	37	64
58-62	70	34	[1] 16	41	71
63-72	91	[1] 21	[1] 15	50	113
73 or more	[1] 224	[1] 130	(2)	(2)	483

[1] Rate based on 10-29 accident involvements.
[2] Less than 10 accident involvements; rate not computed.

Ref. (22) pg.34

Table 21-Percentage of involvements by type of collision, by travel speed, day and night.

Travel speed, m.p.h.	Accident involvements	Percentage of accident-involvements by type of collision				
		Rear-end	Head-on	Angle	Other	None
DAY						
Standing	493	78	6	9	5	2
22 or less	1,183	47	8	38	3	4
23-32	331	58	10	16	8	8
33-37	355	56	10	9	10	15
38-42	558	47	16	12	10	15
43-47	698	45	16	11	11	17
48-52	911	41	17	12	12	17
53-57	700	35	14	14	11	26
58-62	441	32	16	15	12	25
63-72	259	32	14	13	12	29
73 or more	54	26	2	7	15	50
TOTAL	5,983	46	13	17	9	15
NIGHT						
Standing	255	64	11	9	15	1
22 or less	473	49	12	33	4	2
23-32	206	52	15	14	12	7
33-37	254	51	20	8	11	10
38-42	418	37	18	9	20	16
43-47	559	40	18	9	21	12
48-52	686	29	17	9	23	22
53-57	454	40	15	7	15	23
58-62	250	30	15	7	18	30
63-72	195	31	7	5	18	39
73 or more	83	23	13	4	11	49
TOTAL	3,833	40	16	12	16	16

Ref. (22) pg.34

Figure (19) and Tables (20 & 21) refer back to part III about types of impacts and compares speed with types of impact. From Figure (19) it can be seen that rear end and angle types of impact follow the trend mentioned in the previous paragraph of occuring more frequently at lower speeds, while head-on and single vehicle non-collision types of accidents tend to be more frequent at the higher speeds.

Table (22) and Figure (23), the last two of this section on speed, refer back to the first paragraphs on speed. They clearly indicate that the least number of accidents occur at speeds just slightly higher than the posted average for a road, whether it be high or low itself. They indicate that the highest rate of accidents occur at speeds lower than the posted average for a particular road, and they give reason for the often posted minimum on some roads.

A significant point brought out by a British Study, as found in the January 13,1968 issue of the British Medical Journal, is that in 103 fatal accidents in a particular county in England, 71/103 of the deaths were attributed to poor vision in some way; poor vision being defined as either poor eyesight or the inability of the driver to see another vehicle or fixed object due to some physical obstruction or weather condition.

The U.S. Department of Commerce bulletin referred to earlier presents two other studies in relation to conditions that lead to accidents which are pertinent to this report.

Tables (24 & 25) indicate accident rates as a function of median and shoulder width. Table (24), regarding the width of the median, indicates that two lane highways have higher accident

Table 22-Speed when involvement rate was a minimum by average of study section, day and night.

Average speed on study sections	Speed when accident-involvement rate was a minimum		Overall accident-involvement rate	
	Day	Night	Day	Night
2-lane sections:	*M.p.h.*	*M.p.h.*	*Rate*	*Rate*
Less than 45 m.p.h.	50	50	289	698
45–50 m.p.h.	50	40	320	587
50–55 m.p.h.	55	55	192	296
55 or more m.p.h.	68	68	182	370
4-lane sections:				
Less than 55 m.p.h.	60	60	138	291
55 or more m.p.h.	68	68	156	470

Ref. (22) pg. 16

Figure 23-Involvement rate by variation from average speed on study section, day and night.

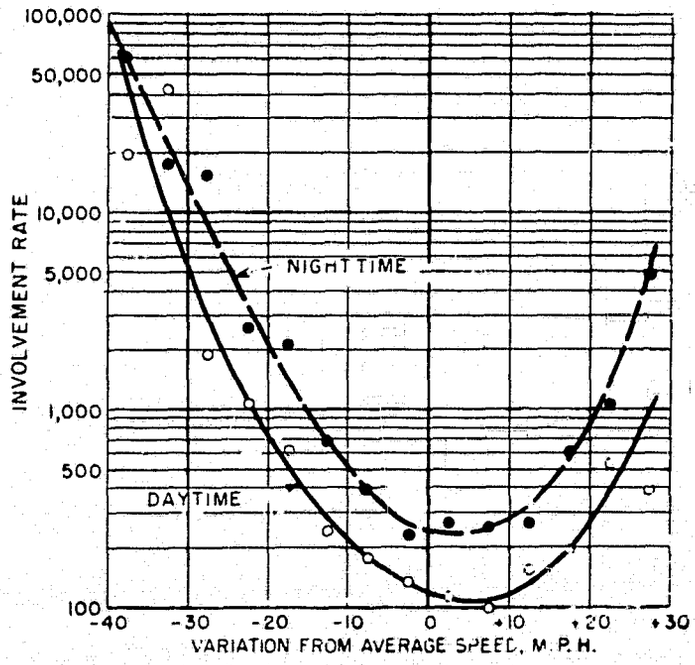

Ref. (22) pg. 16

Table 24- Median width related to total involvements and head-on collisions on 2-and 4-lane highways, day and night

Median width	Vehicle-miles	Total accident involvements		Head-on collisions [2]		Head-on collisions as a percentage of total
		Number	*Rate*	*Number*	*Rate*	
DAY						
Feet						
2-lane:						
All sections	1,749,317,000	4,352	249	701	40	16
4-lane:						
Less than 15 [1]	322,087,000	440	137	26	8	6
15-39	484,970,000	928	191	20	4	2
More than 40	222,290,000	263	118	8	4	3
NIGHT						
2-lane:						
All sections	554,144,000	2,569	464	548	99	21
4-lane:						
Less than 15 [1]	130,874,000	433	331	16	12	4
15-39	164,126,000	663	404	22	13	3
More than 40	43,368,000	168	387	9	21	5

[1] Minimum median width was 8 feet.
[2] Includes opposite direction sideswipes.

Ref. (22) pg. 38

Table 25-Shoulder width related to type of collision, day and night

Shoulder width	Vehicle-miles	Total accident involvements		Type of collision								
				Rear-end [1]			Head-on [2]			Angle		
DAY												
Feet		*Number*	*Rate*	*Number*	*Percent*	*Rate*	*Number*	*Percent*	*Rate*	*Number*	*Percent*	*Rate*
2-lane:												
0-5	740,896,000	1,605	217	640	40	86	267	17	36	233	15	31
6-9	679,018,000	1,777	262	829	47	122	273	15	40	208	12	31
10 or wider	329,403,000	970	294	470	48	143	161	17	49	181	19	55
4-lane:												
All	1,029,347,000	1,631	158	828	51	80	54	3	5	400	25	39
NIGHT												
2-lane:												
0-5	209,509,000	947	452	302	32	144	188	20	90	79	8	38
6-9	225,487,000	988	438	299	30	133	219	22	97	95	10	42
10 or wider	119,148,000	634	532	231	36	194	141	22	118	87	14	73
4-lane:												
All	338,368,000	1,264	374	706	56	209	47	4	14	183	14	54

[1] Includes same direction sideswipes.
[2] Includes opposite direction sideswipes.

Ref. (22) pg.39

rates than four-lane highways sections, (as expected since two-lane sections have no median), and that during the day wider medians produce less accidents on four lane sections while at night the opposite seems to be true. Table (25), regarding the width of highway shoulders, again indicate a higher rate of accidents for two lane sections over four lane sections and indicates that as these shoulder widths increase for two lane sections the involvement rate increases. This conclusion seems very incongruous and the author of the particular section of the bulletin indicates this also, but he gives no reasons for the data being so opposite to what would be expected.

Tables (26 & 27) are from the U.S. Commerce Department study and refer to the last topic of this section. These tables analyze the relation of automobile body style to accident involvement rate. A significant point that can be concluded from these tables is that convertibles lead the list in most categories as being the most dangerous. Whether this conclusion implies that convertibles as such are more dangerous or that the people who drive them are poorer drivers is a question that has not been answered in any of the available data, but I tend to think it is a combination of both.

Table 26-Involvement rate by travel speed and body style of passenger car, day and night

Travel speed, m.p.h.	Day					Night				
	Accident-involvement rate by body style of passenger car					Accident-involvement rate by body style of passenger car				
	2-door sedan	4-door sedan	Soft-top convertible	Hardtop	Station wagon	2-door sedan	4-door sedan	Soft-top convertible	Hardtop	Station wagon
32 or less	7,803	6,023	9,663	[1] 1,986	6,969	12,474	5,645	11,963	(2)	[1] 1,024
33-42	323	255	[1] 264	[1] 104	[1] 167	772	524	[1] 735	[1] 213	[1] 213
43-52	189	131	210	50	128	611	352	896	[1] 114	300
53-62	169	122	157	54	61	544	379	886	[1] 60	171
63 or more	147	110	[1] 102	(2)	[1] 24	793	407	[1] 414	[1] 133	(2)

[1] Rate based on 10–29 accident involvements.
[2] Less than 10 accident involvements; rate not computed.

Ref. (22) pg. 21

Table 27-Involvement, injury, fatality, and property damage rates by body style of passenger car, day and night

Body styles	Vehicle-miles	Accident involvements	Persons						Property damage		
			Injured			Killed					
DAY											
	Number	*Number*	*Rate*[3]	*Number*	*Rate*[3]	*Per 100 involvements*	*Number*	*Rate*[3]	*Per 100 involvements*	*Amount*	*Rate*[3]	*Per 100 involvements*
2-door sedan	698,483,000	1,969	282	810	116	41	46	7	2	$624,800	$90,000	$32,000
4-door sedan	933,764,000	1,907	204	764	81	39	39	4	2	618,200	66,000	32,000
Convertible	64,119,000	164	256	80	125	49	3	(2)	(2)	54,350	85,000	33,000
Hardtop	210,403,000	153	73	78	37	51	1	(2)	(2)	59,750	28,000	39,000
Station wagon	264,366,000	307	116	135	51	44	8	(2)	(2)	104,050	39,000	34,000
Other	13,137,000	34	259	6	(2)	17	3	(2)	(2)	12,700	97,000	37,000
TOTAL	2,186,262,000	4,534	207	1,863	85	41	100	5	2	1,473,850	67,000	32,000
NIGHT												
2-door sedan	167,243,000	1,481	886	757	453	51	63	38	4	$521,050	$312,000	$35,000
4-door sedan	211,669,000	1,153	545	520	246	45	48	23	4	412,700	195,000	36,000
Convertible	19,557,000	186	951	86	440	46	11	[1]56	13	67,200	344,000	36,000
Hardtop	61,304,000	84	137	16	126	19	1	(2)	(2)	31,650	52,000	38,000
Station wagon	68,311,000	157	230	61	89	39	2	(2)	(2)	55,250	81,000	35,000
Other	2,341,000	13	[1]555	3	(2)	23	0	(2)	(2)	3,100	133,000	[1]24,000
TOTAL	530,425,000	3,074	580	1,443	272	47	125	24	4	1,090,950	206,000	36,000

[1] Rate based on 10-29 accident involvements.
[2] Less than 10 accident involvements; rate not computed.
[3] Rate is the number of involvements, persons injured, persons killed, or amount of property damage per 100 million vehicle-miles.

Ref.(22)pg.33

Part V - Auto Injuries - Their Severity, Their Causes, and the Most Common Areas of the Body Which Are Effected.

In this section, although many sources will be referred to, one particular article [17] which was published in the 11th Stapp Car Crash Conference Report of 1967 will be referred to several times. This article is a comparison of two studies done, one in an urban area and one in a rural area. For convience in the article each study's name was abreviated. One study was abreviated TARU, which stands for the Traffic Accident Research Unit, and which was done at the University of Adelaide in Australia and represents an urban area study. The second study's name in the comparison was abreviated ACIR, which stands for the Automobile Crash Injury Research, and was done by the Cornell Aeronautical Laboratory in the U.S. and represents a rural area study.

Auto injuries in general are caused either from the direct penetration of another automobile or object into the passenger compartment or by what is called the "secondary collision. The "secondary collision" is the collision of the car occupant with some area of the interior of the car. In this type of collision the occupant may not be harmed by the intial impact but is rather injured when he is thrown into something within the interior of the car. No data is readily available with a breakdown of the frequency of these two types of collisions, therefore the data to follow has been assumed to apply to both types of accidents.

Dr. F. D. Woodwad, in the same article[23] as mentioned earlier in the Southern Medical Journal, states that "As a result of the Cornell Crash Studies, we know that, in order of occurence, the most frequent sources of death or injury are from the steering assembly, ejection, dashboard, and windshield, and back of the front seat. The most frequent body areas effected are (1) the head and neck, (2) the chest, (3) the extremities, etc. " [23]

Table (28) and Figure (29) give actual figures from a total of three different studies which tend to agree quite will with the ranking of Dr. Woodwad. Figure (29) indicates the differences between injury in the driver and occupants of the car. One can see that the passenger seems to have more head injuries, (probably from hitting the dash), while the driver seems to have more chest injuries, (probably from hitting the steering wheel and column).

Table (30) and figures (31 & 32) give a ranking from two different sources of the various areas of the inside of the car which cause injury the most frequently. These studies agree with Dr. Woodwad's rankings also quite well.

Table 28- Frequency of Injury to Each Body Area (%of those injured)

Body Area	ACIR (Braunstein 1957)	TARU
Head	72.3%	70.1%
Neck & Cervical Spine	6.8%	-
Thorax	36.6%	19.4%
Abdomen	15.3%	3.6%
Spine and Pelvis	-	2.0%
Upper Limb	29.4%	30.7%
Lower Limb	47.0%	52.4%
No. Injured	1,678	509

Ref. (17) pg.311

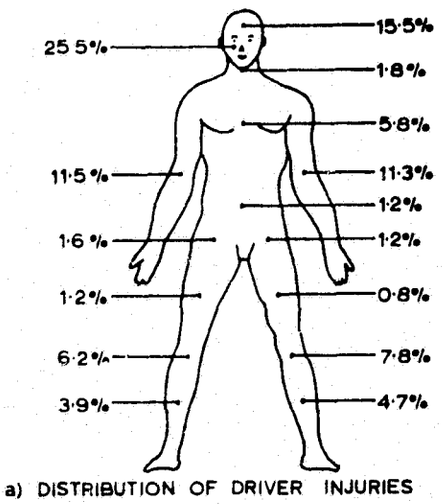

a) DISTRIBUTION OF DRIVER INJURIES

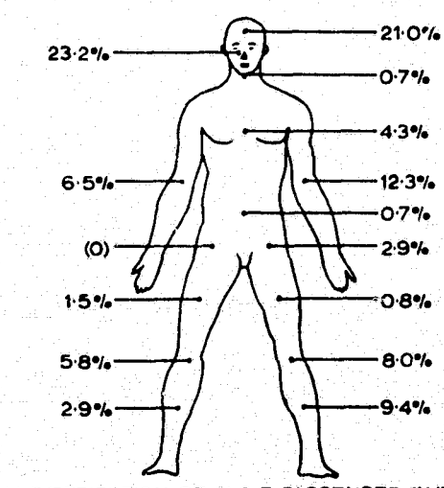

b) DISTRIBUTION OF N.S.F. PASSENGER INJURIES

Figure 29-Car Occupant Injuries Ref. (13)pg. 76

Table 30-Rank of Causes of Injury According to Frequency of Injury for Car Occupants

All Injuries	Moderate & Greater Injury
Instrument Panel	Door-Windshield
Door	Instrument Panel
Windshield	Head Area & Rear View Mirro
Head Area & Rear View Mirror	Ejection
Steering Wheel	Other
Ejection	Steering Wheel
Front Seat	Front Seat
Other	Corner Post
Corner Post	Not Known
Not Known	

Ref. (18)

Figure 31-Ranking of components causing injury

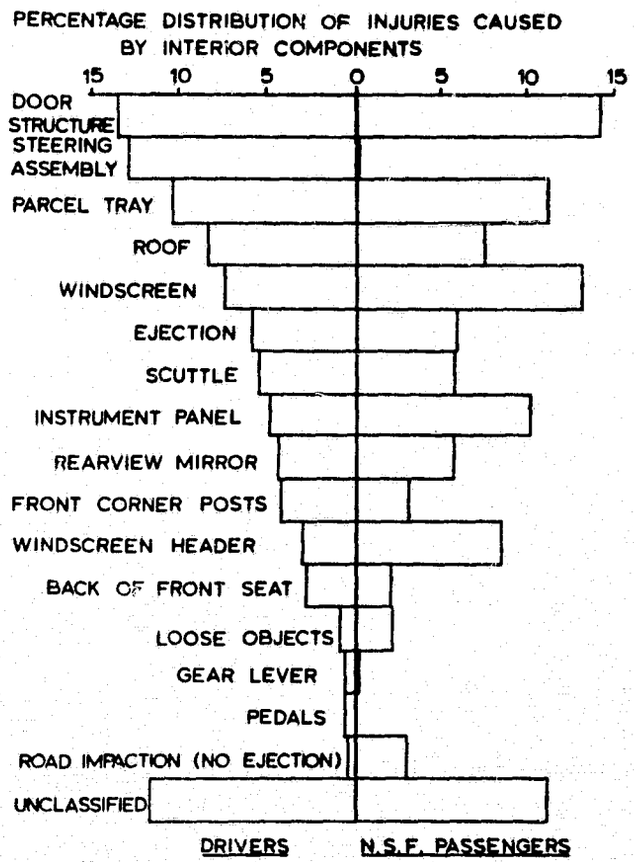

Ref. (13) pg.76

Figure 32-Position of Body Impacts on the Interior of a Car

"Head impacts cluster near the top of the windshield and doors, knee impacts on the lower part of the instrument panel, and the thorax and upper-limb impacts on the steering wheel and doors."

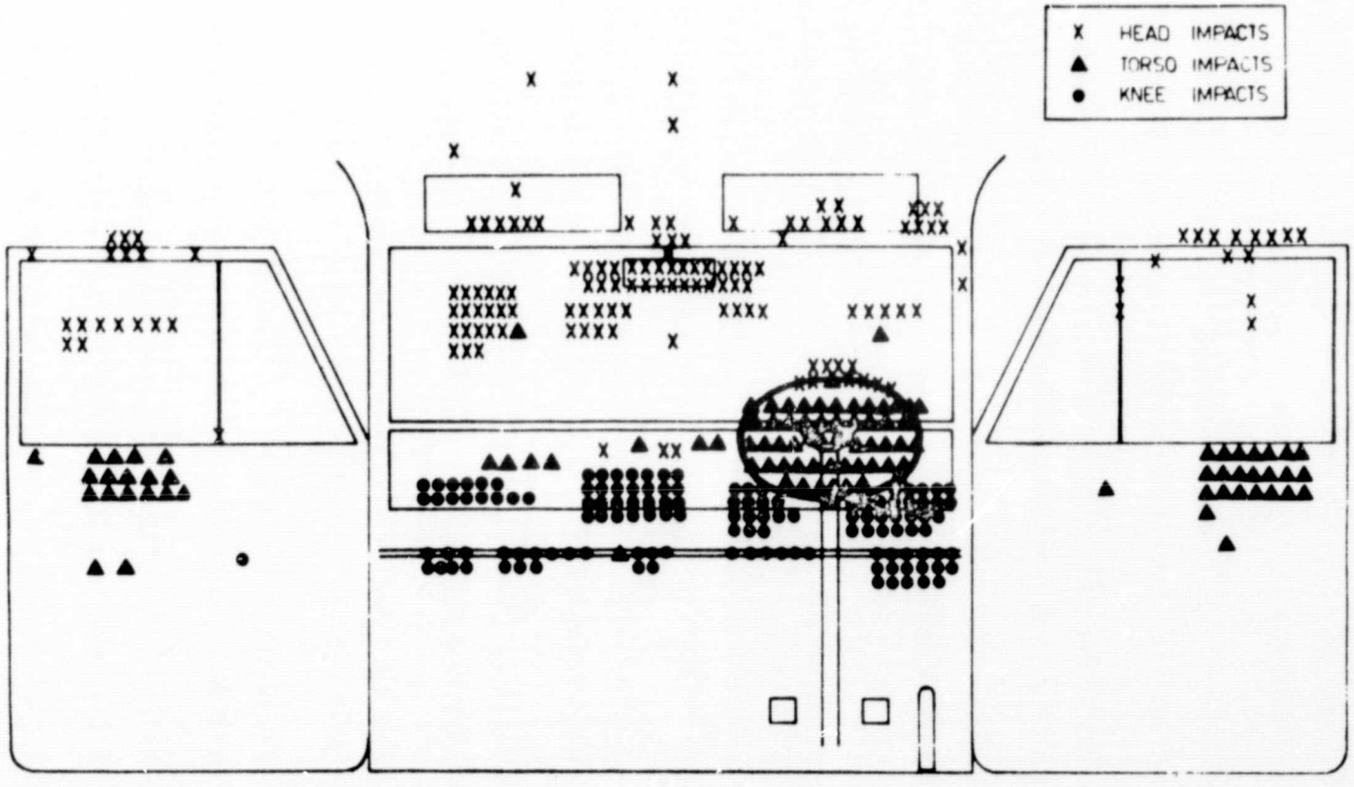

Ref. (18) pg. 1074

Table 33

Body Area and Cause of Injury

% With Injury to Each Body Area by Cause Where Known
All Car Occupants

TARU Number of Injured Persons = 509

Head & Neck	Door	Windscreen	Header	Steering Wheel	Other	Ejection
	24.0	23.2	22.0	7.2	5.6	4.8
Thorax	Door	Steering Wheel	Instrument Panel	Other	Ejection	Front Seat
	40.0	22.0	10.7	10.7	5.3	4.0
Abdomen	Door	Ejection	Front Seat	Other		
	50.0	25.0	16.8	8.3		
Spine & Pelvis	Door	Ejection	Other	Corner Post	Header	
	25.0	25.0	25.0	12.5	12.5	
Upper Limb	Door	Ejection	Windscreen	Steering Wheel	Instrument Panel	Other
	56.7	17.9	7.5	7.5	4.5	3.0
Lower Limb	Instrument Panel	Door	Front Seat	Ejection	Other	Windscreen
	71.8	11.5	8.6	3.8	1.9	1.4

Ref. (17) pg. 314

Table 34

Body Area and Cause of Injury

% With Injury to Each Body Area by Cause Where Known for Drivers and Front Seat Passengers

ACIR (Kihlberg 1965) Number of Injured Persons = 1615

Head	Windscreen	Steering Wheel	Ejection	Instrument Panel	Other	Door
	54.6	14.3	8.6	8.1	7.9	6.5
Neck	Other	Ejection	Steering Wheel	Windscreen	Door	Instrument Panel
	53.8	20.9	7.8	6.7	6.7	3.9
Thorax	Steering Wheel	Instrument Panel	Ejection	Door	Other	Windscreen
	41.6	20.9	12.6	8.1	7.9	2.6
Abdomen	Other	Ejection	Door	Instrument Panel	Steering Wheel	Windscreen
	29.5	26.7	21.9	15.1	12.3	1.4
Upper Limb	Ejection	Instrument Panel	Windscreen	Door	Steering Wheel	Other
	20.7	20.4	18.9	17.8	13.6	5.6
Lower Limb	Instrument Panel	Ejection	Door	Other	Steering Wheel	Windscreen
	74.4	15.9	9.7	8.9	4.5	2.2

Ref. (17) pg. 313

Table 35- Major Cause of Injury

(Braunstein, Moore and Wade, 1957)	% of Occupants Injured		
	Any Degree	Moderate to Fatal Degree	Dangerous to Fatal Degree
Steering Assembly	29.4	8.4	2.5
Ejection	14.6	6.9	3.2
Instrument Panel	20.6	4.2	0.7
Windshield	16.9	4.6	0.6
Back of Front Seat (Top)	11.0	2.4	1.1
Door Structures	7.7	2.4	0.5
Back of Front Seat (Bottom)	15.1	2.5	0
Front Corner Post	2.0	1.2	0.7
Flying Glass	3.0	0.5	0.02
Top Structures	1.2	0.6	0.2
Rear View Mirror	2.2	0.6	0.02

Ref. (17) pg. 312

Table 36- Degree of Injury

	ACIR (Braunstein 1957)		TARU	
Nil	25.5%		36.5%	
Minor	35.3%		41.8%	
Non-Dangerous	19.4%	74.5%	19.7%	63.5%
Dangerous	4.8%		0.9%	
Fatal	4.8%		0.2%	
Survived, injury unknown	10.0%			
No. of Cases	2,253		801	

Ref. (17) pg. 311

Tables (33 & 34) combine the two types of ranking mentioned above into the "Per Cent Injury to Each Body Area by Cause" and the results are consistent with the previous singular rankings.

The severity of injury each area of the car produces is tabulated in Table (35) and indicates, along with Dr. Woodwad's rankings, that the steering assembly, ejection, and the instrument panel cause the most serious injuries. Table (36) gives an indication of the degree of injury most likely to be found in the majority of accidents.

Referring back to previous sections on types of impacts, Table (37) below indicates how people die in two different classifications of accidents. The information relates to rural accidents in Canada.

Table 37

% of Every 100 Persons Killed in Collisions

36 Head Fractures
28 Trunk, Limb and Multiple Fracture Injuries
24 Internal Injuries
12 Other

% of Every 100 Persons Killed by Overturning, Running Off Road, Etc.

31 Head Fractures
24 Trunk, Limb and Multiple Fracure injuries
22 Internal Injuries
23 Other

Ref. (9)pg. 38

The last area to be covered in this section and in the paper regards the death rate as a function of the seat in an automobile. Table (38) and Figure (39) clearly indicate that the death rate

and injury rate are highest for the driver, as would be expected, with the rates for the right front passenger being second. These graphs also indicate that the injury and death rates for all occupants of the car are almost three times as great for night-time as for the daytime.

Table 38.—Occupant-mile injury and death rates by seated position in passenger car, day and night

Seated position	Occupant-miles of travel		Occupants injured		Occupants killed		Injury rate [3]		Fatality rate [3]	
	Day	Night	Day	Night	Day	Night	Day	Night	Day	Night
Left front	2,186,000,000	530,000,000	849	706	49	66	39	133	2	12
Right front	1,398,000,000	293,000,000	503	356	29	26	36	121	2	9
Center front	401,000,000	93,000,000	81	58	5	4	20	62	[1] 1	[1] 6
Left rear	385,000,000	74,000,000	74	58	3	6	19	78		
Right rear	495,000,000	91,000,000	97	69	4	6	20	76		
Center rear	285,000,000	62,000,000	39	24	0	2	14	[1] 39	([2])	([2])
Rear seat in station wagon and other	23,000,000	4,000,000	6	5	0	0	([2])	([2])	([2])	([2])
TOTAL	5,173,000,000	1,147,000,000	1,649	1,276	90	110	32	111	2	10

[1] Rate based on 10–29 occupants injured or killed.
[2] Less than 10 occupants injured or killed; rate not computed.
[3] Injury and fatality rates are number of occupants killed or injured per 100 million occupant-miles of travel.

Rural Accidents Ref. (22) pg.33

Figure 39-Occupant-mile injury rates by seated position, day and night

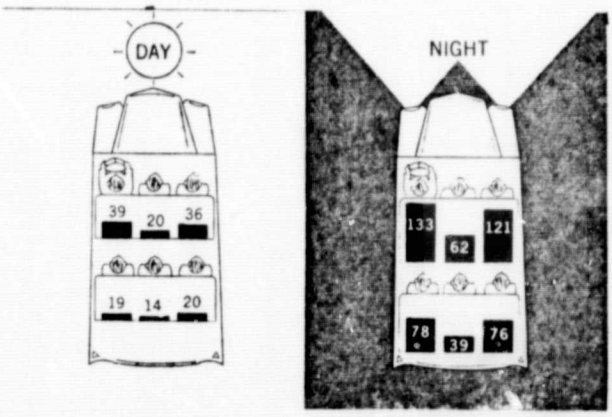

Ref. (22) pg.33

BIBLIOGRAPHY:

1. "1967 Automobile Facts and Figures," Detroit,Michigan: Automobile Manufacturer's Association, 1967.

2. Clark, C., and Blechschmidt,C. "Human Transportation Fatalities and Protection Against Rear and Side Crash Loads by the Airstop Restraint," Ninth Stapp Car Crash Conference,1966.

3. Desilva, H. Why We Have Auto Accidents, New York:John Wiley & Sons, Inc., 1956.

4. Golimparel, D. (ed.) Information Please Almanac-Atlas and Yearbook-1969. 23rd Edition, New York:Simon & Schuster,1968.

5. Goodhard, A. C. "Statistics and Road Accidents," Medicine, Science, and Law, 3:439-47, Oct.1962.

6. Gralton, E. "Medical Factors and Road Accidents,"British Medical Journal, 1:75-9, Jan. 15,1968.

7. Huelke, D. F., and Gilkas, P.W. "Now We Know How They Died," Society Of Automotive Engineers Journal, 73:80, May 1965.

8. Huelke, D. F. "Causes of Death in Automobile Accidents," Journal of the AMA,203:1100-7, March 25,1968.

9. Harris, F. F. "Statistical Summary of Traffic Accidents in Canada,"International Conference on Medical Aspects of Traffic Accidents,1st, Montreal, 1955,pp.25.

10. Kilby, J.K. "Driver and His Right Front Passenger in Automobile Accidents," Ninth Stapp Car Crash Conference,1966, pp.19-64.

11. Kulouski, J. Accidental Injuries of the Conjoined Femur, Springfield Thomas, 1964.

12. Kulouski, J. Crash Injuries, the Integrated Medical Aspect of Automobile Injuries and Deaths, Springfield Thomas,1960.

13. Macky, G. M., and deFonseka, C. P. "Some Aspects of Traffic Injury in Urban Road Accidents," Eleventh Stapp Car Crash Conference,1967.

14. Moore, J. O. "A Study of Speed in Injury Producing Accidents: A Preliminary Report," American Journal of Public Health, 48:1516-25,1958.

15. Nader, R. "Unsafe At Any Speed,New York:Pocket Books Inc.,1966, pp.222.

16. Page, W. J. "Travel by Motor Vehicles in 1965 and 1966," Public Roads,34:267-270, February 1968.

17. Ryan, G. A. "Injuries in Urban and Rural Traffic Accidents: A Comparison of Two Studies," Eleventh Stapp Car Crash Conference, 1967.

18. Ryan, G. A. "Injuries in Traffic Accidents," New England Journal of Medicine, 276:1066-76, May 11, 1967.

19. Solomon, D. "Accidents on Main Rural Highways Related to Speed, Driver, and Vehicle," Bureau of Public Roads, U.S. Dept. of Commerce, Washington, D.C., July 1964.

20. Stone, K. A. "Let's Cut Single-Car Accidents," Society of Automotive Engineers Journal, 73:46-53, April 1965.

21. Twelfth Stapp Car Crash Conference, New York: Society of Automotive Engineers, 1968.

22. "Accidents on Main Rural Highways," Bureau of Public Roads, U.S. Dept. of Commerce. Washington, D.C.: United States Government Printing Office, July 1964. C37.2 Ac2

23. Woodwad, F.D. "Seven Medical Proposals for the Prevention of Injury and Death on the Highway," Southern Medical Journal, 59:557-63, May 1966.

GLOSSARY OF DEFINITIONS FOR REFERENCE 22---ADDED TO REPORT AFTER ITS COMPLETION.

RURAL-2 & 4 LANE HIGHWAYS OF THE NONFREEWAY TYPE. STATES SURVEYED IN THIS STUDY INCLUDED: ARIZONA, CALIFORNIA, CONNECTICUT, IOWA, MINNESOTA, MISSOURI, MONTANA, NEW JERSEY, NORTH CAROLINA, OREGON, AND VIRGINIA.

INVOLVEMENT RATE--NUMBER OF VEHICLES INVOLVED IN ACCIDENTS PER 100 MILOION VEHICLE MILES OF TRAVE.

VEHICLE MILES OF TRAVEL--NUMBER OF VEHICLES TRAVELING OVER STUDY SECTION TIMES THE LENGTH OF THE SECTION IN MILES.

OCCUPANT - MILE RATES---RATE OF OCCURENCE FOR AN OCCUPANT OF A CAR PER SO MANY MILES HE HAS ACTUALLY TRAVELLED ON THE TEST SECTION IN THIS STUDY.

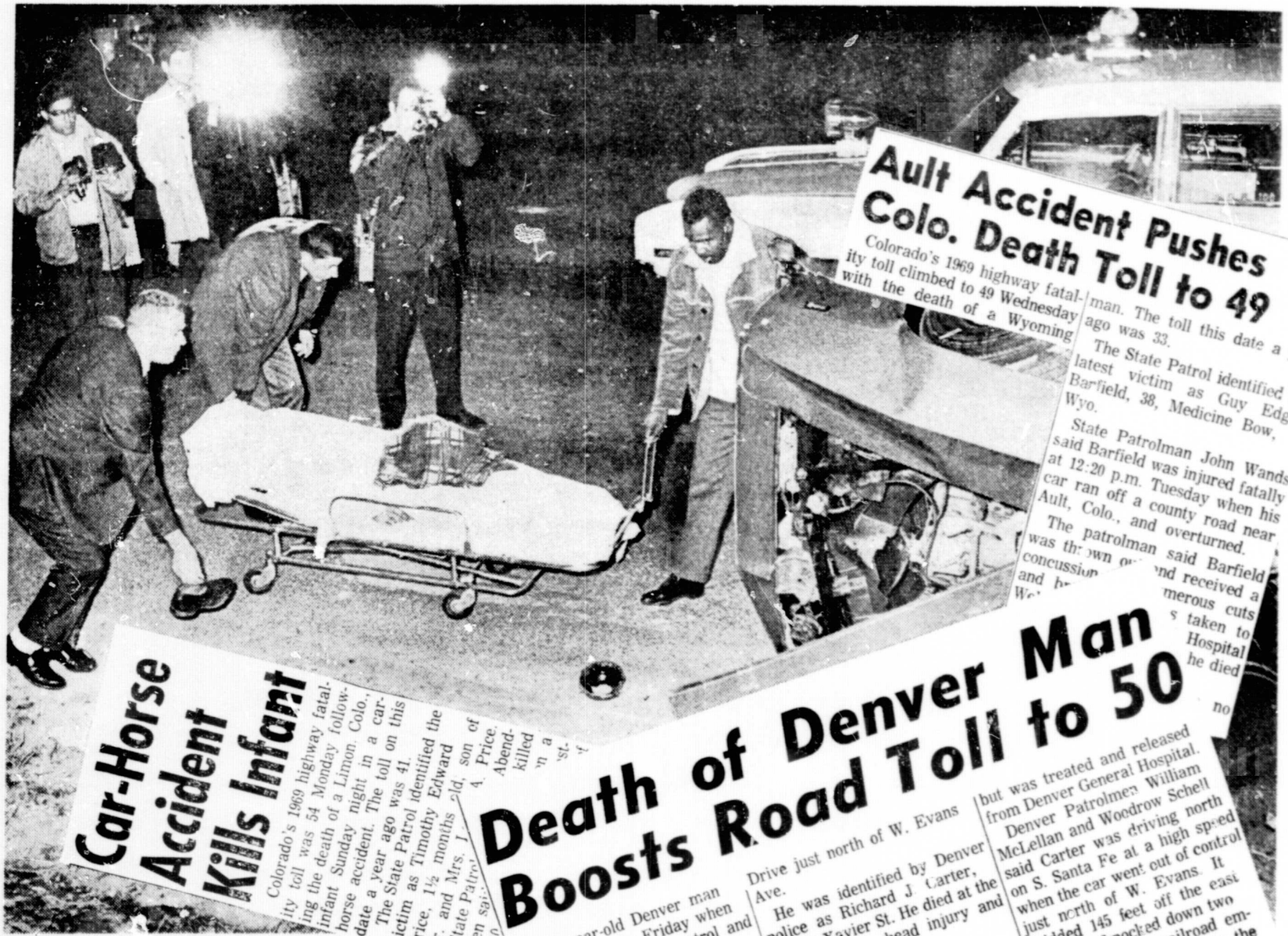

Ault Accident Pushes Colo. Death Toll to 49

Colorado's 1969 highway fatality toll climbed to 49 Wednesday with the death of a Wyoming man. The toll this date a year ago was 33.

The State Patrol identified the latest victim as Guy Edgar Barfield, 38, Medicine Bow, Wyo.

State Patrolman John Wands said Barfield was injured fatally at 12:20 p.m. Tuesday when his car ran off a county road near Ault, Colo., and overturned.

The patrolman said Barfield was thrown out and received a concussion and numerous cuts and bruises. He was taken to Hospital where he died

Car-Horse Accident Kills Infant

Colorado's 1969 highway fatality toll was 54 Monday following the death of a Limon infant Sunday night in a car-horse accident. Colo., date a year ago was 41. The toll on this

The State Patrol identified the victim as Timothy Edward Price, 1½ months old, son of Mr. and Mrs. J. A. Price.

State Patrol

Death of Denver Man Boosts Road Toll to 50

A 21-year-old Denver man was killed early Friday when his car flew out of control and turned on S. Santa Fe Drive just north of W. Evans Ave.

He was identified by Denver police as Richard J. Carter, 1349 S. Xavier St. He died at the scene from a head injury and

but was treated and released from Denver General Hospital.

Denver Patrolmen William McLellan and Woodrow Schell said Carter was driving north on S. Santa Fe at a high speed when the car went out of control just north of W. Evans. It skidded 145 feet off the east shoulder, knocked down two ran up a railroad em- and went into the